JULY 2021 | HydrocarbonProcessing.com

HYDROCARBON PROCESSING®

PLANT DESIGN, ENGINEERING AND CONSTRUCTION

HYDROCARBON PROCESSING®

JULY 2021 | Volume 100 Number 7
HydrocarbonProcessing.com

8

SPECIAL FOCUS: PLANT DESIGN, ENGINEERING AND CONSTRUCTION

PROCESS OPTIMIZATION

BONUS REPORT: THE DIGITAL PLANT

DIGITALIZATION

VALVES, PUMPS AND TURBOMACHINERY

MAINTENANCE AND RELIABILITY

DEPARTMENTS

COLUMNS

WEB EXCLUSIVE

Cover Image: A panoramic view of the ZapSibNeftekhim construction site in western Siberia. Photo courtesy of Sibur.

99TH ANNIVERSARY 1922–2021

HP Industry Perspectives

Mid-year market update

Last month, *Hydrocarbon Processing* presented its mid-year market update to a global audience. The webcast highlighted major trends affecting the hydrocarbon processing industry, as well as a detailed analysis of active capital projects around the world. The following provides a brief overview of the many topics that were covered. An on-demand version of the webcast "*Hydrocarbon Processing's* Industry Market Outlook: 2021 Update" is available at www.HydrocarbonProcessing.com/webcasts.

Demand. According to several industry reports, global fuels demand is forecast to rebound this year and increase in 2022. The U.S. Energy Information Administration forecasts global fuel demand to average 98 MMbpd this year an increase to more than 101 MMbpd in 2022. This is a significant increase in fuels consumption from 2020 levels, which saw widespread fuels demand destruction due to lockdowns and travel restrictions imposed around the globe due to the COVID-19 pandemic.

Both petrochemicals and natural gas will continue to see stark increases in demand. Developing countries continue to witness demand increases for petrochemicals products, which will continue to, at least, 2050. This trend will lead to increases in LPG, ethane and naphtha feedstock consumption, a direct result of new cracker builds in locations such as China, Russia and the U.S.

As many countries around the world initiate carbon reduction/emissions regulations, demand for natural gas will lead to a significant rise in global LNG trade. This trend is leading to the construction of hundreds of millions of tons per year of new LNG liquefaction and regasification capacity, along with the use of floating vessels (e.g., FSRUs and FLNGs).

Capital investments. Gulf Energy Information's Global Energy Infrastructure database is tracking nearly 1,100 active capital projects around the world. In total, these projects represent more than $1.8 T in capital expenditures to 2030.

Approximately 40% of total capital investments ($745 B) are in the Asia-Pacific region. The region is followed by the U.S. at $320 B in total capital expenditures and the Middle East at $280 B. These three regions represent 70% of active capital investments globally.

At present, more than 42% of active projects are within the refining sector. Market share for active projects in the petrochemicals and natural gas/LNG sectors are 34% and 24%, respectively. Nearly 70% of active projects are in preconstruction stages.

Year-over-year, new project announcements have decreased by approximately 6%. Over the past year, nearly half of all new project announcements were in the Asia-Pacific region. Most new Asian project announcements were in China (40%) and India (26%). Both countries continue to buildout refining, petrochemicals and LNG infrastructure to satisfy increasing demand for refined fuels, petrochemical products and natural gas for power generation. The Asia-Pacific region is followed by Eastern Europe, Russia and the CIS and the U.S., both with 12% market share. HP

HYDROCARBON PROCESSING®
www.HydrocarbonProcessing.com

P. O. Box 2608
Houston, Texas 77252-2608, USA
Phone: +1 (713) 529-4301
Fax: +1 (713) 520-4433
Editors@HydrocarbonProcessing.com

PUBLISHER Catherine Watkins

EDITOR-IN-CHIEF/ ASSOCIATE PUBLISHER Lee Nichols

EDITORIAL

Executive Editor	Adrienne Blume
Managing Editor	Mike Rhodes
Digital Editor	Stephanie Bartels
Technical Editor	Sumedha Sharma
Reliability/Equipment Editor	Heinz P. Bloch
Contributing Editor	Alissa Leeton
Contributing Editor	ARC Advisory Group
Contributing Editor	Anthony Sofronas

MAGAZINE PRODUCTION / +1 (713) 525-4633

Vice President, Production	Sheryl Stone
Manager, Advertising Production	Cheryl Willis
Manager, Editorial Production	Angela Bathe Dietrich
Assistant Manager, Editorial Production	Melissa DeLucca
Graphic Designer	Krista Norman

ADVERTISING SALES
See Sales Offices, page 89.

CIRCULATION / +1 (713) 520-4498 / Circulation@GulfEnergyInfo.com
Director, Circulation Suzanne McGehee

SUBSCRIPTIONS
Subscription price (includes both print and digital versions): One year $399, two years $679, three years $897. Airmail rate outside North America $175 additional a year. Single copies $35, prepaid.

Hydrocarbon Processing's Full Data Access subscription plan is priced at $1,995. This plan provides full access to all information and data *Hydrocarbon Processing* has to offer. It includes a print or digital version of the magazine, as well as full access to all posted articles (current and archived), process handbooks, the *HPI Market Data* book, Construction Boxscore Database project updates and more.

Because *Hydrocarbon Processing* is edited specifically to be of greatest value to people working in this specialized business, subscriptions are restricted to those engaged in the hydrocarbon processing industry, or service and supply company personnel connected thereto.

Hydrocarbon Processing is indexed by Applied Science & Technology Index, by Chemical Abstracts and by Engineering Index Inc. Microfilm copies available through University Microfilms, International, Ann Arbor, Mich. The full text of *Hydrocarbon Processing* is also available in electronic versions of the Business Periodicals Index.

DISTRIBUTION OF ARTICLES
Published articles are available for distribution in a PDF format or as professionally printed handouts. Contact Foster Printing at Mossberg & Co. for a price quote and details about how you can customize with company logo and contact information.

For more information, contact Jill Kaletha with Foster Printing at Mossberg & Co. at +1 (800) 428-3340 x 149 or jkaletha@mossbergco.com.

Hydrocarbon Processing (ISSN 0018-8190) is published monthly by Gulf Energy Information, 2 Greenway Plaza, Suite 1020, Houston, Texas 77046. Periodicals postage paid at Houston, Texas, and at additional mailing office. POSTMASTER: Send address changes to Hydrocarbon Processing, P.O. Box 2608, Houston, Texas 77252.

Gulf Energy Information

BPA WORLDWIDE

President/CEO	John Royall
CFO	Alan Millis
Vice President, Upstream and Midstream	Andy McDowell
Vice President, Finance and Operations	Pamela Harvey
Vice President, Production	Sheryl Stone
Vice President, Downstream	Catherine Watkins

Publication Agreement Number 40034765 Printed in USA

Other Gulf Energy Information titles include: *Gas Processing™, Petroleum Economist®, World Oil®, Pipeline & Gas Journal* and *Underground Construction.*

LEE NICHOLS, EDITOR-IN-CHIEF/ASSOCIATE PUBLISHER
Lee.Nichols@HydrocarbonProcessing.com

IRPC Process: A sincere thanks to all

Last month, *Hydrocarbon Processing* hosted the International Refining and Petrochemical Conference (IRPC). The virtual event—IRPC Process Technology—was viewed by more than 1,500 people from nearly 70 countries around the world. The event's primary focus was to provide hydrocarbon processing industry (HPI) personnel the latest processing technologies in the refining and petrochemical industries.

IRPC Process Technology was kicked off by a pre-conference innovation showcase held by Sulzer GTC Technology. The event was led by Joe Gentry, Vice President, Licensing and Technology, who presented a look at the refinery of the future from a process licensor point-of-view. "We see the refinery of the future having three essential elements," said Gentry. "These elements include changes in feedstocks and product mix (incorporating petrochemicals production), an intense drive to optimize energy efficiency, and the creation of an environmentally-sound facility."

The three elements highlighted by Mr. Gentry were echoed by many presentations throughout the event. Refiners are making concerted efforts to increase the production of biofuels and renewable fuels, boost energy efficiency, invest in carbon mitigating technologies and incorporate more petrochemical production units into existing operations. Petrochemical producers are also investing in curbing emissions from their facilities and working at increasing energy efficiency, as well as developing and partnering with licensing companies on new plastics recycling technologies.

The industry's move into the energy transition was highlighted by both opening keynotes. First, Leon de Bruyn, CEO, Lummus Technology, spoke on the licensor of the future and how sustainability and the circular economy will play a vital role in its development. "When you have this long-term view of where you will be in 10 yr or 20 yr, you start with your customer. For us, the customer is the end consumer and clearly there is a drive for more circularity. Our job as a technology licensor is to innovate and bring those innovations to a commercial state and to the market. The reliability of resources, the circularity to minimize waste and carbon reduction are all going to be key ingredients, along with economics, to drive the success of the licensor of the future," said Mr. de Bruyn.

Day 2's keynote address showed the energy transition in action. Petri Lehmus, Vice President of Research and Development, Neste Corp., provided an overview of how their facilities are investing in reducing emissions and producing the latest biofuels and circular solutions in the market, including renewable diesel and sustainable aviation fuel.

The keynote presentations were followed by deep technical presentations on various conventional and energy transition technologies within the refining and petrochemical industries. IRPC Process Technology can be viewed on-demand by visiting www.IRPC-Process.com.

Sincere thanks to all. *Hydrocarbon Processing* sends a heartfelt thank you to all presenters for their time and effort. Your contributions undoubtedly made IRPC Process Technology an outstanding success. The technologies presented showcased the ingenuity of the HPI and the evolution of the industry.

Lastly, IRPC Process Technology would not have been possible without the financial backing of our sponsors. *Hydrocarbon Processing* would sincerely like to thank the following companies for their help in making this event a reality: Sulzer GTC Technology, BASF, Aggreko, Beyond Limits, ExxonMobil and Jotun.

We hope you will all join us for the next installment of IRPC—IRPC Operations—to be held virtually September 21–22. For more information, visit www.IRPC-Operations.com. HP

INSIDE THIS ISSUE

LEE NICHOLS, EDITOR-IN-CHIEF/ASSOCIATE PUBLISHER
Lee.Nichols@HydrocarbonProcessing.com

AFRICA

Anchorage Investments is developing a nearly $2-B petrochemical complex in Suez, Egypt. The Anchorage Benitoite Petrochemical project will produce 1.75 MMtpy of petrochemical products and intermediates, including propylene, polypropylene (PP), acrylic acid, n-butanol and butyl acrylate. **Honeywell UOP** will license its C_3 Oleflex technology for a 750,000-tpy propylene unit, while **Lummus Novolen Technology** will provide its proprietary technology for the 590,000-tpy PP unit. Once completed, the complex will help satisfy increasing demand for petrochemicals in Egypt.

Maire Tecnimont's subsidiaries—**MET Development, NextChem** and **Stamicarbon**—are developing a power-to-fertilizer plant in Kenya. The project, being developed by **Oserian Development Co.,** will be built at the Oserian Two Lakes Industrial Park approximately 100 km north of Nairobi. NextChem plans to complete front-end engineering design (FEED) by 2022. Once completed in 2025, the facility will produce 550,000-tpd of calcium ammonium nitrate and/or nitrogen, phosphorous and potassium fertilizers.

UTM Offshore Ltd. is in collaboration with **Nigerian National Petroleum Corp.'s** subsidiary, **LNG Investment Management Services,** for Nigeria's first-ever FLNG project. The 1.2-MMtpy vessel will help monetize natural gas from Nigeria's Yoho offshore field. UTM has awarded **KBR** an owner's engineer contract for the project. KBR's scope includes due diligence for pre-FEED activities being executed by **JGC Corp.**

ASIA-PACIFIC

Hindustan Petroleum Corp. Ltd. (HPCL) purchased a 50% stake in **Shapoorji Pallonji's** grassroots LNG import terminal. Located in Chhara, India, the new $585-MM, 5-MMtpy LNG import terminal will supply the Indian national grid with natural gas. Once completed in late 2022, the LNG import terminal will help India reach its goal of increasing natural gas to 15% in the country's total energy mix. The terminal can be expanded to 10 MMtpy, if needed.

Refining Technology Solutions, a subsidiary of **DuPont Clean Technologies,** was awarded a contract from **North Huajin Refining and Petrochemicals** for a new diesel hydrotreater. The 37,000-bpd grassroots unit, to be built in Liaodong Bay New Area, Panjin, China, will help the operator produce fuels that adhere to jet 3 fuel and China 6 specifications. The diesel hydrotreater is scheduled to begin operations in late 2023.

Prime Polymer, a JV between **Mitsui Chemicals** and **Idemitsu Kosan Co. Ltd.,** is developing a PP plant in Chiba, Japan. The 200,000-tpy facility will use Mitsui Chemicals' HYPOL process to produce PP. Construction of the plant will begin in August, with operations scheduled to being in late 2024.

The Australian government plans to pay the country's two remaining refineries up to $1.8 B to stay open. The investment, to be provided to **Ampol** and **Viva Energy,** will help the country protect its fuel security. The package includes funds to help both refiners upgrade their facilities to produce ultra-low-sulfur fuels by 2025.

Adani Group and **TotalEnergies** plan to begin operations on the 5-MMtpy Dhamra LNG import terminal in July. The terminal will be India's seventh in operation. If needed, the Dhamra LNG terminal can be expanded to 10 MMtpy.

A collaboration between **Neste, Mitsui Chemicals** and **Toyota Tsusho Corp.** plan to develop Japan's first plant to produce renewable plastics and chemicals from 100% bio-based hydrocarbons. Mitsui will use Neste's proprietary Neste RE technology to replace part of the fossil feedstock in the production of a variety of plastics and chemicals at its crackers. This will enable Mitsui to produce renewable ethylene, propylene, C_4 fraction and benzene, among others, and process them into basic chemicals such as phenol or plastics.

Axens was awarded a licensing contract for **Hengyi Industries'** integrated complex in Pulau Muara Besar, Brunei. Axens will provide FLEXICOKING technology for the complex. FLEXICOKING was developed by **ExxonMobil Catalysts and Licensing.** In January 2020, Axens and ExxonMobil Catalysts and Licensing signed a licensing alliance agreement.

This is the second FLEXICOKING license at the Pulau Muara Besar integrated complex. The first unit—with a capacity of 1.1 MMtpy—began operations in late 2019. The new unit is part of Hengyi Industries' New Crude to Aromatics Phase 2 expansion project.

Indian Oil Corp. Ltd. (IOCL) has awarded **Technip Energies** an engineering, procurement, construction and commissioning (EPCC) contract for a new petrochemical plant in India. IOCL is making a significant investment to incorporate petrochemical units into the Paradip refinery, including the installation of a paraxylene and purified terephthalic acid (PTA) complex. Technip Energies' scope includes the construction of a 1.2-MMtpy PTA plant onsite.

Korea Petrochemical Industries Co. Ltd. will use **Lummus Technology's** butadiene extraction (BDE) technology—Lummus Technology has been licensing the BDE process from **BASF** since 1990—at its chemical plant in Ulsan, Korea. The 146,000-tpy unit will produce butadiene, which will also lead to the production of more valuable products from existing C_4 streams and generate feed for an existing olefins conversion unit.

Axens will supply several technologies for **Chennai Petroleum Corp. Ltd.'s** Cauvery Basin refinery project. The 9-MMtpy

refinery will be located at Nagapattinam, Tamil Nadu, India. Axens will provide technologies for a naphtha hydrotreating unit, a reforming unit, a C_5–C_6 isomerization unit, a vacuum gasoil hydrotreater, a cracked gasoline selective desulfurization unit and a sulfur block consisting of a Claus unit and a two-train tail gas treatment unit.

Numaligarh Refinery Ltd. is making a significant capital investment to expand its refinery in Numaligarh, Assam, India. The Numaligarh Refinery Expansion Project (NREP) will increase the Numaligarh refinery by 6 MMtpy to 9 MMtpy. The NREP expansion is part of India's Hydrocarbon Vision 2030 initiative to expand production in northeast India. Once completed, the facility will produce fuels that adhere to Bharat Stage-6 specifications.

Air Liquide Engineering and Construction will continue its partnership with **Samsung Engineering** to build a methanol plant in Sarawak, Malaysia. The 5,000-tpd facility will use Air Liquide's Lurgi MegaMethanol technology. The company will also provide engineering, related equipment, as well as an air separation unit to produce 2,200 tpd of oxygen. The methanol plant is scheduled to begin operations in 2023.

Indo-Rama Synthetics is investing more than $80 MM to upgrade equipment and expand polyethylene terephthalate (PET) production at its manufacturing site in Nagpur, India. Scheduled for completion in 2Q 2022, the new PET facility will expand production by 700 tpd.

Yangtze Petrochemical Corp. is investing $811 MM to upgrade several units at its refinery in Nanjing, Jiangsu province, China. The upgrade, to be completed in 2023, includes the upgrade of eight facilities, including a 2.8-MMtpy catalytic cracker and a 2.6-MMtpy residue hydrocracker. The project will enable the refinery to boost the production of ultra-low-sulfur fuels.

Crown LNG plans to build a 7.2-MMtpy LNG receiving terminal on India's east coast. The facility will be located 11 km offshore Kakinada. Crown LNG announced it will take FID on the project by 2023. If built, the facility will begin operations in 2026. The terminal will help east India increase natural gas imports, which will be used for power generation and fertilizer and petrochemicals production.

Hyundai Chemical, a JV between **Hyundai Oilbank** and **Lotte Chemical,** announced its capital-intensive petrochemicals project in Daesan, South Korea will start operations by the end of the year. The $2.4-B project includes the construction of an 850,000-tpy ethylene unit to feed an 850,000-tpy PE plant and 500,000-tpy PP unit.

CANADA

Woodside Energy has announced it will sell its 50% stake in the Kitimat LNG export terminal. Located in British Columbia, the 21-MMtpy project is a JV between Woodside and **Chevron Canada.** Woodside announced it will focus on its Scarborough project in Australia. In December 2019, Chevron Canada announced plans to sell its 50% share in the project.

EUROPE

Air Liquide Engineering and Construction will provide license, process design and technical services for a Cryocap flue gas plant for Zeeland refinery, a JV between **TotalEnergies** and **Lukoil.** The technology will enable the capture of more than 90% of emissions from the facility's two hydrogen production units.

Neste has awarded **Technip Energies** multiple contracts for the company's renewables plant to be built in Rotterdam, the Netherlands. According to Technip Enegies, the first contract covers EPC management (EPCm) services to modify Neste's existing renewables plant to produce sustainable aviation fuel (SAF). The more than $200-MM project will enable Neste to produce 500,000 tpy of SAF.

The second contract covers FEED for a grassroots renewables refinery in Rotterdam. FEED will help Neste make an FID by 2022. Both plants will use Neste's proprietary NEXBTL technology, which allows the conversion of waste and residue feedstock into renewable products like renewable diesel, SAF and renewable solutions for the polymers and chemical industry.

Liquid Wind has awarded a FEED contract to **Worley** for a new power-to-fuel project in Sweden. The facility will use biogenic carbon dioxide from a biomass-fired power plant and combine it with green hydrogen—made from renewable electricity and water—to produce 50-000 tpy of renewable methanol.

Hellenic Petroleum announced plans to invest nearly $5 B by 2025, half of which will be spent on clean energy projects. These investments are part of the company's plan to transition to cleaner energy to cut carbon emissions.

In June, **Jizzakh Petroleum,** a JV between **JSC Uzbekneftegaz** and **Gazprom,** signed a memorandum of understanding with several banks to help finance its grassroots methanol-to-olefins complex. The $2.8-B complex—to be built in the southwestern area of Uzbekistan's Bukhara region—will process 1.5 Bm^3y of domestically produced natural gas to produce 500,000 tpy of polymers, including low-density polyethylene, ethylene vinyl acetate, PET and PP.

TotalEnergies awarded **NextChem,** a subsidiary of **Maire Tecnimont,** a FEED contract for a SAF plant in Granpuits, France. Upon completion in 2024, the plant will produce 400,000 tpy of biojet fuel from animal fats and used cooking oil. The facility will also adhere to France's aviation biofuels program, which calls for bio-content in jet fuel to reach 2% by 2025 and 5% by 2030.

In late May, **Gazprom** announced it broke ground on its capital-intensive Ust Luga integrated complex. The facility will be in Ust Luga, Leningrad Oblast, Russia. The complex will consist of a gas processing plant, LNG liquefaction terminal and petrochemicals complex. **RusKimAlyans,** a JV between Gazprom and **RusGazDobycha,** will be responsible for developing the integrated gas processing and liquefaction complex. The gas facilities will process 45 Bm^3y of wet natural gas that will act as a feedstock for the 13-MMtpy LNG liquefaction plant. The ethane will be used as a feedstock for the $13-B Baltic Chemical complex. Once completed, the chemical complex will produce 3 MMtpy of polymers.

As part of its ORLEN 2030 strategy, **PKN ORLEN** has begun its capital-intensive Olefins 3 Complex project. Lo-

cated at the operator's Plock facility, the nearly $3.7-B project will increase steam cracker capacity by nearly 400,000 tpy to more than 1 MMtpy. **Hyundai Engineering** and **Tecnicas Reunidas** were awarded the EPCC contract for the project. Once completed in 1Q 2024 (production launch is scheduled for early 2025), the expanded olefins complex will enable PKN ORLEN to increase the production of ethylene and ethylene derivatives, as well as increase its stature among the larger petrochemical producers in Europe.

Nizhnekamskneftekhim (NKNK), a subsidiary of **TAIF Group,** awarded **Lummus Technology** a technology and licensing contract for the company's EP-600 petrochemical complex expansion project. The expansion is taking place at NKNK's complex in Nizhnekamsk, Tatarstan, Russia. According to Lummus Technology, the company will license proprietary technologies for four units: an ethylbenzene unit, a styrene monomer unit and two propylene units. **OOO Gemont** was awarded an EPC contract for the petrochemical complex expansion project in early 2020. The EP-600 project is scheduled to be completed in 2023.

LATIN AMERICA

As part of **Raizen Argentina's** Buenos Aires modernization and expansion program, **Axens** will supply its Prime G+ technology for an FCC gasoline hydrodesulfurization unit. The 10,200-bpd unit will help the refinery upgrade its fuel quality to adhere to stringent specifications that will go into effect in Argentina in 2024.

In May, **Petrobras** announced plans to invest approximately $300 MM through 2025 to improve efficiencies at its domestic refineries—referred to as the RefTOP initiative. However, at the time of this publication, Petrobras did not provide details on this investment.

Panama plans to build a 670-MW power plant in Colon. The $1-B project, announced by the country's president in early June, will use imported natural gas to produce electricity. **Consortium Consorico Group Energy Gas Panama,** a consortium comprised of **InterEnergy Group, AES Panama** and the Panamanian government, will build the facility. At the time of this publication, the power plant is expected to begin operations in late 2023.

U.S.

In May, **Chevron Lummus Global (CLG)** announced the successful start-up of a 100% renewable base oils unit in **Novvi's** Deer Park, Texas plant. The unit will use CLG's ISODEWAXING technology to produce renewable base oil.

Haldor Topsoe will supply its HydroFlex renewable fuel technology for **Seaboard Energy's** 6,500-bpd renewable diesel plant. Located in Hugoton, Kansas, the plant will use various renewable feedstock to produce sustainable diesel fuel. Haldor Topsoe will provide basic engineering, proprietary equipment, catalyst and technical services for the plant. Seaboard Energy plans to begin operations on the renewable diesel plant by 2022.

Due to severe weather and equipment delivery delays, **CVR Energy** announced a delay in startup of its renewable diesel plant. Located in Wynnewood, Oklahoma, the $135-MM–$140-MM plant will use feedstock such as corn oil, tallow, cooking oil and soybean oil to produce renewable diesel fuel. The plant is scheduled to begin operations by 4Q.

CVR Energy has also announced it may convert its 132,000-bpd Coffeyville, Oklahoma plant to produce renewable diesel. At the time of this publication, no decision has been announced.

Nacero has awarded **Bechtel** a FEED contract for the company's $6.5-B natural gas-to-gasoline plant. The 115,000-bpd plant will be built in two phases, the first phase consisting of a 70,000-bpd plant. Located in Penwell, Texas, the gas-to-gasoline plant will also feature carbon capture technology and run off renewable power.

Chevron Phillips Chemical has broken ground on a new 266,000-tpy 1-hexene unit. The plant, located in Old Ocean, Texas, is scheduled to be completed in 2023.

Cheniere Energy announced in early May that Train 6 at **Sabine Pass LNG's** export terminal was more than 80% complete. Train 6, which will increase the terminal's total production capacity to 30 MMtpy, is expected to be commissioned in 2022. HP

MIKE RHODES, MANAGING EDITOR
Mike.Rhodes@HydrocarbonProcessing.com

HP Industry Metrics

U.S. Gulf Coast margins increased, supported by unplanned refinery outages that limited a stronger recovery in run rates and kept product outputs relatively supressed. Margins in Europe and in Asia performed negatively as refining economics showed losses, reflecting the growth in product availability following the maintenance season in Europe and constrained fuel consumption levels due to high case numbers of the new COVID-19 variant in Asia. HP

An expanded version of Industry Metrics can be found online at HydrocarbonProcessing.com.

U.S. gas production (Bft³d) and prices (US$/Mft³)

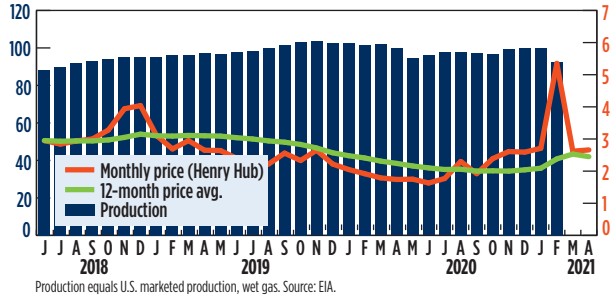

Production equals U.S. marketed production, wet gas. Source: EIA.

Selected world oil prices, U.S. $/bbl

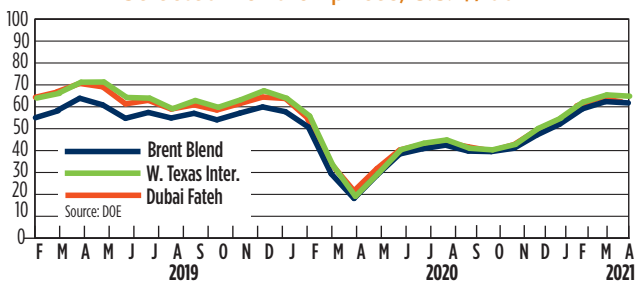

Brent dated vs. sour grades (Urals and Dubai) spread, Jan. 2021–June 2021*

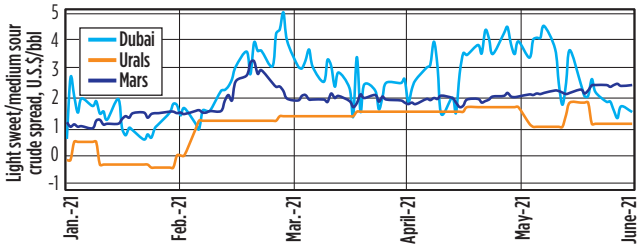

World liquid fuel supply and demand, MMbpd

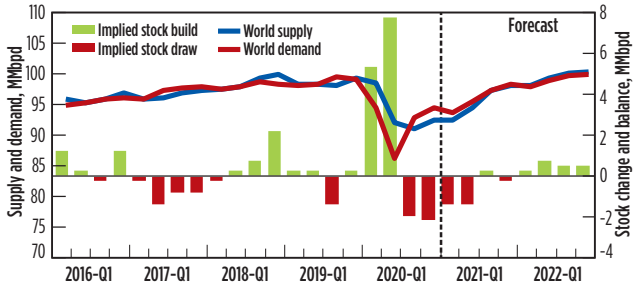

Source: *EIA Short-Term Energy Outlook*, June 2021

Global refining margins, 2020–2021*

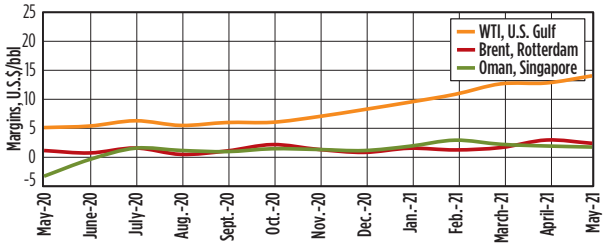

Global refining utilization rates, 2020–2021*

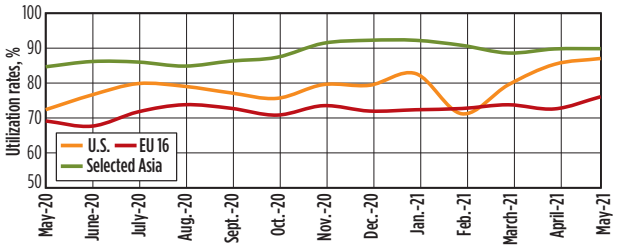

U.S. Gulf cracking spread vs. WTI, 2020–2021*

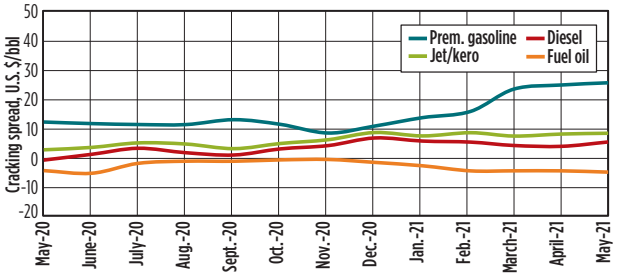

Rotterdam cracking spread vs. Brent, 2020–2021*

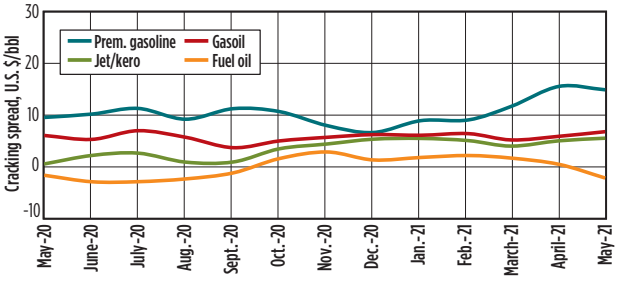

Singapore cracking spread vs. Dubai, 2020–2021*

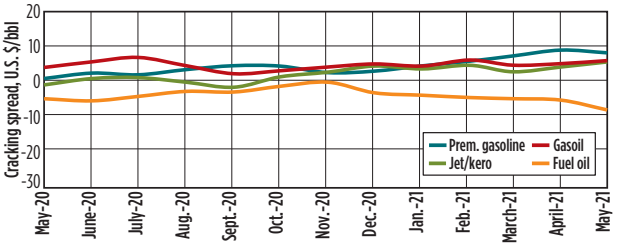

LEE NICHOLS, EDITOR-IN-CHIEF/
ASSOCIATE PUBLISHER
Lee.Nichols@HydrocarbonProcessing.com

HP Global Project Data

Gulf Energy Information's Global Energy Infrastructure database is tracking nearly 1,100 projects around the world. At 40%, the Asia-Pacific region holds the largest market share in total active projects followed by the Middle East and the U.S. These three regions represent nearly 70% of all active projects in the hydrocarbon processing industry. When analyzed by activity level, nearly 70% of active projects are in preconstruction phases. Finally, in terms of capital expenditures, the Asia-Pacific region dominates in total announced investments at nearly $750 B. The closest contender is the U.S. at $320 B, followed by the Middle East at $280 B. HP

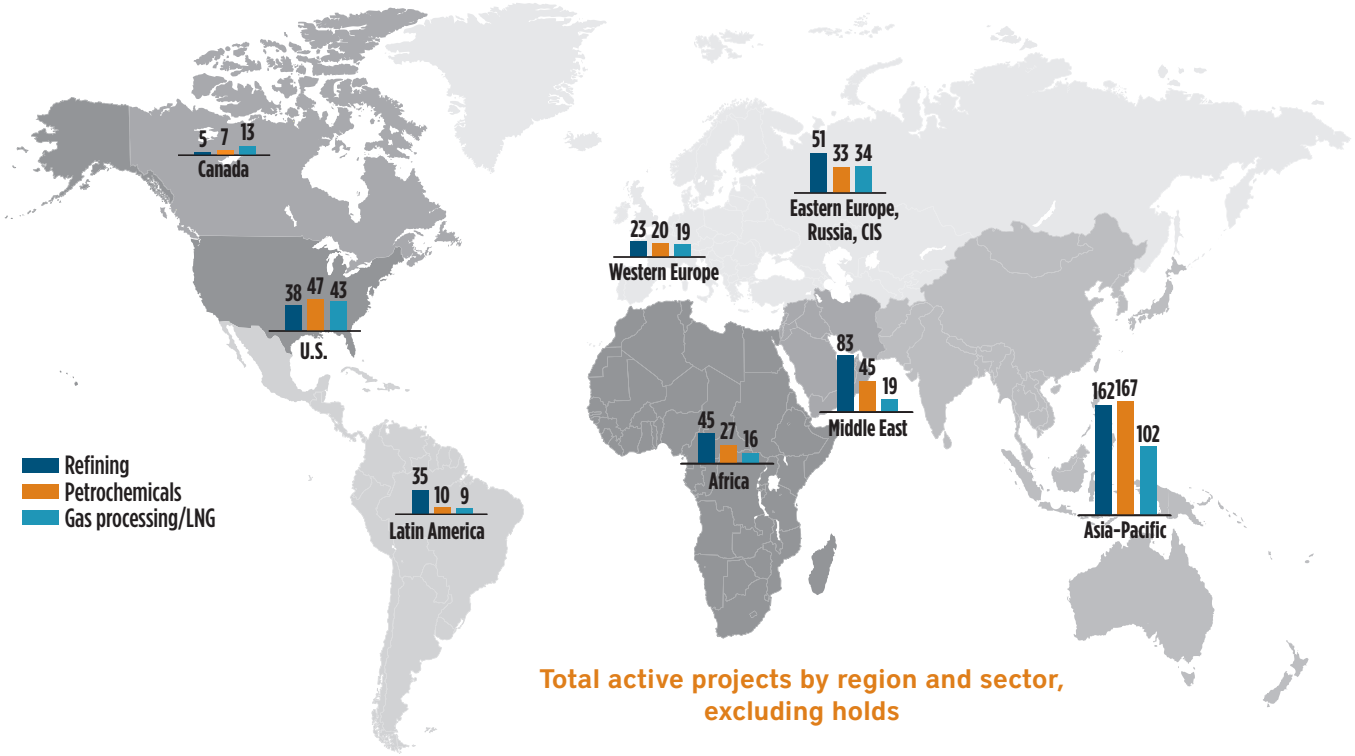

Total active projects by region and sector, excluding holds

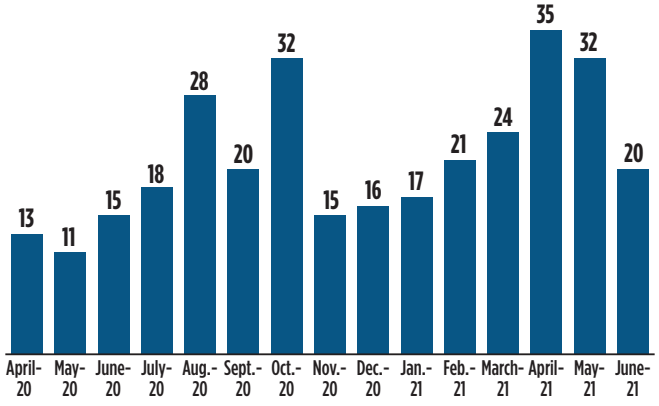

New project announcements, April 2020–June 2021

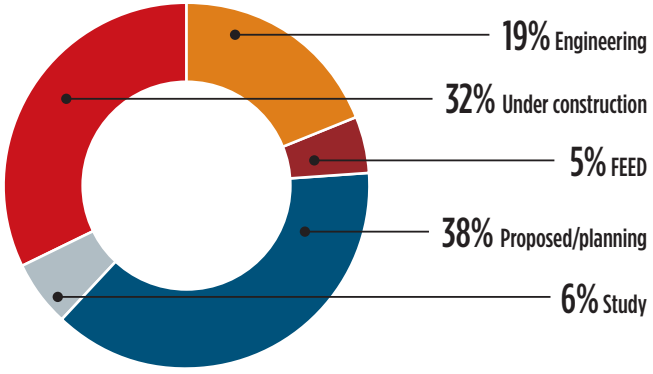

Active project market share by activity level

HEINZ P. BLOCH, RELIABILITY/EQUIPMENT EDITOR
Heinz.Bloch@HydrocarbonProcessing.com

Thinking outside of the box

In late 1989, the Milwaukee Metropolitan Sewage District asked the author to present a three-day equipment maintenance course at one of its large effluent treatment facilities. Situated on Jones Island, the treatment plant makes a pelletized fertilizer byproduct, which we choose to call "Millfort." The fertilizer is still sold today by several major-brand hardware stores for about $28 per 32-lb bag.

Among the raw material that flows into a sewage treatment plant is industrial waste, including fluids from a world-scale beer brewery. Contaminated water byproduct greatly exceeds the final beverages produced by breweries. However, this byproduct is a high-value, nitrogen-rich, slow-release fertilizer. While the inflow captured by thousands of sewage treatment plants is basically the same wherever we find ourselves, the differences are still remarkable. Each municipality and its local industries are different, and while the Milwaukee Metropolitan Sewage District is a quality provider of totally deodorized pellets containing at least 6% nitrogen, 4% phosphate and 2.5% iron, the prevailing percentages can vary from place to place.

A measure of similarity exists between the Milwaukee Metropolitan Sewage District and hydrocarbon processing or plain plastic raw material facilities. With dry pellets as the end product, the Milwaukee Metropolitan Sewage District sends the incoming material through four primary processing phases: screening, settling, secondary treating (i.e., thickening) and disinfecting. The plant contains tankage, agitators, mixers, filter presses, heated dryers, baggers, pallets, strap-wrap units and many other machines. At both the Milwaukee Metropolitan Sewage District and a plastics plant, the personnel work in many different job functions that add value to whatever flows in as feed. By the time the Milwaukee Metropolitan Sewage District discharges a clean stream of liquid into Lake Michigan, heavy metals will have been removed and reclaimed.

Perhaps the similarity with a plastics plant ends there. However, sewage treatment plants elsewhere stop short of turning dried and deodorized sludge into an in-demand fertilizer. Elsewhere, the smelly semi-liquid is usually loaded into railcars and sent to landfills. In Milwaukee, it provides jobs and a desirable product; elsewhere, it often fills the air with odors that make the neighbors wish they lived upwind.

So, what is the point of this page? It is an encouragement to think outside of the box. We might aim for association with people who have determined the cost-vs.-benefit of constructing and erecting small, Millfort-style plants near cities exceeding a certain population. After that, we might ask how many apprenticeships would be created at the factories that make the machines needed to produce a Millfort-like product. Perhaps we would ask about the feasibility of creating many jobs if the clean pellets would be conveyed into hopper cars that would take them near the rim of government-owned land.

FIG. 1. Morning dew collects on the underside of plastic sheets covering vegetables near Lake Galilee.

A few pellets would accelerate the growth of vegetables watered by early morning dew that collects under plastic sheets near Lake Galilee (FIG. 1). For many decades, the facts about drip-feed irrigation have confirmed beyond any reasonable doubt that drip-feed irrigation equals resource conservation. Similarly, experts in reforestation and soil stabilization could hold seminars on crown vetch and many other beautiful shrubs we know well from New Jersey. Vegetation saved miles of embankment on New Jersey's Garden State Parkway, as well as thousands of imperiled hillside homes, from frequent landslides.

Having seen the results of such endeavors, I vividly recall the flagrant blossom and seemingly happy swarms of bees that also added value to parts of New Jersey. So, near the rims of our deserts, there would be tree nurseries that grow seedlings for sensible reforestation with a sound and insect-resistant mix of leafy trees and maintenance-free evergreen needle trees. Subject matter experts would teach whatever is needed to gainfully employ large numbers of willing workers in jobs and activities that create another side benefit: An elevation of one's sense of self-worth, because just like the workers at the Milwaukee Metropolitan Sewage District, the willing workers would be producing much more than waste. They would add lasting value to be enjoyed by many generations to come—if only we gave more thought to thinking outside of the box and stopped arguing against facts and science. HP

HEINZ P. BLOCH resides in Montgomery, Texas. His professional career commenced in 1962 and included long-term assignments as Exxon Chemical's Regional Machinery Specialist for the U.S. He has authored or co-written more than 770 publications, among them 23 comprehensive books on practical machinery management, failure analysis, failure avoidance, compressors, steam turbines, pumps, oil mist lubrication and optimized lubrication for industry. Mr. Bloch holds BS and MS degrees (cum laude) in mechanical engineering. He is an ASME Life Fellow and was awarded lifetime registration as a Professional Engineer in New Jersey.

M. CAPRA
Aggreko Process Services EMEA, Klundert, The Netherlands

Improve propylene recovery at FCC and DCU gas plants with mobile industrial refrigeration

Polypropylene demand remained strong through the 2020 pandemic crisis and is booming in the Asia region, driven by strong Chinese import growth. Consequently, propylene did not suffer the same weak demand and increased volatility experienced by fuels. As polymer grade propylene prices favorably stepped up, reaching $870/t by the end of November 2020, the collapse of the fuels market generated a cash flow shortage across the refining industry: projects and turnarounds were delayed, capital investments cancelled and general spending was reduced.

Refineries contribute approximately 30% of the global propylene supply—taking advantage of this short-term market opportunity by quickly enhancing the recovery yield of this valuable olefin secures additional marginal value to sustain overall profitability.

In the present context, industrial mobile refrigeration for lease is a strong response to these limited favorable market conditions, as solutions are easily deployable, project time schedules are extremely short, no capital investment is necessary, and solutions are tailor-made for specific plants. Additionally, the risks of financial failure are minimized because leasing costs can be terminated as soon as the benefits decline, so no unproductive capital assets will be retained at project termination.

Optimize the costs/benefits ratio. Considering cash constraints and propylene trading prices, one necessary condition for success is for refiners to partner with industrial refrigeration specialty rental companies skilled in evaluating the impact of improved utility conditions on propylene recovery yield and overall project profitability.

The structure of typical gas recovery plants equipped with fluid catalytic cracking units (FCCUs) and delayed coking units (DCUs) is represented in FIG. 1. Extra refrigeration can be applied to the water coolers in the process: the stripper condenser, FCCU/DCU main fractionator condenser, stabilized naphtha trim cooler, sponge oil cooler and eventually the primary absorber condenser and top/bottom pumparounds, when present. The maximization of the benefits/costs ratio clearly implies testing how sensitive the propylene recovery yield improvement is to extra-refrigeration applied in the above listed water coolers. This analysis is generally conducted on every gas plant under examination and indicates the most convenient water cooler on which to apply external refrigeration.

The case study presented here was engineered in four weeks—including the customer's hazard and operability (HAZOP) analysis—and deployed in two weeks as the tie-ins to connect the refrigeration solution were present already.

Gas plant case study. The gas plant, processing the overhead (OVHD) of the FCC main fractionator, was operated with cooling water available at 28°C and ambient air at 30°C. Downstream of the primary absorber, the sponge absorber (not indicated in FIG. 1) has a very low recovery efficiency of

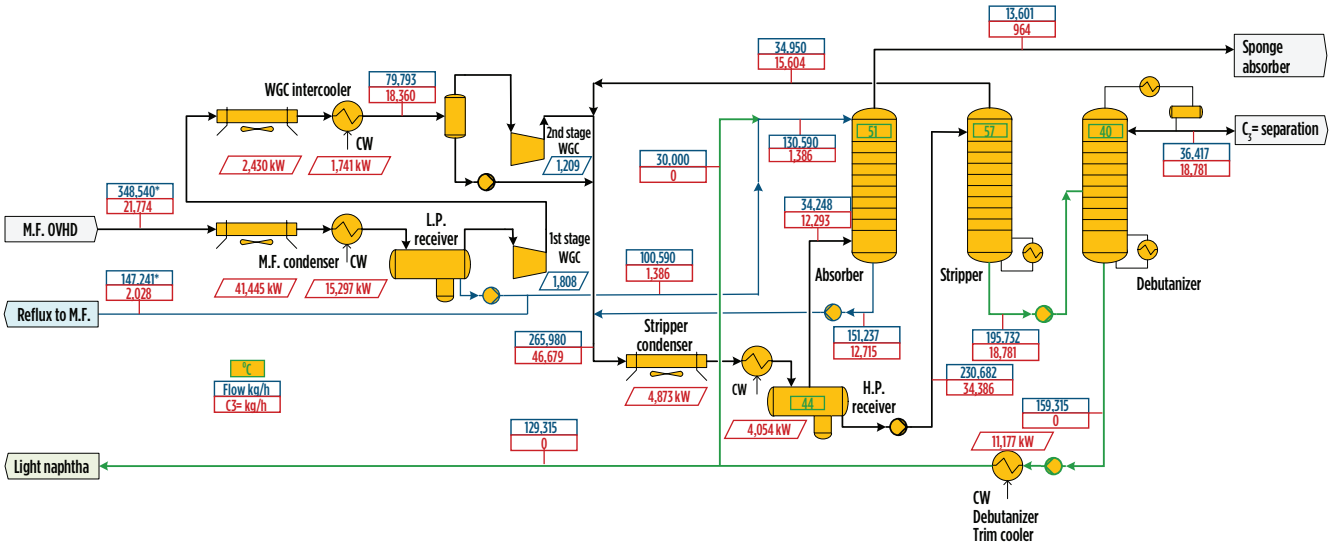

FIG. 1. Gas plant at initial conditions.

light gases, such as liquefied petroleum gas (LPG) and propylene. Any light hydrocarbon released by the primary absorber is generally sent to the fuel gas pool or to flare. In this example, 964 kg/hr of propylene were lost; at $870/t, this translated into $6.71 MM/yr sent to flare.

A key to increased propylene recovery was the improved efficiency of the primary absorber, operated with a mix of un-stabilized naphtha from the M.F. condenser and stabilized naphtha from the debutanizer bottom. The recovery yield performed was 95% based on a net propylene flowrate to the gas plant. The mix of naphtha supplied to the absorber included 1 wt% of propylene, and the offgas to the sponge absorber was at 51°C.

The sensitivity analysis conducted on all candidate water-cooled exchangers—the M.F. condenser, WGC intercooler, debutanizer trim cooler, stripper water-cooled condenser and sponge oil cooler—showed maximum propylene recovery when targeting the stabilized naphtha recycled to the primary absorber. The same analysis should include the primary absorber water-cooled condenser as well as the top and bottom pumparounds, not present in this case study.

It was determined to apply external refrigeration to the stabilized naphtha fed to the primary absorber top tray. The following changes were considered:

- Operating the debutanizer bottom pump at maximum capacity to improve the propylene concentration in the scrubbing naphtha mix to 0.78 wt%.
- Installation of a high-efficiency shell and plate exchanger on the stabilized naphtha line to the primary absorber to perform 1.5-MW refrigeration. This decreased the primary absorber top temperature down to 36°C and the H.P. receiver temperature down to 40°C.

This addition reduced the propylene lost to flare from 964 kg/hr to 440 kg/hr—at $870/t, this translates to $3.65 MM/yr. Considering a chillers' COP=5, 0.30 MW of electrical power had to be supplied from the refinery network. At a cost of $30/MWh, the energy cost totalled $72,000/yr, leaving a margin of $3.58 MM/yr before rental costs.

Several criteria can be applied to guide a future project (FIG. 2): maximization of the benefits/costs ratio, maximization of propylene recovery yield, minimization of a plant's piping modification costs or required power, as well as maximization of the temporary refrigeration solution's reliability, as low probability of refrigeration downtime will reduce costs of flared propylene.

Hiring engineered temporary cooling solutions allows harvesting new profitability during short-term market opportunities at reduced financial and technological risk without committing CAPEX.

Takeaway. When facing limited opportunities to improve overall refinery profitability, engineered temporary cooling solutions for lease offer a strong alternative to capital investment, with low financial and technological risk. The case study presented here allowed new profitability on a lucrative short-term opportunity; benefits were collected as soon as costs started. Additionally, any cost can be terminated as the benefits decline, so no unproductive capital assets are left behind. HP

MASSIMO CAPRA is the manager of Aggreko Process Services in Europe, supporting the Russian and Caspian areas, as well as the Middle East's refining and petrochemical sectors. He has 31 yr of experience in the refining and chemical process industries as a process and project engineering manager for companies that include AGIP, Foster Wheeler Italiana, Tecnimont, Aramco Overseas Co., and as a freelance consultant. He worked as a Process Technologist and Team Leader at OPCW, conducting more than 150 process assessments in chemical facilities. Mr. Capra has earned an MS degree in chemical engineering from Politecnico di Torino (IT), a PGC in project management from the University of Wales (UK), an MBA from Robert Kennedy College (CH), Lean 6 Sigma Black Belt from BMGI (USA) and ISO9001 Lead Assessor certification from SGS (NL).

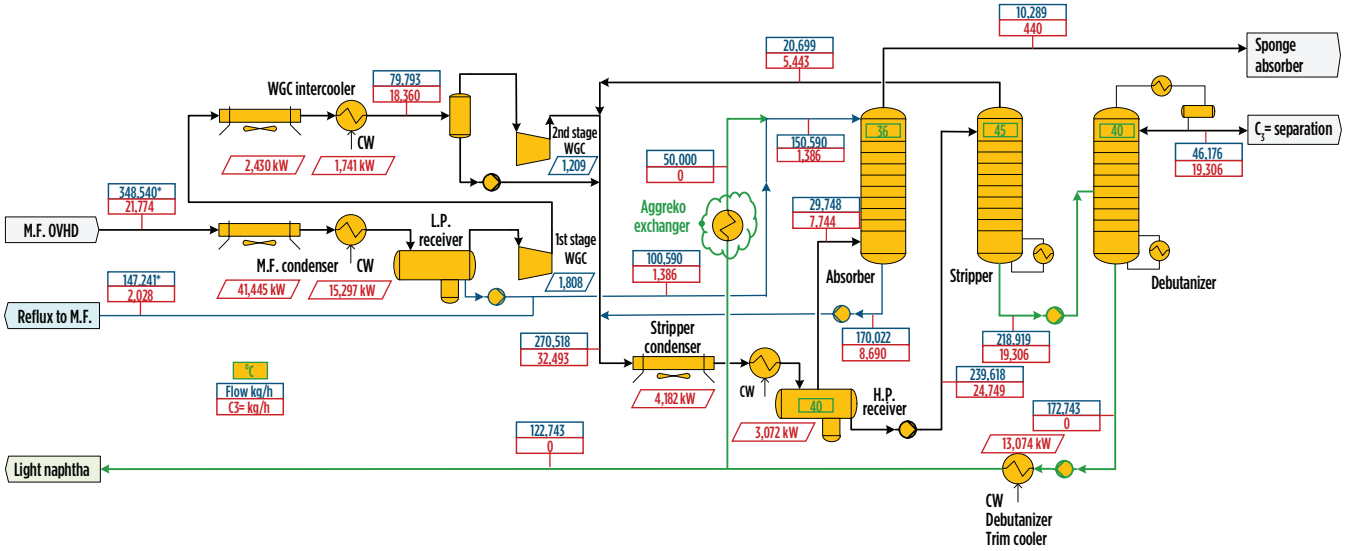

FIG. 2. Gas plant at improved conditions.

A. SOFRONAS, CONSULTING ENGINEER
http://mechanicalengineeringhelp.com

Case 113: The benefits of an engineering education and advanced degrees

It has been a long time since I graduated with my engineering degrees, but I feel qualified to discuss them after many years in industry. Over the years, people have asked me if it is worthwhile to pursue an advanced degree.

Having worked in industry, I've noticed the benefit of the following degrees:

- Associate of applied science in mechanical power technology, a 2-yr degree.
- Bachelor of science in mechanical engineering, a 4-yr degree.
- Master of engineering with an emphasis on mechanical engineering, a 2-yr degree.
- Doctor of engineering with an emphasis on mechanical engineering, a 3-yr degree.

I have always been a "hands-on" type of person who likes to fix and build mechanical things. I like to weld, do lathe work and restore old cars and engines. A 2-yr technical degree was a good way to develop expertise in new technologies. I always felt I could have had a successful career utilizing this degree, as many of my colleagues have done. Some opened car dealerships and automotive repair shops, and others became engineering technicians and troubleshooters.

After receiving this degree and working for a while, I decided that I wanted to work in design and research and have more job flexibility. It was suggested that I pursue a BSME degree. By selecting the correct 2-yr program, much of the course work for a 2-yr technical degree can be transferred toward a BSME degree.

FIG. 1. Construction utilizing 3D printing and robotics.

A BSME degree is excellent for mechanically minded people. It allowed me the flexibility to do the kind of work I wanted to do and to move from company to company as opportunities developed. With this degree, I was able to do interesting failure analysis and design work on machines and structures, using analytical methods. It allowed me to develop my analytical niche.[1] The willingness to observe what other successful engineers did and the benefit of having excellent mentors certainly helped.

The fear of being desk-bound was unfounded, as I was at my desk less than 50% of the time, mostly doing analytical work. The rest of the time was spent in the plant facilities, at machinery vendors, at seminars teaching and learning, or on worldwide trips installing or troubleshooting equipment at other facilities.

The master's and doctorate degrees allow an engineer to proceed into research and development or into university teaching. These degrees allowed me to teach in a university and to work in a government-sponsored scientific research facility. I was able to work on everything from sampling devices for a Martian lander to new machining and testing methods. The ability to provide locomotive design, ship system design, design for government projects and to select and troubleshoot equipment in the refining industry illustrate the flexibility of these degrees.

I chose to pursue these degrees because I enjoy learning new skills and also for my own satisfaction. My advanced degrees were paid for by the companies I was working for at the time, along with scholarships and teaching fellowships, so the education was cost-effective. I was pleasantly surprised with all of the additional benefits they brought me. Each advancement did increase my compensation, but I also could have achieved this by moving into a management role. I tried a position as Manager of Advanced Engineering, but quickly realized that I was more satisfied with technical work.

In the master's degree program, the thesis is a compilation of research that proves one is knowledgeable about the information learned throughout the graduate program. It is very different than a doctorate dissertation. I wrote my master's thesis on the topic of torsional vibrations, an area I was working on for my company at the time.

The doctorate program in engineering is a full-time, demanding program. The coursework is not the difficult part; the choice of dissertation is the key challenge. The intent of the dissertation is to contribute new knowledge to expand the understanding on a given subject in your field. The point is to come up with an entirely new concept, develop it and defend its worth. I wrote my dissertation on analytical modeling of the drilling process to develop a new drill. This modeling was needed and paid for by the company I was working for at the time.

Defending a dissertation before a committee of professors can be intimidating, and one must completely understand one's chosen subject and one's coursework. Luckily, I had a heavy interest in analytical modeling, which helped me immensely in deciding on and defending my dissertation topic.[1]

The selection of an academic advisor is also extremely important. In the unlikely event that the relationship does not take off, it is wise to seek another advisor before starting on one's dissertation. I was fortunate to have an excellent advisor who became a lifelong friend and helped me earn my doctorate in less than

3 yr. Some of my fellow students took 7 yr to complete their doctorate degrees with their advisors.

Advanced degrees can also create difficulties. In my case, I almost lost a very attractive job opportunity because the employer thought I was over-qualified. Only after someone in the hiring department noticed the hobbies listed on my resume, which showed my practical abilities and work history, did I obtain the position. Using my troubleshooting skills, I grew into a worldwide group leader for failure analysis for the company. When I retired after 20 yr with the company, I started my own consulting business doing similar work.[2]

Employment of mechanical engineers and engineers in general is projected to grow at 5% over the next 10 yr. Good jobs are always available for those who stay ahead of the most recent advances in technology and engineering skills.

It is difficult to predict the longer-term future in mechanical engineering. With the development of new computer systems and advanced technologies, the future will look much different than the present. When I started working in engineering 50 yr ago, personal computers were not available. What we have today would have seemed like science fiction back then. Now I can sit at my home computer and design a structure in a day that would have previously taken a month, a draft person and a technician or two.

In the future, we will probably have quantum computers with unlimited capacity and speed. Troubleshooting of equipment will be done using computer simulations, as will be the engineering involved for design. Equipment will be scanned, engineered and constructed using totally different technologies. FIG. 1 illustrates construction techniques, now in their infancy, totally performed by 3D scanning and printing using concrete or polymers as the printing ink and robotic construction.[3] Human organs will also be made in the operating room using bioprinting, with surgeries performed by robots. Some of these things are being done today, in a very simplified manner.

The point to all of this is that engineers will be part of this exciting future, and those with imagination and technical skills of all levels will always be in demand. HP

NOTE

Case 112 was published in *HP* May 2021. For past cases, please visit www.HydrocarbonProcessing.com.

LITERATURE CITED

[1] Sofronas, A., *Survival Techniques for the Practicing Engineer,* Wiley, Hoboken, New Jersey, 2016.

[2] Sofronas, A., *Unique Engineering Methods for Analyzing Failures and Catastrophic Events: A Practical Guide for Engineers,* Wiley, Hoboken, New Jersey, to be published in 2021.

[3] Sofronas, A., "Examining the creation of the universe and humankind into the far future, using research, scientific thought and visualization experiments," Amazon Publications, 2022.

TONY SOFRONAS, D. Eng, was the worldwide lead mechanical engineer for ExxonMobil Chemicals before retiring. He now owns Engineered Products, which provides consulting and engineering seminars on machinery and pressure vessels. Dr. Sofronas has authored several engineering books and numerous technical articles on analytical methods.

P. DONNELLY, AspenTech, Bedford, Massachusetts

Why EPC firms are accelerating digitalization

Even before the challenges of the COVID-19 pandemic emerged, engineering, procurement and construction (EPC) firms were already under considerable stress. Combining low net margins with the burden of carrying much of the project risk was resulting in general underperformance by the sector. When plant owner-operators announced capital spending cuts in the range of 20%–50%, it looked like engineering firms were about to enter another cyclical downturn. Interestingly, the management of these firms, with the hard-won wisdom gained in previous downturns, did not act as one might have predicted. Instead of immediate deep cuts to personnel, engineering firms looked for alternative ways to pare costs, such as cutting dividends, reducing bonuses and eliminating certain non-employee contractors.

While layoffs have not been completely avoided, these actions have mitigated the deeper reductions in the workforce that were seen in 2014–2015 and have also better positioned these firms to capitalize as a recovery slowly emerges. It is also worthy to note that, in addition to carefully managing cost reductions, certain investments have continued and even accelerated—most notably in digitalization. According to McKinsey & Company's 2020 report *The Next Normal in Construction,* two-thirds of the 400 surveyed EPC executives were accelerating their investments in digitalization. These managers and executives understand that smart investments in digitalization will help preserve core competencies and personnel, and, over the long term, protect their ability to compete as business conditions improve.

Often, the objectives of digitalization investments include streamlining software and technology portfolios, along with automating the flow of project data. This enhances collaboration internally and externally, while making data available for reuse across disciplines and project phases. In addition, many firms are now seeking to continue leveraging project engineering data to provide value-adding services in operations and maintenance. This can increase customer intimacy, while adding necessary and more stable revenues based on operating budgets. The digitalization of project data is a key enabler of these digital-twin-based services, which will be enhanced through a digital handover.

Four key challenge areas for EPC firms. Many EPC firms are well underway on their digital journey, while others are still in the planning phase. However, where are these investments going? Common digital initiatives can be categorized into four key areas. These include:

1. **Data management:** Digital technologies can play a hugely important role in helping EPC firms manage and move massive amounts of data more efficiently. This means a reduced reliance on physical documents to store and share information and making that information more available for review and use by others, as well as making it faster and easier to hand off to other disciplines, partners, vendors, owner-operators, regulators and other parties in the project ecosystem.
2. **Technology consolidation:** Many EPC firms have dozens (if not hundreds) of unique software solutions in the engineering department. Comprised of Tier 1 providers, niche commercial applications and engineers' homegrown applications, these types of solutions create a bird's nest of technology that prevents any real progress toward digitalization. By standardizing and reducing the overall number of software providers, eliminating redundancies, and using stricter criteria for the support of smaller niche apps, chief information officers (CIOs) and heads of engineering departments can simplify the landscape of the software that they rely on, while creating the conditions required for automating the flow of data.
3. **Apps and data integration:** Once the software portfolio is rationalized and consolidated, the work of integrating the remaining applications should start. Connecting the remaining apps with the intent of automating flow and reusing data should be the priority.
4. **Expansion of digital-twin-based services:** The engineering data used to design and build the plant can also be used to enhance startup, training and operations, while providing additional and diverse revenues for EPC firms. Examples might include the use of engineering tools to ensure that the models used for running the plant are accurate and up to date; that dynamic models and operator training tools ensure safe, profitable operations; and that predictive maintenance services maximize asset uptime.

Digital twins of the physical asset and its operating conditions are a marriage of the digital representation of the physical plant (e.g., equipment data) and the information about the process occurring within that physical equipment.

A digital twin can be viewed in three ways. The first is the plant digital twin, which provides equipment and process models of the plant, along with relevant cost data. These types of digital twins are typically used for plant design, debottlenecking and revamping, as well as for tuning of the asset during operations and maintenance. Plant digital twins can be

deployed offline and online and can be calibrated to plant operating conditions through autonomous model tuning. Used for equipment monitoring, operator open-loop advice or autonomous optimization, their scope may range from a single piece of equipment to an entire unit's operations (e.g., catalytic cracking), and to plant-wide (e.g., energy and utility systems) or enterprise-wide (e.g., risk models encompassing multiple plants and sites). They can be simulated dynamically to provide operator training.

The second type is the operational digital twin. This provides plant operations—from a business level all the way to the control level—that are modeled and virtually viewed as planning, scheduling, control and utility models. These twins inform business decisions such as crude selections and products trading. They also inform technical decision making, like optimizing quality, throughput, energy use, emissions compliance and safety.

The third type is the operational-integrity digital twin. This twin provides guidance on both tactical and strategic decisions around prescriptive maintenance, offering real-time recommendations to maximize uptime, adjust production to deal with failing equipment, minimize environmental impacts, mitigate production losses and prioritize safety. EPC firms can also assist the owner-operator in obtaining a future view of equipment and asset health, as well as risk profiles and root causes of failures, to improve overall uptime and operational integrity.

Increasingly, EPC firms are seeking to deliver digital twin-based services to their clients. Creating, delivering and maintaining these three types of twins make good use of engineering talent and resources, while adding considerable value to plant owners. They can enhance staff utilization and billings while increasing customer intimacy, which aids business development for new projects.

Digitalization successes. While some may be just beginning their digital journey, many firms have already seen notable successes with leveraging this digital engineering data. The following are a few examples.

Worley's digital platform[a] initiative is designed for speed without compromising the quality of the engineering work. It relies on digital information from concept and front-end engineering design (FEED) to inform a digital estimating platform that helps clients reach a final investment decision (FID) up to 50% faster. Benefits include expedited evaluation of concepts through process simulation software, automated artificial intelligence-driven 3D plant layout and piping designs, and coordinated estimates tied to the engineering information.

Hargrove Engineers + Constructors provides digital twin-based services that improve plant operations, profitability and reliability. The company provides digital twins that represent a virtualized copy of the historical, current and future behavior of the physical plant asset, along with the physical and chemical processes occurring within that plant, so their customers can improve throughput and quality, lower operating costs and increase equipment uptime.

Leveraging digital design and engineering tools, Burns & McDonnell created a digital representation of a conceptual plant design to quickly redesign a column from traditional design specifications to a more efficient divided wall column. The redesign was accomplished in a matter of hours instead of the normal weeks-long effort. This was only possible because the multidisciplinary team could collaborate around digital project information.

Takeaway. Prior to 2020, the majority of EPC firms were already embracing initiatives to digitalize areas of their businesses. With uncertain market conditions likely to continue into the foreseeable future, digitalization is accelerating and will fundamentally change the way EPC firms bid and execute project work, hand over projects to customers, and support projects throughout their operating lifespan. Digitalization also enables closer collaboration with owner-operators, which can drive significant new value for the entire ecosystem, while enhancing the quality and sustainability of the asset. HP

NOTES

[a] Worley's SpeedFEED

PAUL DONNELLY is the Director of Industry Marketing for AspenTech, where he is responsible for the company's engineering and construction business segment. Mr. Donnelly has more than 25 yr of global experience in engineering, construction and supply chain management. He earned a BS degree in geology, along with an MBA degree, from the University of Massachusetts.

R. CHUANG and A. FAN, CTCI Corp., Taipei, Taiwan

Execution features of modularization projects

Due to growing global environmental awareness in recent decades, the petrochemical industries have been seeking more cost-effective construction solutions. This initiative is an impetus to the adoption of modularization, which helps to provide safer working environments, improve quality and secure firm scheduling, as the prefabrication of modules is usually performed offsite in independent module fabrication yards to avoid interference with ongoing site activities.

While modularization provides a better solution for various issues regarding labor, budget or space, there are new aspects and criteria that must be considered. Dealing with complex project interfaces is becoming more of a challenge, since modularization involves multiple tasks working in parallel throughout the world. In this case, modularization project management involves more than just creating work timetables and schedules, managing and prioritizing construction work orders, and communicating with clients and stakeholders. Coordination between multiple taskforces and project locations becomes even more essential, and often requires more timely decisions or mitigations than are required for conventional construction projects.

This article will first introduce the advantages of modularization—a trend in today's demanding petrochemical industries—before delving into planning strategies. Using a mega-module project as an example, this article will discuss how such projects are planned and executed, along with typical challenges and how decisions are made under various project execution scenarios.

ADVANTAGES OF MODULARIZATION

The concept of modularization is to bring systematic integration to the systems that are originally intended to be installed at job sites by design, and to categorize them as module components and have them fabricated or tested separately based on refinery process requirements and productivity. Breaking project development into smaller programs at the early planning stage allows a variety of tasks to be conducted simultaneously in various locations. This shortens project duration, since fabrication, along with the assembly and testing of process modules, can be performed in parallel with onsite activities. Other benefits include better quality control, more efficient use of materials, reduced safety risks, a smaller field crew and less required space onsite. In addition, module preassembly units can be designed to accommodate specific locations or limited spaces. Such a flexible work scope provides owners the confidence to take on any project where geographical or climate conditions are far from ideal. The following is a further explanation of the advantages of modularization.

Improve project management flexibility. Modules for modularization projects are fabricated offsite, allowing site development and foundations to proceed simultaneously across countries and time zones (**FIG. 1**). Given that module fabrication is a time-consuming process that usually takes up nearly half of the entire project period, the engineering team can make good use of this fabrication period to finalize detailed designs and save some room for future adjustments on design changes due to specification alterations or owner instructions. This period also provides the procurement team with sufficient time to develop robust material delivery plans to prioritize supplies based on urgency or locations. Conversely, the construction team can focus more on setting up construction plans and raising safety awareness when commencing site activities.

Enhance fabrication safety and quality. Safety has always been the primary focus for every construction project, regardless of scale or properties. In modularization projects, module fabrication and preassembly are performed in independent module yards that offer established and safe working environments. By employing pancake and deck stack-up techniques, which is a typical module steel structure installation method, safety risks can be reduced. This can also help prevent process errors from occurring and eliminate defects in fabricated products, thus ensuring quality.

Optimize plant facility configuration. With modules being fabricated offsite, the work onsite becomes simpler, as most of the remaining work involves underground activities such as piles, foundations or underground piping. Proper module plan-

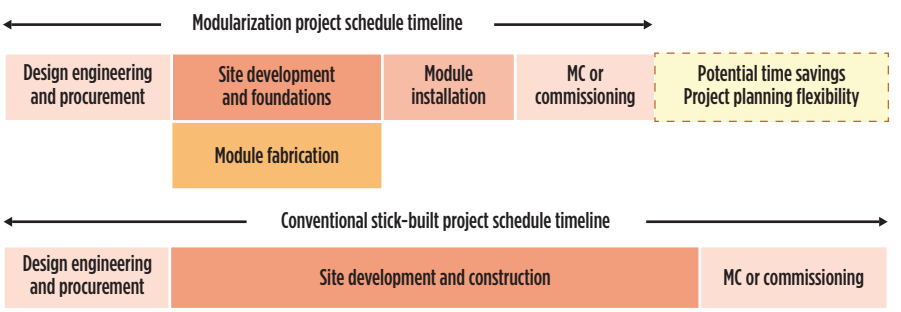

FIG. 1. Modularization vs. stick-built project schedule timeline.

ning leads to better space utilization. This is a huge benefit from an owner's point of view because the extra spaces saved can be used to install more facilities to improve future productivity.

Minimize the need for construction labor onsite. Modularization showcases the perfect solution for onsite labor shortage, which has long been a bottleneck in modern construction projects. By modularizing most of the process-related systems and equipment for preassembling and testing in the module yards, construction work hours can be significantly reduced. Such simplified site infrastructure configuration results in lower resource requirements for onsite labor and machinery, thus creating a more spacious work environment. This not only enhances safety and quality, but also helps improve work sequences and resource allocations throughout the project.

High level of adaptability to various environmental conditions. Modularization projects are less susceptible to unfavorable climate or geographical conditions since the process is performed in independent module yards. In addition, they are highly adaptable to changes, allowing adjustments or modifications to module engineering designs, such as for size and weight, structural reinforcement and fixation, module layout, heat insulation, and anti-corrosive or anti-rust coating treatments as required on job sites.

MEGA-MODULE PROJECT EXECUTION: EXPERIENCE AND STRATEGIES

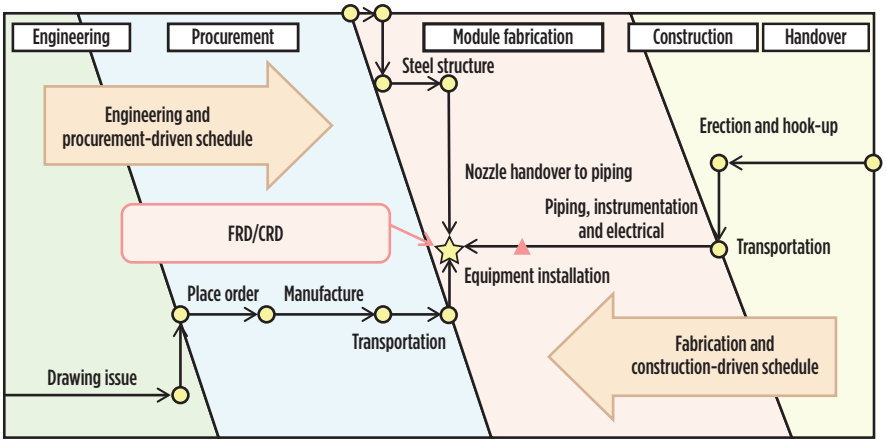

FIG. 2. The FRD and CRD are the most important dates in a project schedule.

The mega-module project that will be discussed here is the world's largest inland petrochemical refinery plant in Texas. It is owned by a JV of two international oil and gas companies that are looking to capitalize on domestic shale gas resources and supply. Once the plant begins operations, it is expected to produce millions of tons per year of mono-ethylene glycol (MEG), along with thousands of local job opportunities. The following will elaborate on the execution features of this mega-module project from three aspects:

1. Project control and schedule planning
2. Procurement and material management
3. Key highlights of module fabrication.

Project control and schedule planning. Successfully planning a modularization project depends on proper integration of work packages with engineering, procurement, fabrication and construction. To achieve this goal, project control aims to manage the following tasks:

- The engineering team supports the construction sequence and schedule
- Vendor-supplied equipment remains on schedule
- Materials are purchased and delivered to support construction
- Communication of specific work tasks is improved throughout the workforce—from the superintendent level through the craft ranks

TABLE 1. Schedule level of detail

Level	Engineering	Procurement	Fabrication	Construction
Level 1	**Milestone—Overall**			
	Model review	LLE	First cut	Air permit(s)
	Major drawing	Critical materials	Sail away	MC Level 1
Level 2	**Master project schedule—Discipline**			
	Primary steel	Static equipment	Steel fabrication and assembly	Foundation erection
	Secondary steel	Rotary equipment	Piping fabrication and erection	Piping fabrication and erection
	ISO drawing IFC	Package equipment	E&I installation	Module erection and hook-up
		Electrical and instrumentation (E&I) equipment		
		E&I bulk material		
Level 3	**EPC CPM network—Module and area**			
	Module discipline	Requisitions	Module discipline	Area discipline
	Area discipline			
Level 4	**Work package**			
	Engineering document index	Equipment and material item	Fabrication work package/deck	Construction work package

- Constraints such as craft availability, material laydowns, scaffolding and approvals for construction drawings are better managed
- Work toward closeout and turnover is better controlled.

In a project, the fabrication required date (FRD) and construction required date (CRD) are of paramount importance. These are the dates on which all engineering drawings and material deliveries are based to meet the project's fabrication and erection requirements in the yard, as well as the construction sequences onsite.

FRD/CRD planning includes the following steps (**FIG. 2**):

- Identify the delivery dates of equipment, materials and engineering deliverables
- Monitor the delivery status to fulfill fabrication and construction requirements
- Obtain management approval for any CRD delays after the schedule engineer updates the delivery schedule
- Inspect or analyze materials, scope, etc., before feeding back to Level 3 and Level 3.5 fabrication or construction schedules.

Module steel structure pancake and deck stack-up are critical to a modularization project. Due to size and weight restraints, equipment on each deck must be installed before the upper deck can be stacked. If major equipment or equipment located at critical locations cannot be installed before deck stack-up, then follow-up work will be delayed. In terms of schedule planning, very few differences exist between modularization and stick-built projects from Level 1 to Level 3. The only difference is Level 4, where fabrication is controlled by each deck of the module (fabrication work package) and procurement is controlled by individual equipment and material items on each deck. Schedule levels are detailed in **TABLE 1.**

Procurement and materials management. Materials management is more complicated in modularization projects because numerous fabrication and construction tasks are performed concurrently in various locations. The challenge lies in selecting suppliers based on their high-value supplies and countries—along with their logistics arrangements, which would greatly affect the workforce in both the module fabrication yards and construction job sites.

Two main strategies were adopted in this mega-module project. The first was vendor pre-bidding. Pre-bidding meetings were scheduled at early stages to introduce solicitation documents and to finalize technical terms and project requirements in exchange for merchandise specifications from interested and prospective bidders. This process helped expedite the technical review process of contractual and vendor documents. By acquiring vendor data as early as possible, engineering design and follow-up work could proceed smoothly.

The second strategy was collaborating with Asian suppliers. The project teamed up with a mega-module fabrication yard in China, which is a conceivable strategy, given that China is where most of the fab-

rication work is concentrated. Therefore, suppliers from local or adjacent countries with high marketing competency (e.g., Taiwan, Japan, Malaysia, India, Thailand and Korea) were listed as strong candidates (TABLE 2). Shorter shipping periods are advantageous for making solid material delivery plans based on fabrication and construction priorities. In addition, shorter shipping periods can also help avoid construction delays due to unexpected material damage and/or design changes by calling up nearby suppliers to cover material shortages.

Module fabrication highlights. To increase efficiency, modularization project planning involves engineering design and fabrication working in parallel. For example, steel structure shop drawings and first cuts in the module yard can be initiated following the completion of primary drawings. This makes weight control management one of the key highlights in the project.

Weight control management starts from the input of engineering data into modeling software based on several design factors. Changes in these variables can affect the quantities and locations in the module layout. The data can be updated accordingly in the modeling software and recorded in the weight control report, which tracks changes in the module's weight, size and gravity from the early project planning period to module completion and sail-away. This provides a solid input basis for arranging transportation and site construction planning.

Choosing a module yard is another key highlight. The basic requirement is adequate fabrication working space and workforce resources. Other considerations include the yard's geographical location, past achievements, affiliated facilities (including indoor/outdoor blasting and painting areas), warehousing, and storage and quay capacities. Facility capacity will directly impact the yard's productivity and stability, while geographical location will determine the accessibility of material coordination and flexibility of transportation planning. It would also help rule out regions with unpleasant environmental conditions that may disrupt or even jeopardize works. A yard's past achievements would serve as strong evidence for its performance and capability and can be used as a reference for decision making. In addition, choosing a module yard located in free-trade or tax-free zones will be beneficial, as custom tariffs can be exempted.

Takeaway. In many aspects, modularization gets the best out of the traditional stick-built construction method, and offers the advantages of improving safety, quality, resource utilization and manageability (TABLE 3). Additionally, it sets a perfect example of how teamwork from various specializations can help speed up a project. HP

TABLE 2. Primary high-value supplies from Asian countries

Country	High-value supplies
China	Pipes, fittings, flanges, pressure vessels, cables and electrical equipment
India	Pumps and noise enclosures
Japan	Compressors and heat transfer equipment
Korea	Reactors, fittings, flanges, high-pressure vessels and heat transfer equipment
Malaysia	Pressure vessels, cables and electrical equipment
Taiwan	Carbon steel/stainless-steel (CS/SS) plates, CS/SS welded pipes, pressure vessels, instruments, cables and electrical equipment
Thailand	Pressure vessels and electrical equipment

ROGER CHUANG is a Project Manager for CTCI Corp.'s hydrocarbon business operations. He has more than 15 yr of experience in the refining and petrochemical industries. Mr. Chuang earned an MEng degree in civil engineering and construction management from National Chiao Tung University, Taiwan.

ALEX FAN is a Project Control Engineer for CTCI Corp.'s hydrocarbon business operations. He has 5 yr of experience in the refining and petrochemical industries. Mr. Fan earned an MEng degree in railway engineering and a BS degree in civil engineering from National Taiwan University, Taiwan.

TABLE 3. Modularization project execution cost-saving initiatives

	Expected benefits			
Item description	Design safety and efficiency	Reduced site workforce	Cost savings	Schedule critical
Leverage suppliers from emerging markets		X	X	X
Fully utilize JV partners' frame agreement			X	X
Process modules simultaneously		X	X	X
Install column internals at fabrication yard		X	X	X
Leverage modular experienced labor			X	X
Maximize fabrication yard pre-commissioning/commissioning		X		X
Utilize one integrated, vertical subcontractor				X
Maximize utilization of module offloading facility (MOF) and self-propelled modular transporter (SPMT)			X	
Maximize precast and preassembly offsite	X	X	X	X
Move the temporary construction facility to the construction worksite		X	X	
Optimize large-scale crane utilization			X	X
Minimize scaffolding erection	X	X	X	X

F. BAARS, Fluor, Amsterdam, Netherlands; and
S. ORUGANTI and **P. KALIA,** Fluor, New Delhi, India

Oil refinery/petrochemical integration in a CO_2-constrained world—Part 1

Petrochemical demand will increase with gross domestic product, while motor fuel demand will only show modest growth and may even decline in certain regions, given environmental/legislative pressure and the introduction of battery-powered electric vehicles. Any new oil refinery will likely include petrochemical facilities, as well. This article evaluates several configurations, highlighting salient differences between them (including economics) and assessing their sensitivity to product and feed price fluctuations, cost of utilities, type of crude and a carbon dioxide (CO_2) tax. These options are evaluated complex-wide as the only way to ensure that schemes are compared on a consistent basis and that all interactions and synergies between units are considered.

While the scenarios and investment costs are based on new facilities, the methodology could equally be applied to revamp projects where options to expand refinery operations with petrochemical units are being considered, along with the revamp costs of existing assets.

The base case refinery scheme includes either a residue fluid catalytic cracking unit (RFCCU) or a hydrocracking unit (HCU). The feed to the RFCCU comes from an atmospheric residue desulfurization (ARDS) unit. The hydrocracker schemes include a delayed coking unit (DCU) or residue HCU (RHCU) as a residue conversion unit. The complex includes motor fuel (Euro-5 gasoline and diesel) and jet fuel production. Where required, ethyl tertiary butyl ether (ETBE) is imported as a gasoline pool component. In some cases, fuel-oil components are produced.

The petrochemical facilities produce base petrochemicals such as polyethylene (PE), polypropylene (PP), butadiene, benzene and paraxylene (PX). The complex includes a hydrogen production unit (HPU)—based on steam reforming—to balance the refinery's hydrogen demand.

The complex processes 10 MMtpy of Urals crude, priced at $70/bbl. The complex will only import natural gas (for process and utility heater service, as well as for hydrogen production), electric power and raw water.

The economic evaluation depends on the prices of raw materials, products and utilities, as well as the unit prices of steel and the costs of construction, labor, etc. The economic analyses detailed in this article are more representative of the differences between certain schemes, rather than of being correct in the absolute sense.

Part 1 introduces the various configurations and how they compare based on investment cost, gross and net margin, and internal rate of return (IRR). Part 2, which will be featured in the August issue of *Hydrocarbon Processing*, will discuss crude effects, CO_2 emissions and the impact of a CO_2 tax on IRR.

RFCCU alternates. The RFCCU is a propylene-optimized unit, with approximately 17 wt% of C_3= from the RFCCU reactor. The RFCCU feed is pretreated in an ARDS unit, taking atmospheric residue directly from the crude distillation unit (CDU). The complex includes ETBE and alkylation units to facilitate Euro-5 gasoline manufacturing. In case of isobutane (iC_4) insufficiency for the alkylation unit, a C_4 isomerization unit processing RFCCU and other refinery butanes is included. The petrochemical extensions include the addition of a PP unit to process polymer-grade propylene from the RFCCU (Case A1) and an aromatics complex (Case A2). The PP unit consists of two trains. An ethylene recovery unit (ERU)—recovering ethylene from FCCU dry gas—is included for cases A1 and A2, with the ethylene co-feed to the PP unit to also produce impact and random co-polymers; excess ethylene is sold. In Case A2, the reformate is sent to the aromatics complex. The raffinate from the aromatics units is used for gasoline blending. **TABLE 1** provides an overview of the units considered under the various schemes.

A graphical depiction of scheme A2 (RFCCU, PP unit and aromatics complex) is shown in **FIG. 1,** with traditional refinery units in green (and blue for the residue conversion units) and with petrochemical units in yellow or pink (aromatics).

The evaluation results are detailed in **TABLE 2.** Gross margin is the value of the products sold minus the cost of all feeds purchased. Net margin in this article is the gross margin minus the cost of utilities, catalyst and chemicals. Investment cost includes the total engineering, procurement and construction (EPC) cost of the complex, excluding the owner's cost. Simple payback is the straightforward calculation of the total EPC investment cost against the net margin, based on a complex operating 8,400 hr/yr. All costs are based on Western European costs in 2019. IRR is based on an 8% weighted average cost of cash, 2% inflation, a yearly maintenance cost of 1% of investment costs, a 4-yr construction period, and a project life of 20 yr. Petrochemicals output is the sum of polyolefins, benzene, PX, propylene and ethylene production.

Adding petrochemical units increases the gross margin. Adding a PP unit increases the gross margin by $52/t and the net margin by $40/t (Case A1), comfortably paying for the $676 MM higher capital cost (with the PP unit consisting of two trains), and

TABLE 1. RFCCU permutations and overview of process units

	A0	A1	A2
Case	**RFCCU**	**RFCCU + PP unit**	**RFCCU + PP unit + aromatics complex**
CDU	X	X	X
Naphtha hydrotreating (NHT) unit	X	X	X
Continuous catalytic reforming (CCR) unit	X	X	X
Isomerization unit	X	X	X
Kerosene hydrotreating (KHT) unit	X	X	X
Diesel hydrotreating (DHT) unit	X	X	X
Atmospheric residue desulfurization (ARDS) unit	X	X	X
RFCCU, including FCC gasoline hydrodesulfurization	X	X	X
ERU		X	X
ETBE manufacturing	X	X	X
Alkylation	X	X	X
C_4 isomerization	X	X	X
HPU	X	X	X
PP unit(s)		X	X
Aromatics complex			X
Sulfur block (sour water stripper, amine regeneration unit and sulfur recovery unit)	X	X	X

TABLE 2. RFCCU permutations when processing 10 MMtpy of Urals crude, with no CO_2 tax

	A0	A1	A2
Case	**RFCCU**	**RFCCU + PP unit**	**RFCCU + PP unit + aromatics complex**
ETBE imports, t/hr	0	0	0
Gross margin, $/t crude	113	165	192
Net margin, $/t crude	84	124	148
Investment, $MM	5,163	5,839	6,428
Simple payback, yr	6.1	4.7	4.3
IRR, %	12.4	16.5	18
Petrochemicals, % of crude	7	9	18

with IRR increasing from 12.4% to 16.5%. Adding an aromatics complex—using reformate as feedstock—further improves the economics (Case A2). The petrochemicals output increases to 18%. In addition, processing FCC gasoline in the aromatics unit has little economic benefit, as it produces less aromatics relative to the reformate, while simultaneously causing the need for more reformate in the gasoline pool to compensate for the loss of FCC gasoline. In this case, FCC gasoline would most likely also require complete hydrotreatment to remove olefins—thus further increasing investment and operating costs, which hurts economics.

HCU alternates. The base case refinery now includes a DCU, along with a middle-distillate-oriented HCU processing the DCU heavy gasoil and straight-run vacuum gasoil from the vacuum distillation unit (VDU). The refinery was subsequently expanded with a steam cracker complex—including pygas hydrotreating, butadiene extraction and polyolefin units—and an aromatics complex. Hexene-1 is imported as co-feed to the PE unit. A full overview of the units included in the evaluation is shown in TABLE 3. A graphical depiction of Case B3 is shown in FIG. 2.

Key results of the evaluation are detailed in TABLE 4. The percentage of petrochemicals on crude is negative when more ETBE is imported than the sum of the petrochemical products sold.

The steam-cracking schemes (Cases B1–B3) include pygas saturation and ETBE production to facilitate Euro-5 gasoline production. Adding alkylation to process the remaining C_4=s is not beneficial, as it would deprive the steam cracker of i+nC_4s. The reduction of petrochemicals does not compensate for the higher gasoline production. Ethylene and propylene are worked up to their respective polymers in generic PE and PP units. These units now consist of multiple trains. Case B2B includes two steam cracker units. The light naphtha isomerization unit disappears for Cases B1–B3, as the C_5–C_6 material is sent to the steam cracker, but it reappears with cases B4 and B5 (TABLE 3).

Expanding the base case (B0)—the DCU/HCU refinery with petrochemical production units—has the potential to more than double (and possibly triple) the gross margin (TABLE 4). However, operating and investment costs increase, as well. The base case is penalized by the high cost of ETBE imports, which is an inherent feature of the DCU/HCU refineries that produce Euro-5 gasoline.

Adding a steam cracker complex to the base refinery (Case B1) improves economics. The steam cracker is a mixed-feed cracker, processing all fuel gas and LPG streams, as well as light naphtha and the bulk of heavy naphtha. The gasoline pool predominantly consists of hydrotreated pygas and ETBE; some reformate is still needed to meet octane specification. Relative to the base case, gasoline production is reduced by approximately 70%.

While gross margin increases by $100/t of crude [from $94/t (Case B0) to $194/t (Case B1)], the net margin only increases

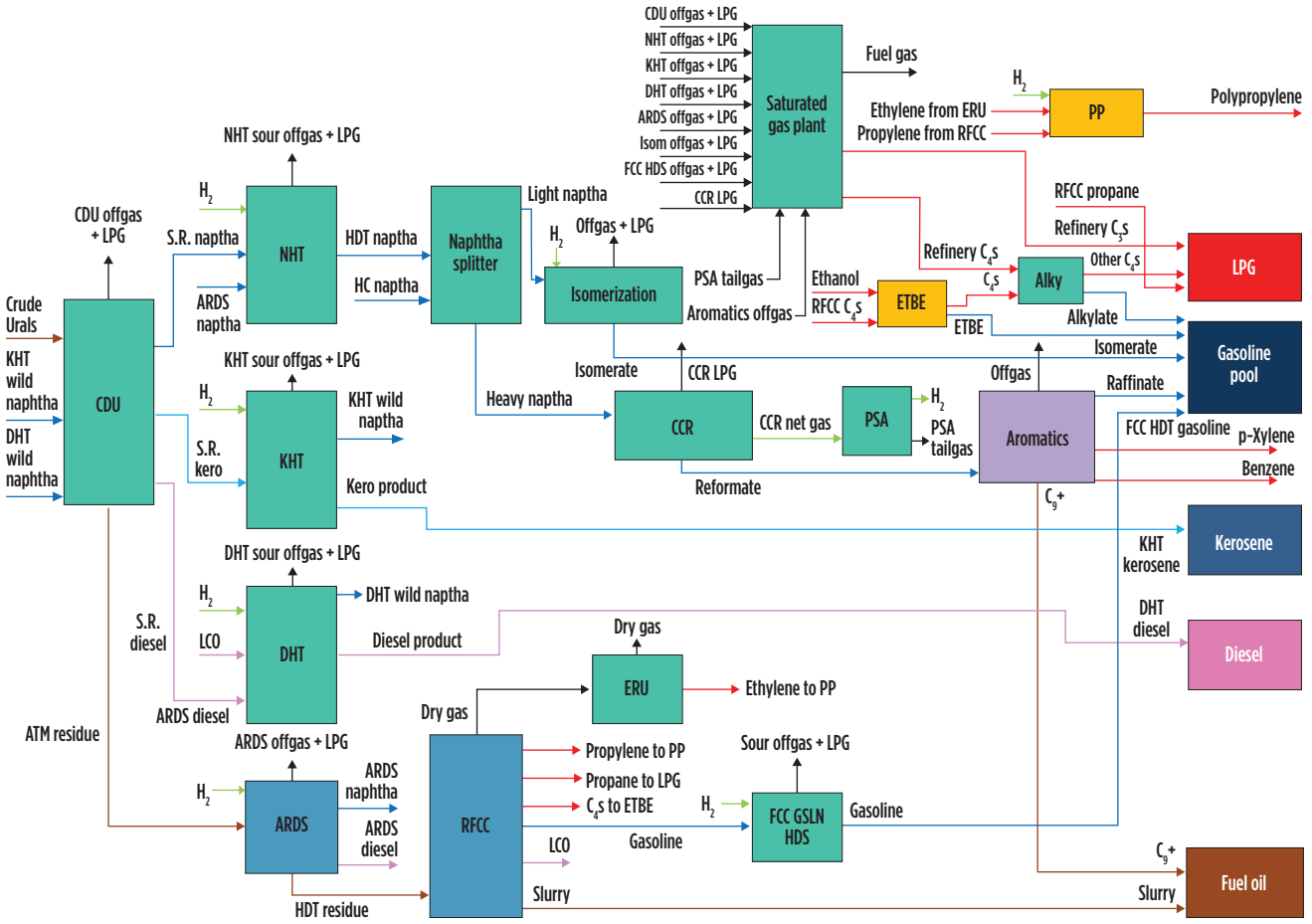

FIG. 1. Block flow diagram of Case A2: An RFCCU, along with a PP unit and an aromatics complex.

by $64/t of crude (from $61/t to $125/t), which is still enough to compensate for the 85% increase in investment cost (from $4.16 B to $7.7 B). IRR increases from 11% to 12.4%.

The value of the steam cracker was further explored by increasing the naphtha flow to the unit, with the additional naphtha produced by the HCU converted to naphtha operation, which produces nearly four times as much naphtha vs. the base case (Case B2A). The gross margin increases from $194/t to $252/t. However, the increase in net margin from $125/t to $151/t does not pay for the higher investment (from $7.7 B to $10.1 B), with IRR decreasing from 12.4% to 11.2%. The petrochemicals output rises to 24% of crude. In addition, sending atmospheric and light coker gasoils to the naphtha hydrocracking unit (NHCU) (Case B2B) further increases the petrochemicals output to 35%, but with poorer economics.

Adding an aromatics complex—with or without a steam cracker—in the scheme (Cases B3 and B4) substantially improves economics, with IRR increasing from 12.4% (Case B1) to 14.1% and 15.4% for Cases B3 and B4, respectively. Despite the lower margin, the case without the steam cracker (i.e., Case B4) has the better economics on account of the lower investment. The gasoline pool properties can only be met by importing supplemental ETBE and sending some reformate to the pool. The petrochemicals output for Cases B3 and B4 is now 37% and 17% of crude, respectively.

In Case B5, the DCU has been swapped for an RHCU, based on slurry technology. Relative to Case B4, the gross margin improves $22/t. This decreases to $17/t on a net margin basis. The RHCU's catalyst cost is a major contributor to the higher operating cost. IRR further improves to 17.7%.

Based on IRR, Case B5—which includes a slurry RHCU that processes the same feed as the DCU previously, along with an HCU geared toward naphtha production and an aromatics complex—has the best economics of the evaluated HCU cases.

Comparisons and sensitivities to product/utility pricing. As a reference case, the obtained IRR results are reported in the first column of **TABLE 5.** The RFCC cases (Cases A0–A2) typically yield better returns than the HCU and NHCU cases (Cases B0–B4) (see also **FIG. 3**). The DCU+HCU case (B0) is penalized by the higher import of ETBE (**TABLE 4**). Adding a steam cracker to the HCU (Cases B1–B2B) does not close the IRR gap with the FCC cases.

Due to the higher capacity of the aromatics complex and the higher naphtha production from the NHCU, adding an aromatics unit is more attractive in an NHCU (moving from Case B2A to Case B3 increases IRR by 2.9%) vs. an RFCC-based configuration (moving from Case A1 to Case A2 increases IRR by 1.5%).

The combination of an RFCC, PP and aromatics complex

TABLE 3. DCU and HCU permutations and overview of process units

Case	B0	B1	B2	B3	B4	B5
	DCU + HCU	DCU + HCU + steam cracker	DCU + NHCU + steam cracker	DCU + NHCU + steam cracker + aromatics complex	DCU + NHCU + aromatics complex	RHC + NHCU + aromatics complex
CDU/VDU	X	X	X	X	X	X
NHT	X	X	X	X	X	X
CCR	X	X	X	X	X	X
Isomerization unit	X				X	X
KHT unit	X	X	X	X	X	X
DHT unit	X	X	X	X	X	X
HCU	X	X				
Naphtha hydrocracking unit (NHCU)			X	X	X	X
DCU	X	X	X	X	X	X
RHCU						X
HPU	X	X	X	X	X	X
Steam cracker complex (includes butadiene extraction and first-stage pygas hydrotreating)		X	X	X		
PE unit		X	X	X		
PP unit		X	X	X		
Pygas saturation		X	X	X		
ETBE		X	X	X		
Aromatics				X	X	X
Sulfur block (sour water stripper, amine regeneration unit and sulfur recovery unit)	X	X	X	X	X	X

TABLE 4. DCU and HCU permutations when processing 10 MMtpy Urals crude, with no CO_2 tax

	B0	B1	B2A	B2B	B3	B4	B5
Case	DCU + HCU	DCU + HCU + steam cracker	DCU + NHCU[a] + steam cracker	DCU + NHCU[b] + steam cracker	DCU + NHCU + steam cracker + aromatics complex	DCU + NHCU + aromatics complex	RHCU + NHCU + aromatics complex
ETBE imports, t/hr	68	0	0	0	19	13	15
Gross margin, $/t crude	94	194	252	312	266	150	172
Net margin, $/t crude	61	125	151	171	165	109	126
Investment, $MM	4,160	7,700	10,132	14,097	9,100	5,540	5,561
Simple payback, yr	6.8	6.2	6.7	8.2	5.5	5.1	4.4
IRR, %	11	12.4	11.2	8.3	14.1	15.4	17.7
Petrochemicals, % crude	-6	13	24	35	37	17	17

[a] NHCU hydrocracking aimed for maximum naphtha production.
[b] Gasoils to the NHCU

(Case A2) has the highest IRR, followed closely by the RHCU, NHCU and aromatics complex (Case B5). The economics depend on the pricing scenarios under consideration. Higher petrochemical prices (an additional 20% relative to the other feed/product and utility prices) greatly improve the economics of the schemes having a high petrochemical output (see FIG. 4 and TABLE 5). IRR is 4%–7% higher as petrochemicals output increases to 20%–40%. With an IRR near 22%, the combination of an RFCCU, PP unit and aromatics complex (Case A2) ranks at the top of the list.

If fuel gas costs are halved, IRR improves between 6% and 33% for all cases, with the high natural gas import cases (B0, B2A and B2B) benefiting IRR the most (TABLE 5). Relative to the reference case, if electricity prices are halved, IRR improves between 5% and 20% (Case B2B).

The effect of electricity and fuel gas prices on economics is most pronounced with the combinations having a high electricity and/or thermal demand. However, the ranking of the cases may change with different assumptions. Whereas Case A2 ranks best in the reference case and Case A2, for example,

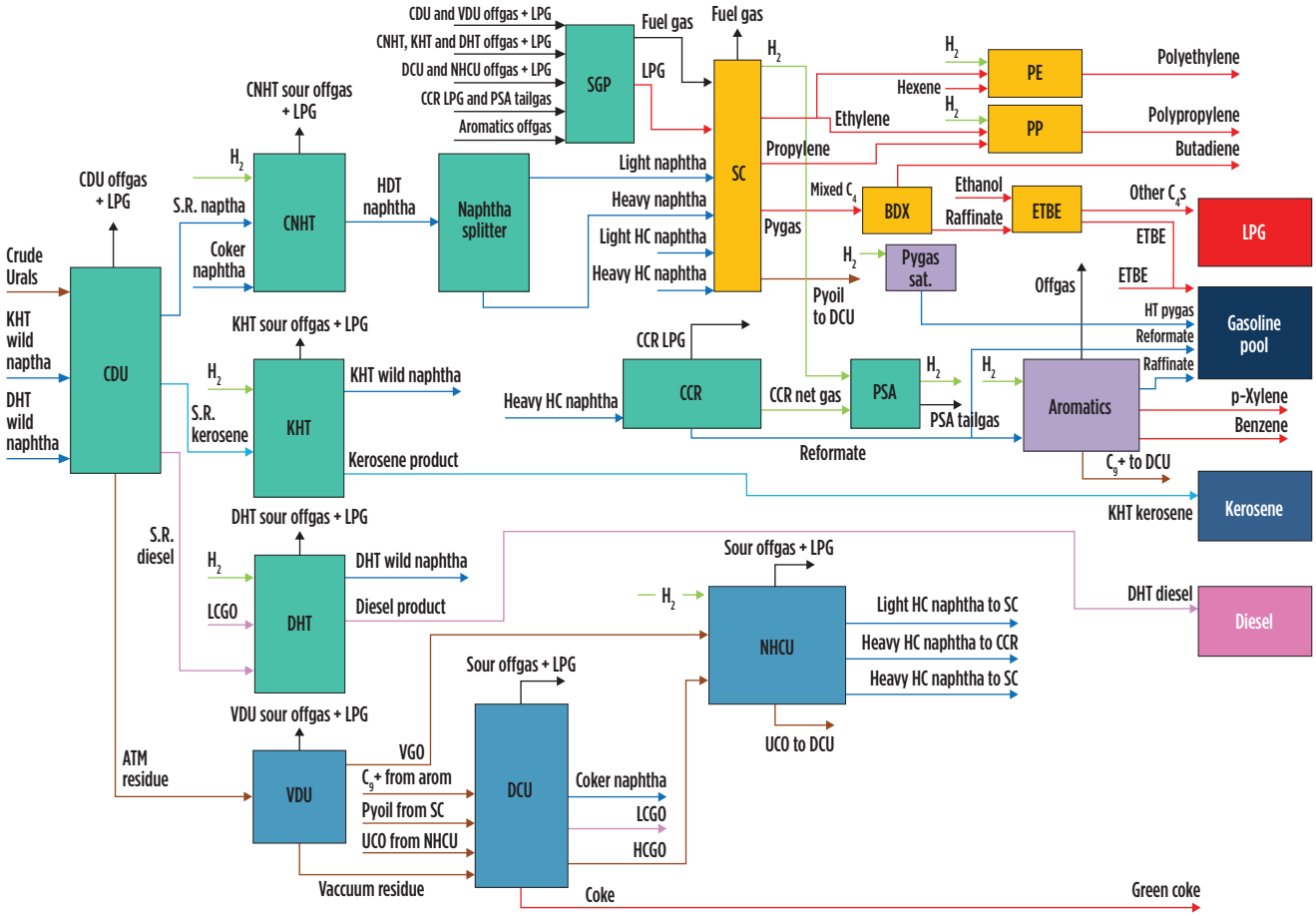

FIG. 2. Block flow diagram of Case B3: An NHCU, along with a steam cracker and an aromatics complex.

still looks best in the high petrochemical price scenario, Case B5 looks best in a scenario of lower fuel gas prices. In case of low electricity prices, Case A2 ranks the highest.

All units have typical fuel gas, steam and electricity consumption levels. No effort has been made to increase electricity consumption by changing steam turbines to electric drives or by considering electric heaters.

Options for further increasing the petrochemical value chain. Making specialty chemicals and/or expanding petrochemicals production will further increase petrochemicals output and/or profitability. Some of the options to be considered include:

- Converting C_4= and recycling it within the steam cracker
- Sending pygas to the aromatics unit
- Sending hydrotreated pygas/raffinate to the steam cracker
- Only producing gasoline blend components
- Incorporating a propane dehydrogenation unit to produce additional propylene
- Adding metathesis to convert C_4= (with C_2=) to propylene and then to PP
- Forward integration with the following:
  - C_2=s processed to glycol and its derivatives and/or polyvinyl chloride
  - C_3= to propylene-oxide and/or its derivatives, which include acrylic acid and acrylonitrile
  - C_3=s and C_4=s to oxo alcohols
  - C_4=s processed to methyl ethyl ketone
  - Butadiene to synthetic rubbers.

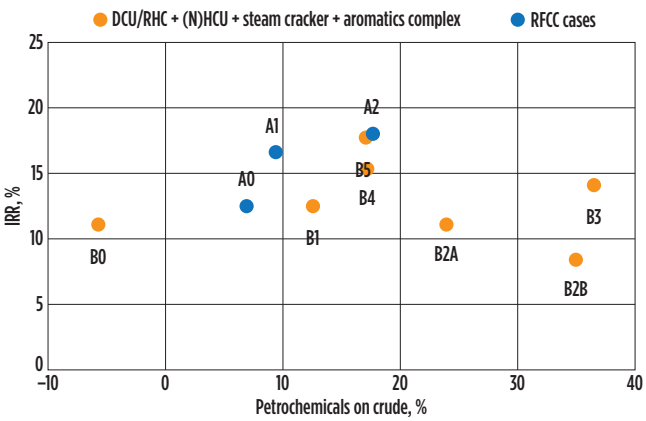

FIG. 3. IRR vs. petrochemicals on crude (%).

Takeaway. Any new refinery complex should integrate petrochemicals manufacturing to produce both transportation fuels and base petrochemical materials. Existing refineries will need to review their options to expand into petrochemical production or integrate with neighboring petrochemical plants.

TABLE 5. Sensitivities: IRR variation with changes in petrochemical pricing and the costs of fuel gas and power (the best scorer is in green, with the runner-up highlighted in yellow and the lowest score in red)

	Case		Reference case	Petrochemicals prices + 20%	Fuel gas at 50% of base case cost	Power at 50% of base case cost
RFCC	A0	RFCCU	12.4	12.2 (−2%)	13.5 (+9%)	13.4 (+7%)
	A1	RFCCU + PP unit	16.5	19.1 (+15%)	17.8 (+8%)	17.5 (+6%)
	A2	RFCCU + PP unit + aromatics complex	18	21.9 (+22%)	19.1 (+6%)	18.9 (+5%)
DCU	B0	DCU + HCU	11	8.6 (−22%)	13.5 (+23%)	11.9 (+8%)
	B1	DCU + HCU + steam cracker	12.4	16 (+29%)	14.7 (+19%)	13.5 (+9%)
	B2A	DCU + NHCU + steam cracker	11.2	16.5 (48%)	13.6 (+22%)	12.6 (+13%)
	B2B	DCU + NHCU + steam cracker, gasoil to NHCU	8.3	14.5 (+75%)	11.1 (+33%)	9.9 (+20%)
	B3	DCU + NCHU + steam cracker + aromatics complex	14.1	20.7 (47%)	15.7 (+12%)	16.5 (+17%)
	B4	DCU + NHCU + aromatics complex	15.4	19.9 (+29%)	17.2 (+12%)	16.3 (+6%)
RHCU	B5	RHCU + NHCU + aromatics complex	17.7	21.8 (+23%)	19.4 (+10%)	18.6 (+5%)

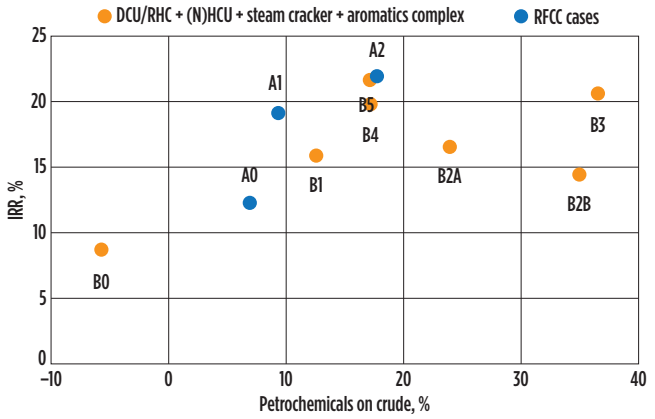

FIG. 4. Impact of 20% higher petrochemical prices on IRR.

Part 1 of this article explored several possible grassroots configurations, including an RFCCU, DCU or RHCU—the latter two combined with a vacuum gasoil hydrocracker. The key petrochemical units included a steam cracker with downstream PE and PP units, as well as an aromatics complex.

While it is theoretically possible to produce large amounts of petrochemicals, it may not always result in better economics, as shown within the confines of this study and regarding market circumstances. A DCU—combined with a naphtha-oriented hydrocracker that processes middle distillates with the bulk of the gases, LPG and naphtha sent to a steam cracker with downstream polyolefin units—can produce nearly 40% of petrochemicals from crude for a refinery processing Urals crude. However, in this study, a propylene RFCC-based refinery with an aromatics complex yielding 23% of petrochemicals from crude has better economics.

FCC-based schemes typically have better economics than DCU/RHCU/HCU-based schemes. However, this depends on many factors. Other than feed/product and utility pricing, it also depends on the design under consideration. For example, for a light crude, DCU/RHCU-based configurations may be more attractive, as will be detailed in Part 2.

This comparison is based on commercially available technologies and does not consider technology developments, which continue unabated. In general, the more-integrated schemes with a high petrochemical output are more robust to changes in feed/product and utility pricing. Higher petrochemical production is possible by ceasing Euro-5 gasoline production (allowing more naphtha to be sent to the aromatics complex or used as feed for the steam cracker), or by using pygas as aromatic feedstock, routing hydrotreated pygas and/or raffinate to the steam cracker, changing unit operations (higher RFCCU severity to produce more C_3=) or adding other units (e.g., metathesis). These projects can be implemented stepwise, with petrochemical units being built in a second phase. Processing bio-based materials and/or streams from plastics recycling plants presents another opportunity to improve economics and sustainability.

The conclusions drawn in this analysis are based on a particular crude diet, feed and product pricing, as well as on operating and investment costs, and could change depending on local circumstances. Feedstock flexibility, along with robustness for feed/product pricing changes, combined with a proper assessment of risks and opportunities associated with each investment, should be part of a proper evaluation. HP

FRED BAARS is a Senior Process Director with Fluor's Energy and Chemicals business line. He has more than 35 yr of experience in refinery operations and processes, and in executing and managing refinery projects in all phases of execution. Mr. Baars was named a Fluor Fellow in 2005.

SRINIVASA ORUGANTI is a Process Director with Fluor New Delhi. He has more than 28 yr of experience in process engineering. Mr. Oruganti previously worked at Uhde India Pvt. Ltd. He earned a BTech degree in chemical engineering from Andhra University and an MTech degree in industrial engineering and management (IE&M) from the Indian Institute of Technology (IIT) in Kharagpur, India.

PARVEEN KALIA is a Linear Programming Modeling Specialist with Fluor New Delhi. He has more than 15 yr of experience in process engineering design for petroleum refinery and chemical plants. Mr. Kalia worked for 5 yr with Reliance Industries Ltd. before joining Fluor. He earned a Bch degree in chemical engineering from Panjab University in India.

A. CHAUDHARI and M. KULKARNI,
BASF Chemicals India Pvt. Ltd., Mumbai, India

Evaluation of high-strength steel SA-517-Gr-F for large pressure vessels

Conventionally, carbon steel material has been widely used around the globe for the fabrication of static equipment—such as tall towers, vessels, heat exchangers, etc.—for less-corrosive service. This material is generally procured in a normalized or quenched and tempered condition to gain benefits towards an exemption from impact test requirements and to obtain a refined grain structure.

In this work, the effect of using a high-strength, low-alloy material SA-517-Gr-F has been studied as an alternative to the conventionally used carbon steel SA-516-Gr-60/70, specifically for large towers in a seismic prone zone and extreme weather conditions. The composition of SA-517-Gr-F is ¾ nickel (Ni)-½ chromium (Cr)-½ molybdenum (Mo-V). The alloying elements are present in very low percentages and this material has a very high mechanical strength. Therefore, it is termed as high-strength, low-alloy steel. The composition of SS 304L is 18 Cr-8 Ni. The alloying elements are present in higher percentages, which improves their corrosion resistance property against SA-517-Gr-F.

In this work, literature on the use of SA-517-Gr-F has been checked in terms of machinability and fabrication, along with commercial factors. Also, fabrication challenges and limitations have been identified by consulting renowned pressure vessel fabricators.

SA-517-Gr-F is a high-strength alloy material that can be explored as an alternative to normal carbon steel (SA-516-Gr-60/70) owing to its very high ultimate tensile strength and, therefore, its higher allowable stresses. **TABLE 1** presents further details. These allowable stresses remain constant for a wide range of temperatures. The difference in thicknesses between SA-517-Gr-F and SA-516-Gr-70 are in the range of 50%–80%, based on design temperature. Recently, the application of SA-517-Gr-F seems to be limited in the industry. The constraints that limit the use of this material have been studied technically as well as commercially.

In this work, the use of SA-517-Gr-F has been holistically explored, and conclusions and key observations have been detailed.

Discussion. The selection of appropriate material of construction (MOC) for the design and fabrication of any pressure vessel is crucial. These are regulated by many factors, including:

- Type of service
- Fluid in contact
- Corrosivity of the fluid
- External environmental factors
- Availability of the material
- Economics (cost of the equipment)
- Overall weight
- Machinability and weldability of material.

The most widely used MOC in the design and fabrication of static equipment is carbon steel—SA-516-Gr-70 (ASME SEC II Part D).[1] However, in specific cases, SA-517-Gr-F (ASME SEC II Part D)—an alternative for SA-516-Gr-70—should be evaluated for reduction in thicknesses and optimization in overall weight. This leads to an overall reduction in associated costs like logistics, transportation, installation (erection) and required civil structure or foundation.

SA-517-Gr-F is evaluated for static equipment with a base MOC of carbon steel and:

- Large static equipment (specifically, large inside diameter)
  - Spheres
  - Large process columns
  - Reactors
- High-pressure equipment
- High-temperature service
- Very high external loads, wind or seismic.

INLFUENCING FACTORS

Type of service. It is imperative to match the most optimal MOC with the type of the service handled by the equipment.

TABLE 1. Comparison of SA-516-70 and SA-517-Gr-F

Parameters	SA-516-Gr-70	SA-517-Gr-F
Type	Carbon steel	Low-alloy, high-strength ¾Ni-½Cr-½Mo-V
Uns	K02700	K11576
Size limitation	No limitation	Available up to 65 mm only
P no.	1	11 b
PWHT requirement	Mandatory over 38 mm	Mandatory over 15 mm
Minimum tensile strength	485 MPa	795 MPa
Minimum yield strength	260 MPa	690 MPa

This can be classified as sour [wet hydrogen sulfide (H_2S)], amine, caustic, etc.[2] Numerous allied factors exist, such as the nature of the fluid's corrosivity in contact with the inner surfaces of the equipment.

SA-517-Gr-F can withstand mild corrosive applications with a suitable internal corrosion allowance, depending on the anticipated rate of corrosion of the metal due to the specific fluid in contact. SA-516-Gr-60/70 can also handle mild corrosive applications, such as hydrocarbons with lower partial pressure of hydrogen (H_2).

For carbon steel, a corrosion allowance of 3 mm–6 mm is considered, depending on the contact fluid and the yearly corrosion rate. However, since SA-517-Gr-F has alloying elements, a lower corrosion allowance is available compared to carbon steel.

Environmental factors. External environmental factors, such as the site location based on its proximity to coastal/marine areas, regulate proper MOC selection to mitigate accelerated external corrosion.[3,4,5] This is accomplished by an external corrosion allowance or even with coating/painting on the external surfaces of the affected equipment.

Availability and expertise. While choosing the appropriate MOC for the given process application, extra attention must be paid to the availability of the chosen MOC and the expertise needed to handle it across various global fabricators.

Economics and overall weight. The overall fabrication and operating weight of the equipment is crucial, particularly for large equipment. Equipment weight is directly proportional to the thicknesses required based on design conditions. The equipment's total investment cost (TIC) comprises:

- Design and engineering cost
- Fabricated weight
- Raw material cost
- Material handling/fabrication allowance
- Associated cost of material and equipment inspection and testing
- Logistics cost
- Installation or erection cost
- Fabricated weight of equipment determines its overall cost
- Fabricated weight of equipment is also significant to determine optimum allied costs like transportation and erection costs
- Operating weight of the equipment determines the overall civil foundation/structure cost
- Thicknesses and weights are a function of the allowable stresses of the selected MOC.

Therefore, overall weight and associated equipment costs are related to correct MOC selection.

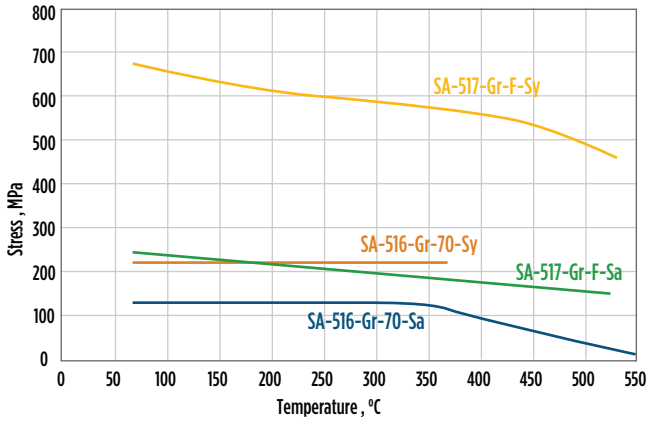

FIG. 1. Yield stress (SY) and allowable stress (SA) variation.

Material machinability and weldability. It is evident that SA-517-Gr-F is characterized by very high tensile and mechanical strength, making the material quite strong, hard and challenging to handle, weld, form, roll and fabricate. During fabrication, steady heating is required for smooth leak-proof joints.

This material also has stringent impact testing and post-weld heat treatment (PWHT) requirements compared to SA-516-Gr-70.

Unlike SA-516-Gr-70, SA-517-Gr-F may also require:

- Vacuum gas while procuring the raw material plate
- Simulated PWHT of mechanical test coupons
- High-temperature tension test, a supplementary requirement in case of high operating temperature
- Post-heating requirement.

COMPARISON OF SA-516-GR-70 VS. SA-517-GR-F

TABLE 1 summarizes the differences in SA-516-Gr-70 and SA-517-Gr-F across various important parameters, ranging from mechanical strength and testing requirements to material costs.

Approach. Detailed design calculations were performed for a specific group of static equipment (**FIG. 1**). These included three nos. large towers (low pressure and large diameters) and two nos. high-pressure spheres (with large diameters).

These calculations were performed in two cases for each piece of equipment:

- Case 1 with SA-516-Gr-70 as the base material
- Case 2 with SA-517-Gr-F as the base material.

A globally recognized and widely used design tool[a] was used to perform these calculations. The equipment was analyzed for the following design conditions:

- Internal pressure and temperature
- External pressure and temperature
- External loading due to wind (unidirectional wind force causing shear force and bending moment)
- External loading due to seismic condition (a transverse inertial force that was analyzed considering the vertical tower as the cantilever system with a lumped mass).

The site location was highly prone to earthquakes, so seismic external loading conditions and internal pressure governed thickness requirements.

Thickness calculation. The pressure vessel thickness calculation formula finds its basis in the thickness evaluation formula of the pressure vessel for the generated hoop stress. The hoop stress formula (cylindrical hoop stress) is shown in Eq. 1:

$$\sigma_H = \frac{Pd}{2t} \quad (1)$$

where:

σ_H = cylinder hoop stress in Pa
P = internal pressure in Pa
d = cylinder inside diameter, m
t = wall thickness, m

As per ASME Section VIII Div.1,[6] the thickness of the cylindrical shell can be calculated using (in circumferential stress) Eq. 2:

$$t = \frac{PR}{SE - 0.6P} \text{ or } P = \frac{SEt}{R + 0.6t} \quad (2)$$

As per ASME Section VIII Div.1, the thickness of the spherical shell can be calculated using Eq. 3:

$$t = \frac{PR}{2SE - 0.2P} \text{ or } P = \frac{2SEt}{R + 0.2t} \quad (3)$$

where:

t = minimum required thickness of shell
P = internal design pressure
R = inside radius of the shell course under consideration
S = maximum allowable stress value of the shell material
E = joint efficiency.

It can be seen from the above formulae that, conceptually, the thickness requirement is inversely proportional to the allowable stress value of the material. The higher the allowable stress value of the material, the lower the thickness required for the given design conditions of the equipment under consideration, and vice versa.

Analyses. Of the five design analyses performed, the results of comparisons of thickness, cost, civil (foundation) forces, etc., for one large tower are presented when analyzed in SA-516-Gr-70 and SA-517-Gr-F for the same conditions.

Technical specifications of the tower:

- Base MOC: SA-516-Gr-70
- Alternate MOC: SA-517-Gr-F
- Design pressure: 9.5 barg
- Design temperature: 120°C/–46°C
- Dimensions: ~ 10.5-m inside diameter, x ~ 100 m
- Skirt length: ~ 5 m
- Design code: ASME Section VIII Div. 1.

The comparison results have been populated in **FIG. 2** and **TABLE 2.**

Results. The following parameters were compared based on the aforementioned analysis:

- Thickness requirement
- Fabricated steel weight
- Operating weight
- Seismic shear force and bending moment

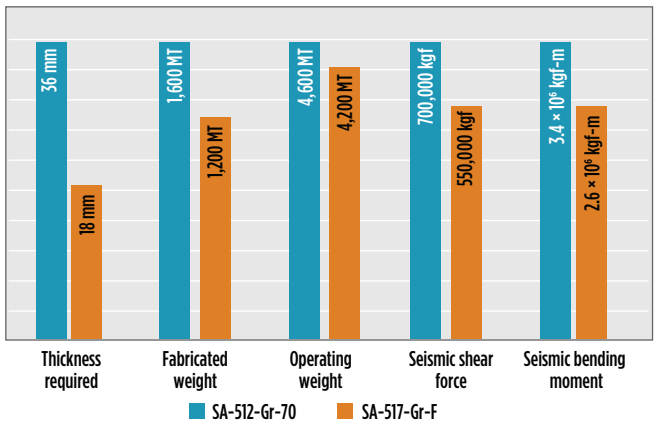

FIG. 2. Comparison plot between various calculation results.

TABLE 2. Comparison of results between SA-516-70 and SA-517-Gr-F

Parameters	SA-516-Gr-70	SA-517-Gr-F
Thickness required, range (mm)	36–44	18–30
Fabricated weight, MT	1,600	1,200
Operating weight, MT	4,600	4,200
Seismic shear force, kg-f	700,000	550,000
Seismic bending moment, kgf-m	34,000,000	26,000,000
Equipment supply cost	The equipment supply cost is almost the same in cases of SA-516-Gr-70 and SA-517-Gr-F. The savings in the equipment weight in the case of SA-517-Gr-F has been nullified, owing to the high material handling cost as compared to SA-516-Gr-70.	
Equipment installation cost	The installation cost of the equipment is reduced by almost 30% in the case of SA-517-Gr-F vs. SA-516-Gr-70 due to significant reduction in equipment weight.	
Foundation related cost	Due to the reduced foundation loads (seismic shear force and seismic bending moment), a reduction in the range of 10% is observed in the piling requirement in the case of SA-517 Gr-F vs. SA-516-Gr-70	

Is this installation's cost reduction a result of reduced thickness alone or has the additional cost that arises with fabrication risk and fabrication specialization required for SA-517 been accounted for?

The reduction in installation cost is a result of reduced erection weight owing to reduced thicknesses in the case of SA-517-Gr-F (due to high mechanical strength of the material). Fabrication and handling costs are considered while deriving the actual capital cost of the equipment.

- Overall equipment cost

For towers, the results can be interpreted as:

SA-517-Gr-F is a good alternative for equipment with larger sizes, high pressures and heavy external loads that may lead to overall cost optimization. Designers must be cautious, as the material comes with fabrication challenges.

- Weight reduction: ~ 35%–40%
- Seismic force and moment reduction: ~ 30%–35%
- Equipment cost optimization: ~ 10%
- Civil foundation/structure cost optimization: ~ 10% of equipment cost
- Installation cost optimization: ~ 20%

For spheres, the results can be interpreted as follows:

- Weight reduction: 35%–40%
- Seismic force and moment reduction: ~ 35%–40%
- Equipment cost optimization: ~ 10%
- Civil foundation/structure cost optimization: ~ 10% of the equipment cost
- Installation cost optimization: ~ 20%

Challenges in using SA-517-GR-F. Although it appears that the use of SA-517-Gr-F in static equipment can lead to significant savings in terms of steel and foundation costs, etc., its use also presents a few challenges:

- **Material availability**—The availability of this material is limited, which can pose a threat to the project schedule. Sourcing and pricing of this material should be studied well in advance.
- **Material handling**—Expertise is needed from the fabricator to handle such hard material—specifically for greater diameters and thicknesses—as know-how and expertise in this area can be quite limited among global static equipment suppliers.
- **Application limitation.** The use of this material cannot be extended to hydrogen service (e.g., hydrogen mounded bullets). Equipment in hydrogen service calls for a hardness limitation requirement (e.g., 235 BHN). This cannot be fulfilled with a low-alloy, high-strength material like SA-517-Gr-F.

Takeaway. When evaluated, SA-517-Gr-F can be a key alternative for critical static equipment with a base MOC like SA-516-Gr-70, with certain conditions. Considering the challenges in sourcing and handling SA-517-Gr-F, its use may be restricted to static equipment such as spheres, towers and reactors with very large-diameter, high-pressure and high-temperature requirements. The use of this material (to a larger extent) is governed by site/plant location, which must be explored and evaluated to ensure proper soil hardness and exposure to severe external loads (wind, seismic, etc.), as well as extended to scenarios where the optimization of the civil foundation (piling) requirements becomes crucial.

When SA-517-Gr-F must be used in any project with critical static equipment, its sourcing must be well planned and ahead of schedule.

It is prudent for the design engineer to consider all important parameters—such as equipment type, design conditions, installation site conditions, availability and handling of SA-517-Gr-F, as well as reliability—before selecting SA-517-Gr-F as an alternative to carbon steel SA-516-Gr-70.

The raw material cost of SA-517-Gr-F is approximately 30% more expensive than SA-516-Gr-70, and the raw material handling and fabrication of SA-517-Gr-F is higher than SA-516-Gr-70. However, due to the overall reduction in weight, civil foundation forces, transportation and erection costs, the capital investment for SA-517-Gr-F could prove more lucrative in specific cases, such as when equipment experiences high pressure and/or temperatures, extreme external shear force and bending moments due to wind or earthquake. Process fluids are compatible with SA-517-Gr-F, when viewed as a substitute for SA-516-Gr-70. HP

NOTE

[a] Hexagon PPM's PVElite-2019

LITERATURE CITED

[1] American Society of Mechanical Engineers (ASME), Sec. II, Part A, and C, 2019.
[2] Teel, R. B., "The stress corrosion cracking of steels in ammonia – A survey – with consideration given to OTEC design," UNT Libraries Government Documents Department, March 1980.
[3] Albrecht, P. and A. H. Naeemi, "Performance of weathering steel in bridges," National Cooperative Highway Research Program Resort #272, 1984.
[4] Online: https://weldinganswers.com/recommendations-for-welding-t-1-steels/
[5] Doty, W. D., "Welding research supplement—Weldability of construction steels: USA Viewpoint," Welding Research Council (WRC), February 1971.
[6] American Society of Mechanical Engineers (ASME), "ASME Boiler and Pressure Vessels," Code Sec. VIII, Div. 1 and Div. 2, 2019.

AEISHWARYA CHAUDHARI works as a Deputy Manager in the static equipment department of the technical expertise and discipline engineering division of BASF, Mumbai, India. She has more than 12 yr of extensive experience in mechanical design, engineering and the execution of various static equipment, such as process columns, pressure vessels and heat exchangers that are widely used in refineries, petrochemical and chemical plants. She earned a B. Tech (Bachelor of Technology) degree from V.J.T.I–Mumbai University, specializing in mechanical engineering. She has achieved the title of Chartered Engineer from the Institution of Engineers, India.

MAHESH KULKARNI works as a Manager-Mechanical in the technical expertise and discipline engineering division of BASF, Mumbai. He has more than 21 yr of experience and specializes in finite element analysis in the process industries, with hands-on experience with static equipment in chemical and petrochemical projects. He has also worked as an FEA expert, project engineer, root cause analysis and troubleshooting expert in refinery projects. He graduated with a degree in mechanical engineering from Pune University and an ME degree in mechanical-heat power engineering in 2002 from Government College of Engineering, Karad, Shivaji University, Kolhapur, India. He achieved the titles of Charted Engineer, Fellow and Professional Engineer from the Institution of Engineers, India.

P. DIXIT, Vadodara, Gujarat, India

Fix nozzle elevations and orientations for distillation columns

An engineering, procurement and construction (EPC) contractor receives a front-end engineering design (FEED) package or basic design and engineering package as an input document from the owner. The information about the process equipment covered in these packages is provided in the form of equipment data sheets. Distillation columns data sheets cover a column line sketch with configuration, the type of internals/trays, the number of trays, and process related details like vapor-liquid hydraulic parameters, properties, etc. The column sketch also covers nozzle connections, with their respective name (purpose), size and indicative locations.

Nozzle connections are broadly categorized into four types: process, safety, instrumentation and inspection/maintenance.

In general, process licensors only provide details of process nozzles that are important to column operation and performance (e.g., feed inlet connections, furnace feed, reboiler feeds). For such connections, elaborate details are provided with internal arrangements, elevation, location and suggested orientation. Other types of nozzle connections and elevations are provided as indicative and their details are left to the detail engineering team.

If the engineering team does not have an internals expert, design engineers normally keep such details under hold. These details are later filled in by the tray designer/supplier. Trays are short delivery items compared to columns, which are required at the site much later and are ordered late in the sequence, putting column fabricator engineering work on hold. This sometimes results in delays by the column vendor or a requested cost escalation.

This article provides an explanation of each type of column nozzle and logic, while fixing nozzle elevation and orientations—accompanying sketches (figures) are provided. The most preferred positions are shown here, as well as alternate options. Using these guidelines, column and piping engineers can perform this work by themselves.

The details discussed here are primarily for sieve and valve trays, which are the most common type of distillation column hardware used in the process industries. The details may also apply for bubble cap trays with some modifications, but may not apply to proprietary trays/internals. Information for these trays/internals should be obtained from their respective designers/suppliers.

Feed nozzles. As shown in **FIG. 1,** a typical distillation column feed is a two-phase (vapor and liquid) flow from a furnace (e.g., crude or vacuum columns). To separate liquid from vapor, special internals—such as a vapor horn with tangential entry (single or double), shown in **FIG. 1A**—are used. These internals uniformly distribute vapor across the diameter. In the case of pressure-sensitive systems like vacuum columns, proprietary internals such as a Schopetentoeter (**FIG. 1B**) or similar are used.

Reboiler nozzles are normally kept flush to the column wall and do not have any internal attached. If the nozzle is located close to liquid levels or directly opposite the bottom downcomer or seal pan, an internal baffle like the one shown in **FIG. 1C** is suggested. All types of feed nozzles require sufficient space above and below the feed. This serves three purposes:

- Avoids disturbing the bottom liquid level
- Avoids the impact of the two phases on the trays or packed bed above
- Distributes vapor across the diameter and knock out liquid.

The details of such feed nozzles and internals are provided in the licenser's data sheet.

Reflux nozzles. Reflux liquid is supplied on the top tray. The feed location is kept opposite the respective tray downcomer in an un-perforated area. Normally, the

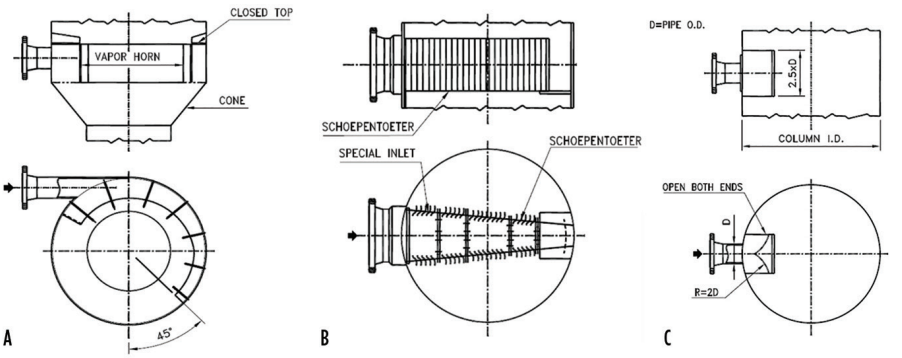

FIG. 1. Feed nozzle with vapor horn (1A), feed inlet with Schoepenteoter (B) and feed inlet deflector baffle (C).

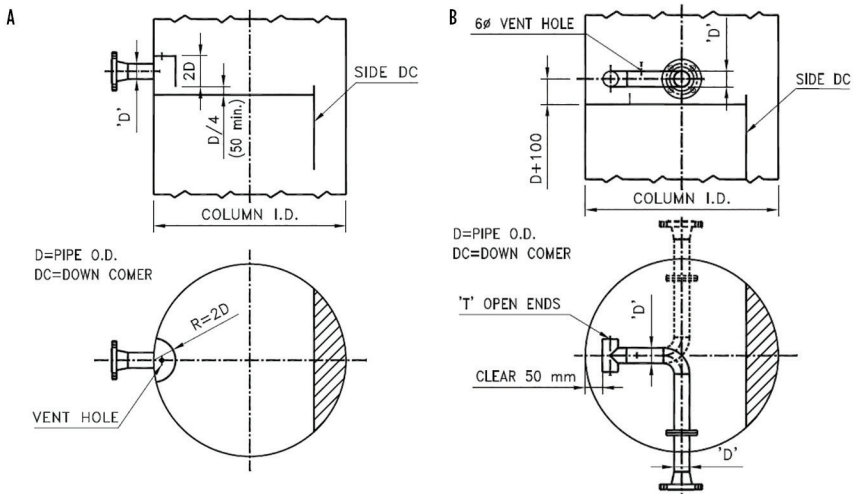

FIG. 2. Reflux inlet one-pass trays.

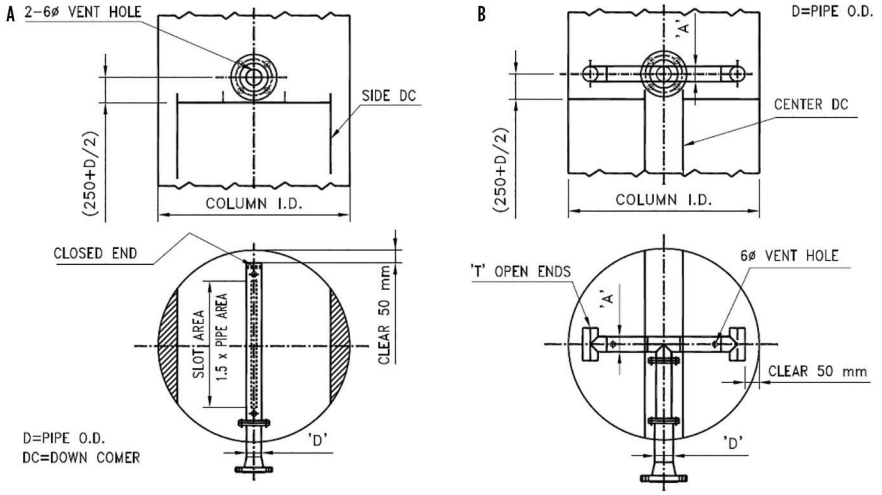

FIG. 3. Reflux inlet two-pass tray, side downcomer (A); and reflux inlet two-pass tray, center downcomer (B).

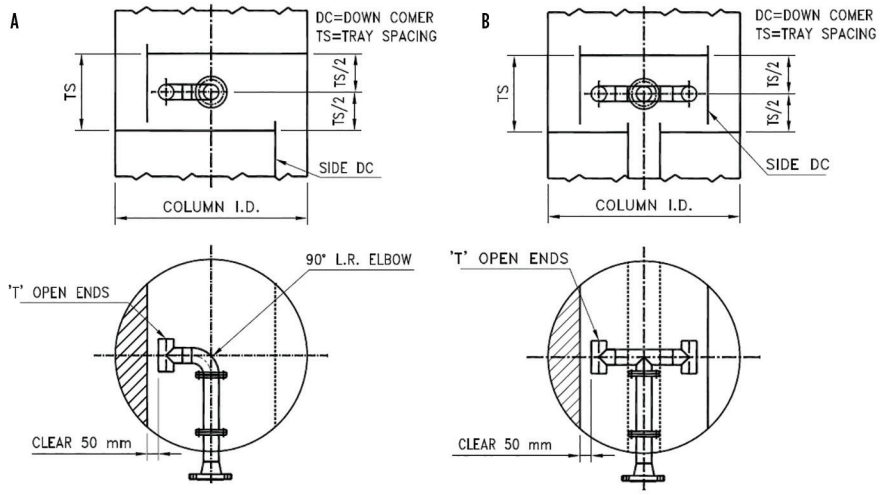

FIG. 4. Intermediate feed one-pass tray (A), and intermediate feed two-pass tray (B).

top tray has an inlet weir height of 100 mm to hold the liquid back and distribute it uniformly over the tray active area flowing over the weir.

FIG. 2 shows the details of a reflux inlet, one-pass tray. For a single-pass tray, **FIG. 2A** is preferred. The internal baffle is made of a half-cut pipe with a bottom gap, as shown. Due to piping orientation, if following **FIG. 2A** is not possible, an internal pipe distributor can be provided as per **FIG. 2B.** This provides the flexibility of fixing the nozzle at any orientation. The reflux nozzle's elevation is kept just above liquid level on the tray to avoid liquid splash from a height.

FIG. 3 shows details of reflux inlet nozzles for two-pass trays. For a side downcomer tray, liquid is fed into the central trough (**FIG. 3A**). For a center downcomer tray, the liquid is fed at two extreme opposites to the downcomers (**FIG. 3B**). In this case, the nozzle elevation is also kept close to the tray liquid level.

Intermediate feed nozzles. The intermediate feeds can be a mix of liquid and vapor or pure vapor. If the feed is only vapor, it can be provided below the active area of the desired tray. Elevation is kept close to the tray level mixing feed vapor-to-vapor zone within the tray spacing. The nozzle is kept about 200 mm–300 mm below the tray.

For intermediate mixed feed (vapor and liquid), arrangements such as those shown in **FIG. 4** are used. Here, the mixture is fed close to the tray downcomer, using equal 'T' as shown. Normally, a clearance of 50 mm is recommended between the tray downcomer and 'T.' With a mixed feed, the elevation is fixed higher than the tray liquid level—good practice is approximately half of the tray spacing. Internal pipe orientation can be routed to the suitable nozzle location determined by a piping engineer.

Manholes. Manholes (**FIGS. 5A** and **5B**) are required for regular inspection of trays and carrying out maintenance work. Nozzle elevations are fixed so that bottom line of the nozzle is at least 100 mm above the tray level. This avoids injuries to an operator from tray studs and other projections while entering. A comfortable and appropriate place for a manhole is in the middle of the tray spacing. Manhole orientation should be arranged so access always opens up in an active area and does not clash with any downcomers or other internals.

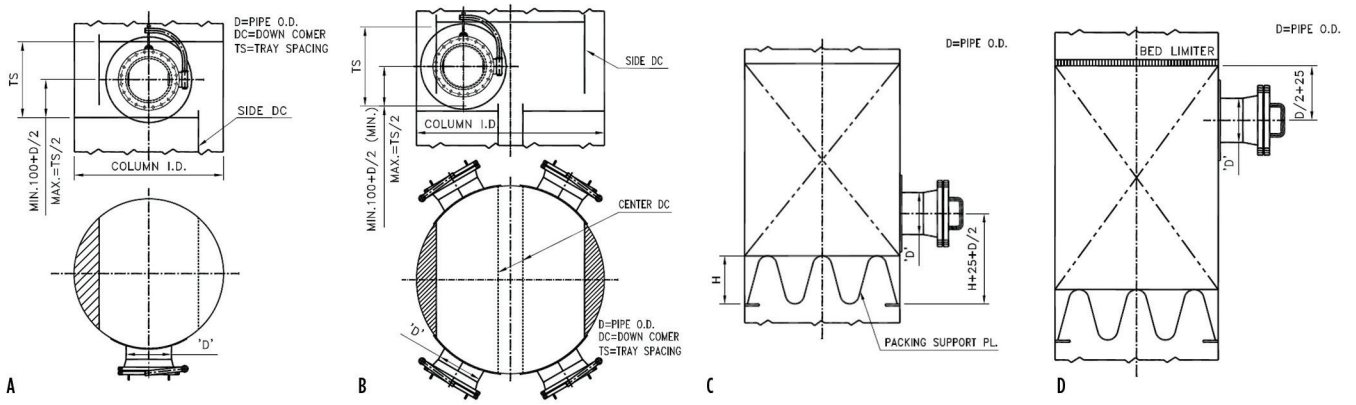

FIG. 5. Manhole one-pass tray (A), options for manhole locations in a two-pass tray (B), a hand hole at the bottom of a packed bed (C) and a hand hole at the top of a packed bed (D).

Fixing the orientation of a manhole in chimney trays and high-quality distributor locations is tricky work. It must be ensured that no chimney riser of a liquid distributor trough is blocking the entry passage.

Hand holes. Hand holes (**FIGS. 5C** and **5D**) are provided mostly in randomly packed towers and are used for either topping up of random packing or removal of packing. Recommended hand hole sizes range from 150 mm–250 mm, depending on column diameter and packing size. For packing removal, hand holes should have a minimum 25-mm gap between the top of the packing support plate and the hand hole inner diameter. Similarly, for topping up of packing, the location should be 25 mm below the bed limiter from the top of the hand hole inner diameter, as shown in **FIG. 5D.**

Pressure and temperature connections. Pressure measurement connections (**FIG. 6**) are always provided in the vapor phase, as most of the pressure measurement instruments work in single phase. The nozzles for pressure measurement are recommended below the active tray area with a minimum gap of 100 mm.

Temperature measuring nozzles are normally provided in the liquid zone due to better heat transfer in the liquid phase. The recommended practice is to provide these nozzles 50 mm above the respective tray. In the case of bubble cap trays, the thermowell is suitably located so it does not clash with the bubble cap.

A thermowell can also be provided in the downcomer area as shown, depending on the available width in the downcomer.

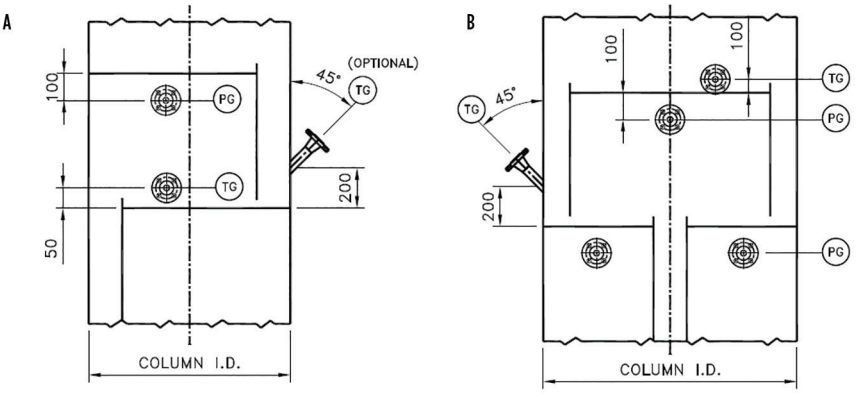

FIG. 6. Pressure and temperature tapping locations in a one-pass tray (A), and pressure and temperature tapping locations in a two-pass tray (B).

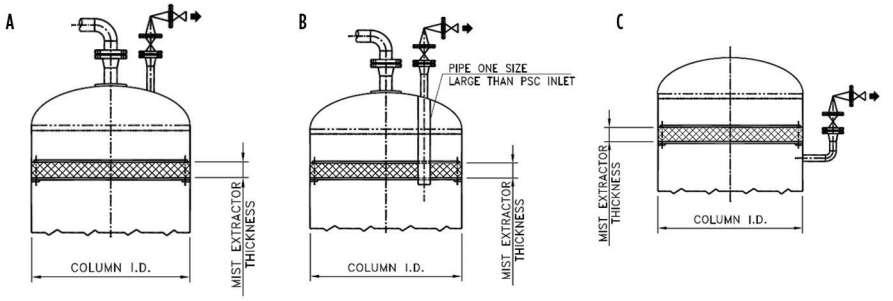

FIG. 7. Safety valve locations options 1 (A), 2 (B) and three (C).

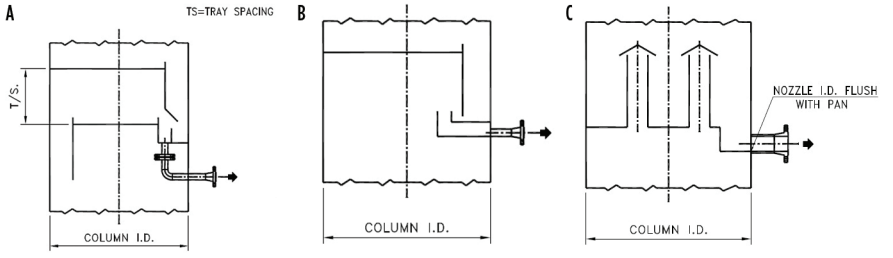

FIG. 8. Partial withdrawal from the tray (A), partial withdrawal from the bottom seal pan (B) and total product withdrawal from the chimney tray (C).

If the width is short and cannot accommodate thermowell projection, it can be made inclined, as shown in FIG. 6.

In a distillation column, fixing nozzles elevation and orientation are based on fixed guidelines. This knowledge helps design engineers shorten the engineering and procurement cycle.

Safety valves (pressure relieving devices). Safety valves are normally provided on the top of the vessel or column (FIG. 7). Normally, the column/vessel has a mist extractor in the top section. Under pressure surges where chances exist of dislodgement of the mist extractor and choking of the safety valve inlet, a good engineering practice is to provide a pipe sleeve larger than the safety valve inlet size and pass it through the mist extractor (FIG. 7B). Under fouling service conditions, it is good engineering practice to provide a safety valve connection below the mist extractor (FIG. 7C).

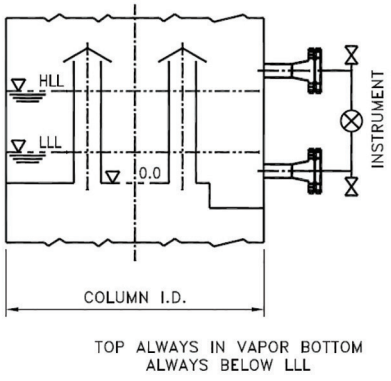

FIG. 9. Level measurements, chimney tray.

Liquid withdrawal nozzle connections. In a distillation column, partial or total liquid withdrawal from the tray is a regular requirement. FIG. 8A shows details of a partial liquid withdrawal from the tray by providing a recessed seal pan and inlet weir as a downcomer seal. Partial withdrawal from the lowest trays can be accomplished by providing a seal pan with a draw-off pan (FIG. 8B). Here, the nozzle is kept flush with the draw-off pan level.

For the total withdrawal of liquid, a collector (chimney tray) is normally provided, as shown in FIG. 8C. The nozzle elevation is kept flush with the recessed pan. Such trays require zero leaks and are generally seal welded.

Level measuring instruments. Most of the instruments in this category are level gauge, level transmitter/controller, level switches, etc. (FIG. 9). Normally, each of these instruments has two connections: top and bottom. Depending on instrument selection, these can be arranged side-side, side-bottom, top-bottom, etc. Before fixing the elevation and orientation of such nozzles, the operating level, alarm level or shutdown levels of each situation must be obtained from the process engineer. The top connection of the instrument must always be above the highest liquid level (HLL) in vapor phase, while the bottom connection must always be below the lowest liquid level (LLL). The elevation of each instrument must be determined based on the operating levels and shutdown or alarm levels. If the tray has a recessed pan, as shown in FIG. 9, the advantage of seal pan depth can be taken to have a wider operating range.

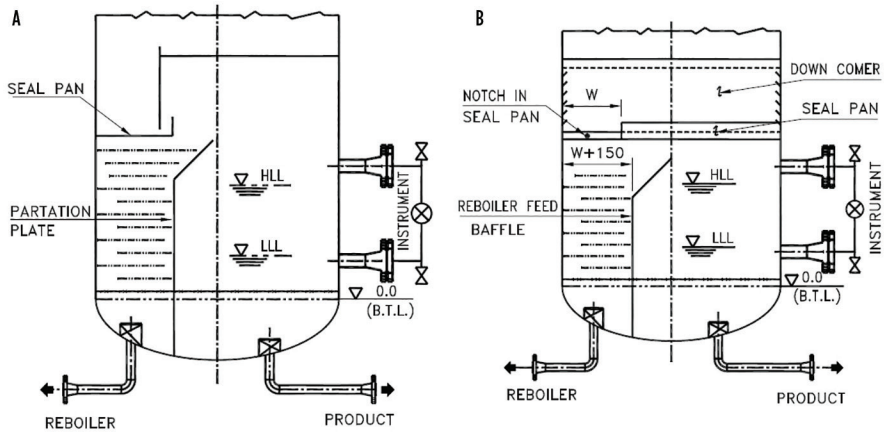

FIG. 10. A reboiler feed baffle in a one-pass tray (A), and a reboiler feed baffle in a two-pass tray (B).

Level control instruments in a reboiler feed baffle. For thermo-siphon reboilers, the reboiler feed from a distillation column is controlled by a pass partition baffle (FIG. 10). The baffle overflow is taken out as product. Baffle height is fixed based on the static head requirement of the reboiler.

In this section, all level instruments and controls are provided in the overflow section, which goes to the bottom product outlet. To fix level instruments in this section, an engineer requires operating levels, alarm levels and shutdown levels. Caution must be taken to provide all these instruments in the product section only. The author noticed a mistake in one case where the sections were reversed.

Sampling connections. Sampling connections are small nozzles sizes ranging from 40 mm–50 mm. Sample collection requirements can be for liquid or vapor; this should be clearly specified in the datasheet. Liquid samplers are placed in the liquid zone, either in the downcomer area or close to the tray level. Vapor collection is done from the vapor zone, mostly from below the tray active area.

Takeaway. With this information about various types of nozzles, their technical requirements and placements, working engineers can apply the given logic and decide for themselves the nozzle elevations and orientation. HP

PRAMOD DIXIT works as a consultant at Baroda India. He spent 20 yr at Engineers India Ltd. as a trays and tower internals specialist, and another 20 yr in EPC companies Larsen and Toubro and Essar Offshore in different senior positions. He provides training to operating company inspection and maintenance engineers in related field and advisory services in the troubleshooting of engineering issues. Mr. Dixit holds a B.Tech degree in mechanical engineering from IIT Roorkee India.

P. WEI and **Q. HONGWEI,** PetroChina Karamay Petrochemical Co., Xinjiang, China; and
L. YANSHENG, China University of Petroleum, Beijing, China

Analyze pressure loss during FCC standpipe catalyst transfer

The fluid catalytic cracking unit (FCCU) is the primary conversion equipment for modern refineries to obtain clean transportation fuels, along with high-grade petrochemical feedstock. With increasing processing capacity, however, standpipe catalyst problems have become a bottleneck, restricting long cycle operation.[1]

The ideal operating mode for industrial FCC standpipe is dense-phase fluidized solids flow, with a range of catalyst density of 500 kg/m^3–600 kg/m^3. This operating mode not only provides high pressure drop for the catalyst circulation, but also has a strong sealing function, preventing gas leakage from the slide valve.[2,3] However, catalyst flow patterns usually vary with operating conditions, standpipe geometry structure, catalyst properties, aeration flowrate, etc. It is difficult to maintain uniform fluidity. Erratic flow patterns often affect pressure buildup in the standpipe.[4,5]

Matsen *et al.*[6] proposed that friction formed in the packed-bed flow was the main reason for the pressure loss. According to the classic single-flow and double-flow pattern models proposed by Leung *et al.*,[7] catalyst flow patterns in the standpipe can be conveniently determined. However, these models did not consider the effect of the slide valve opening value on catalyst flow patterns, and FCC engineers still could not explain some pressure-reversal phenomena in the industrial standpipe using the theory.

This article analyzes the influencing factors of pressure loss on a 1-MMtpy industrial FCCU by measuring the dynamic pressure in the regenerated standpipe under different operating conditions. A half-pipe flow model is established and a linear relationship equation between the catalyst circulation rate and the standpipe pressure loss is proposed, which can be used to guide the operating adjustment for the industrial FCC standpipe.

Experimental setup. The schematic diagram of the 1-MMtpy industrial FCCU is shown in **FIG. 1.** The riser terminal is connected with the vortex separation system (VSS). The regenerator contains a combustor, the dilute phase pipe and the disengager. The inlet pressure of the regenerated standpipe, p_i, is shown in kPa. The pressure above the regenerated slide valve is p_s. The outlet pressure of the regenerated slide valve, p_o, is shown in kPa. The pressure drop of the slide valve is expressed in kPa as $\Delta p = p_s - p_o$.

The key operating parameters are listed in **TABLE 1.** The corresponding catalyst circulation rate, G_s, changed from 435.4 kg × m^{-2} × s^{-2} to 857.4 kg × m^{-2} × s^{-2} between Case 1 and Case 4. The ratio of catalyst to oil was calculated according to the heat balance between the reactor and the regenerator system. The opening value of the regenerated slide valve increased from 45% to 65% with the increase in processing capacity, which was very large and not conducive to the operating adjustment. For Case 3 and Case 4, the processing capacity and reaction temperature were lower than in other cases. To ensure the gas velocity in the inlet of the cyclone separators and the VSS under an appropriate scope, the pressures of the reactor and regenerator were reduced to 165 kPa and 160 kPa, respectively.

Regenerated standpipe structure. The schematic diagram of the regenerated standpipe is shown in **FIG. 2.** The standpipe consists of two inclined pipes. The angle between the upper inclined

FIG. 1. Photo and schematic diagram of the 1-MMtpy industrial FCCU.

pipe and the vertical line is 10°. The upper inclined pipe encompasses two parts with inner diameters of 760 mm and 630 mm, respectively, and a total length of 18.2 m. The top wider part is used to degas bubbles. The angle between the lower inclined pipe and the vertical line is 45°, with a length of 2.3 m and an inner diameter of 630 mm.

C1–C11 are the 11 axial cross-sections of the standpipe. One aeration nozzle is installed on each cross-section, and the angle between the nozzles and the wall surface is 30°. Nozzles on C2, C4, C6 and C8 are located at the bottom inclined pipe. The rest of the nozzles are installed on both sides, and the angle with the central busbar is 60°. The aeration gas above the regenerated slide valve is nitrogen with a pressure of 1.4 MPa and a normal temperature. The aeration gas below the regenerated slide valve is steam with a pressure of 1 MPa and a temperature of 265°C. The aeration flowrate is controlled by the flow limiting orifice with a diameter of 2 mm–5 mm.

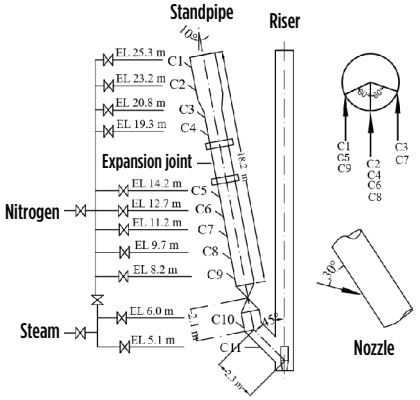

FIG. 2. Schematic diagram of the regenerator standpipe. EL is elevation; C1–C11 are cross-sections of the standpipe.

TABLE 2 shows the analysis of material properties of the equilibrium catalyst at 20°C. Pressure measurement was carried out with the selected aeration nozzles (C1, C2, C3, C6, C9 and C10) at the same time under different operating conditions. Measuring frequency and time were 1 Hz and 60 sec, respectively.

Results and discussion. In looking at the pressure profiles of the standpipe, FIG. 3 shows the axial pressure profiles of the regenerated standpipe from Case 1 to Case 4. The p_i depended on the regenerator pressure and the static pressure of the dense-phase bed in the regenerator, with little change under the different operating conditions. The axial pressure increased gradually along the standpipe, but the pressure between the C6 and C9 cross-sections was greatly affected with G_s.

When G_s was 857.4 kg × m^{-2} × s^{-1}, the pressure at the bottom standpipe increased and had a maximum pressure of 255.6 kPa at the C9 cross-section. In the other three operating conditions, the pressure below the C6 cross-section decreased. When G_s was 435.4 kg × m^{-2} × s^{-1}, pressure at the C9 cross-section had a minimum pressure

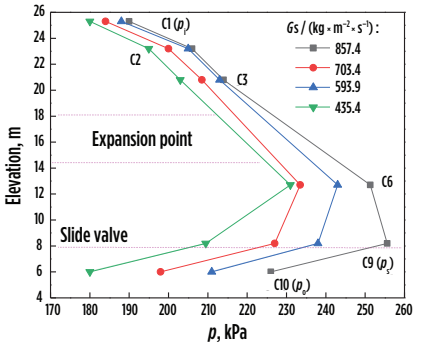

FIG. 3. Axial pressure profiles in the standpipe.

of around 210 kPa. The p_o below the slide valve ranged in pressure from 180 kPa–223 kPa, which was mainly affected by the pressure drop of the riser, and increased with the increase of G_s.

FIG. 4 shows the dynamic pressure at the C6 and C9 cross-sections under different operating conditions. When G_s was 857.4 kg × m^{-2} × s^{-1}, the mean pressure at the C6 cross-section was less than that at the C9 cross-section, as shown in FIG. 4A. In the other three operating conditions, the pressure at the C6 cross-section was greater than that at the C9 cross-section. Moreover, the pressure difference between the C6 and C9 cross-sections increased gradually with the decrease of G_s. When G_s was 435.4 kg × m^{-2} × s^{-1}, the mean pressure difference increased to 30 kPa.

In analyzing the flow patterns in the standpipe, FIG. 5 shows the single and double flow pattern modes in the FCC standpipe proposed by Leung *et al.*[7] Generally speaking, the sliding speed of the gas solids at the top standpipe is large, and the catalyst flow pattens are dense-phase fluidized solids flow. The fluidized gas volume in the bottom standpipe is reduced because it is compressed. If the aeration flowrate is approximately equal to the decreased gas volume, then the axial pressure gradually increases along the standpipe, as shown in FIG. 5A.

If the aeration flowrate is insufficient, then the pressure gradient along the standpipe decreases. The catalyst flow pattern on the top standpipe is in a fluidized state. Catalyst voidage, ε, decreases gradually, and the axial pressure increases continuously. However, in the bottom standpipe, when ε is less than the incipient fluidization voidage, ε_{mf}, the catalyst flow patterns change to transitional

TABLE 1. Operating parameters of the FCCU

Case	Feedstock, t/hr^{-1}	Gs/ (kg × m^{-2} × s^{-1})	Reactor pressure, kPa	Regenerator pressure, kPa	Reactor temperature, °C	Regenerator dense phase temperature, °C	Catalyst-to-oil ratio	Opening of slide valve
1	120	857.4	173	165	530	705	8	65
2	105	703.4	173	165	520	705	7.5	60
3	95	593.9	165	160	510	705	7	55
4	75	435.4	165	160	500	705	6.5	45

TABLE 2. Properties of the equilibrium catalysts

Apparent packing density, kg × m^{-3}	Skeletal density (ρ_s), kg × m^{-3}	ρ_{mf}, kg × m^{-3}	APS, μm	ϕ%					
				0–20, μm	20–40, μm	40–60, μm	60–80, μm	80–110, μm	> 110, μm
840	2,400	760	76	0	7	29	27	27	10

Notes: ϕ = Particle size volume distribution; APS = Average particle size; ρ_{mf} = Incipient fluidization density

packed-bed flow or packed-bed flow, and the friction loss increases rapidly. In the transitional packed-bed flow, ε continues to decrease but is larger than ε_0. The friction loss is smaller than the static pressure, and the axial pressure continues to increase. The pressure gradient along the standpipe is negative but lower than that of the dense-phase fluidized solids flow, as shown in FIG. 5B, Curve 1. In the packed-bed flow, ε drops to ε_0, and the frictional loss is larger than the static pressure. The axial pressure gradually decreases, and the pressure gradient becomes positive, as shown in FIG. 5B, Curve 2.

Industrial FCC standpipes consist of vertical pipe and inclined pipe. Catalyst flow patterns in a standpipe are complex. Generally speaking, catalyst flow patterns in the top standpipe are in a fluidized state. When the aeration flowrate is insufficient in the middle pipe, the catalyst flow patterns change to the transitional packed-bed flow. The pressure loss increases and the pressure gradient decreases, which results in a decreased catalyst circulation rate. The actuator of the slide valve will increase the opening value to raise the G_s and ensure the stability of the reaction temperature. However, the height of the catalyst sealing column above the slide valve decreases with the increase of the opening value, which may result in gas leakage from the slide valve into the riser. The pressure gradient will become positive, as shown in the curve in FIG. 6C. However, if the catalyst sealing column is high enough, then the gas at the bottom standpipe will only flow

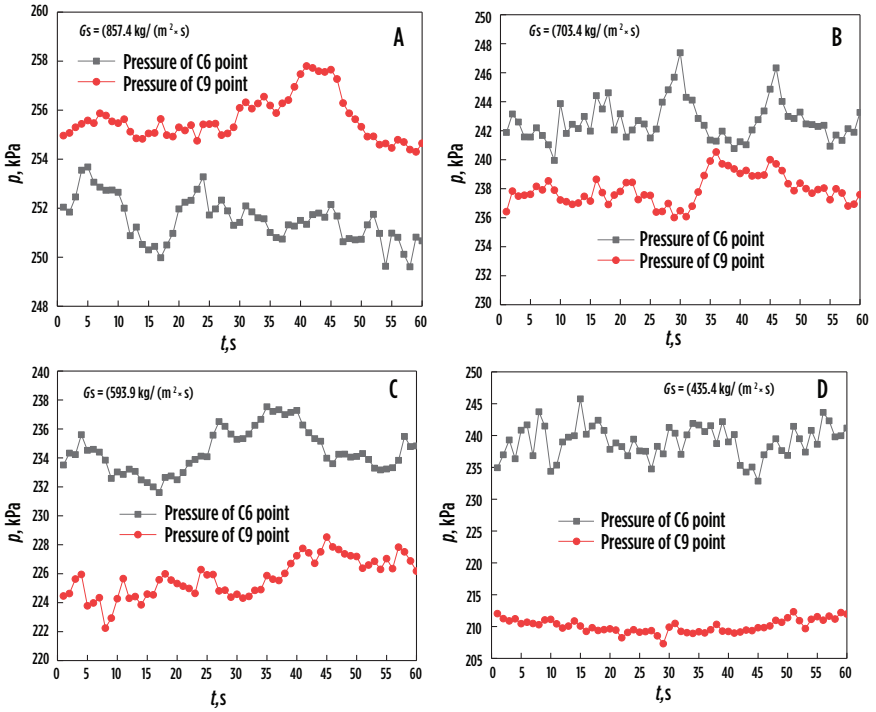

FIG. 4. Dynamic pressure at C6 and C9 cross-sections.

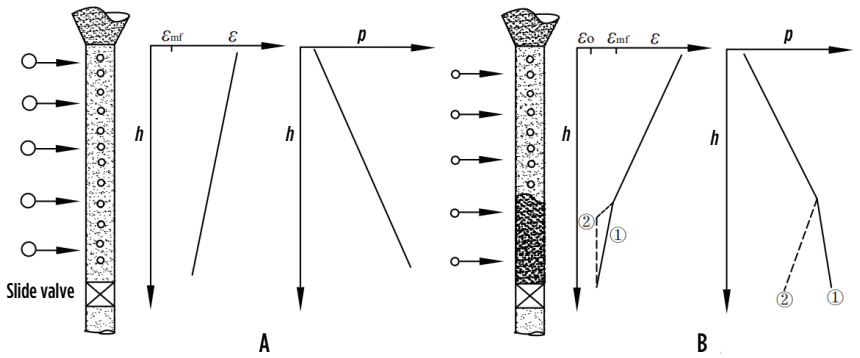

FIG. 5. Different catalyst flow patterns in the FCC standpipe.

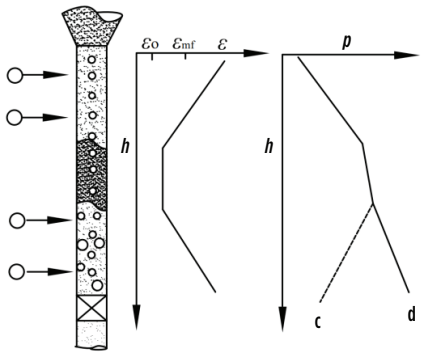

FIG. 6. Three flow patterns in an industrial FCC standpipe. Point (c) represents the gas leakage formed and the gas above the slide valve flowing into the riser, while point (d) represents the catalyst sealing ability above the slide valve.

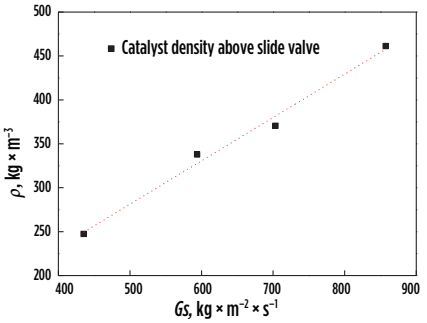

FIG. 7. Catalyst density above the slide valve under different operating conditions.

upward and the pressure gradient is still negative, as shown in the curve in **FIG. 6D.**

Catalyst density above the slide valve. For the parallel FCCU, Eq. 1 is used to calculate the catalyst density above the slide valve:

$$A = (6.29Fs \times 10^{-2})/[C_s(\Delta p \times \rho)^{0.5}] \quad (1)$$

where:

A = Actual catalyst flow area, cm^2
A_o = Full open area of the slide valve plate = 936.95 cm^2
F_s = Catalyst circulation rate, kg/hr
ρ = Catalyst density above the slide valve, kg/m^3
Δp = Pressure drop of slide valve, kPa
C_s = Flowrate coefficient.

For the single acting slide valve with a throttling cone, C_s equals 0.85. According to **TABLE 1** and Eq. 1, catalyst density above the slide valve under different operating conditions can be calculated as shown in **FIG. 7.**

Within the operating conditions, catalyst density above the slide valve varied

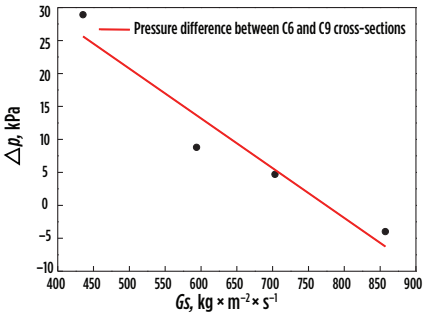

FIG. 8. Relationship curve between G_s and Δp_{loss}.

from 247 kg/m^3–461 kg/m^3, which was much less than ρ_{mf}. In Case 1, catalyst density above the slide valve was around 461 kg/m^3, which had a strong sealing capacity to prevent gas leakage from the slide valve. However, catalyst density decreased gradually with the reduced G_s. In Case 4, catalyst density dropped to only 247 kg/m^3. Catalyst flow patterns transformed into the lean-phase fluidized solids flow, and the catalyst sealing function disappeared. Gas leakage was the fundamental reason for the bottom standpipe pressure reversal.

According to the double flow pattern model shown in **FIG. 3,** pressure in the bottom standpipe decreased, which suggested that catalyst density above the slide valve would be close to ρ_{mf}. In reality, however, catalyst density above the slide valve from Case 2 to Case 4 was much less than ρ_{mf}, as shown in **FIG. 7.** This indicated that the gas leakage flow pattern had a similar pressure distribution to the packed-bed flow in the industrial FCC standpipe.

Pressure loss in standpipe. The average pressure difference between the C6 and C9 cross-section was defined as the standpipe pressure drop loss in kPa ($\Delta p_{loss} = p_{C6} - p_{C9}$). According to the average value of dynamic pressure in **FIG. 4,** the relationship between Δp_{loss} and G_s was established as shown in **FIG. 8.** Within the operating conditions (G_s = 435.4 kg × m^{-2} × s^{-1} to 857.4 kg × m^{-2} × s^{-1}), there was a linear relationship equation between Δp_{loss} and G_s, $\Delta p_{loss} = -0.07554G_s + 58.51208$.

Takeaway . The dynamic pressure in the regenerated standpipe was measured at different operating conditions in a 1-MMtpy FCCU. Process parameters and pressure distribution in the standpipe were used to determine the catalyst flow patterns. The main conclusions were summarized as:

1. Different catalyst flow patterns were present in the industrial FCC standpipe. Dynamic pressure characteristics could be adopted to determine the catalyst flow patterns.
2. Catalyst flow patterns in the standpipe varied with the catalyst circulation rate. Under the low catalyst mass rate, gas leakage appeared from the slide valve into the riser, which was the fundamental reason for the axial pressure reversal in the bottom standpipe.
3. Gas leakage reduced the standpipe pressure drop. A linear relationship equation between G_s and pressure loss was expressed as: $\Delta p_{loss} = -0.07554G_s + 58.51208$, which could be used to calculate the catalyst mass rate. HP

ACKNOWLEDGMENTS

The authors acknowledge financial support by the 2021 Technical Talents Innovation Foundation Project of CNPC and the Natural Science Foundation of China.

LITERATURE CITED

Complete Literature Cited available online at www.HydrocarbonProcessing.com.

PENG WEI is a Senior Engineer in the FCC division of the petrochemical branch company of PetroChina. He has worked in FCC plant production, management and technical revamp for 11 yr. He holds a PhD in chemical engineering from the China University of Petroleum in Beijing. His research interests include oil and gas processing and fluidization technology, among others.

QI HONGWEI is a Senior Engineer and the Director of the science and technology department of the petrochemical branch company of PetroChina. With more than 30 yr of experience, he is responsible for technology management of the fuel oil system. He also oversees the technical revamp of many units, including the catalytic cracking, delayed coking and distillation units. He also has abundant experience in process optimization.

LIU YANSHENG is a Professor of chemical engineering at the China University of Petroleum in Beijing and is engaged in the distillation process, equipment development and application of basic research. His research interests include transmission and separation, distillation, equipment development and fault diagnosis. He has worked in chemical engineering for more than 30 yr and is responsible for the technical revamp of several FCCUs, having abundant experience in debottlenecking the production process.

G. R. MARTIN, Sulzer GTC Technology, Irving, Texas

Advances in light ends processing units using DWCs

For those who have been in the refining industry for many years, it is obvious that significant changes are occurring. Refining is not going away, but refineries built for long-term existence will not be built like those of the past. Forces and needs are dictating changes in the refining business climate.

Dividing wall columns (DWCs) are a useful tool for helping meet these demands. Using DWCs in the design of complex light ends processing units can provide a lower-CAPEX design over that of a conventional gas plant. DWC technology has already proved its value through numerous applications. However, it must be used in the appropriate application to yield a successful outcome. This article addresses the use of DWCs to fractionate light hydrocarbon streams. While the applications shown are common for the refining industry, this technology also can be used in other types of processing plants where light hydrocarbon streams are processed.

DWCs reduce the amount of materials of construction and, in many applications, reduce the energy required to produce end products. In other applications DWCs may only reduce the materials of construction. The reduction in energy consumption has a continuous benefit, with DWCs often saving 10%–30% over conventional distillation configurations. This varies depending on the process, and comparisons should always be evaluated to justify the design selection.

In the past, CAPEX savings in materials of construction were the primary and often *only* interest, but changing business dynamics are forcing businesses to consider even nonprofit issues, such as carbon footprint. With the use of DWCs it is common for the materials of construction of the major processing equipment to be reduced by 30%. Not only is CAPEX reduced, but this reduction in materials of construction also results in energy savings and less impact on the environment.

Pressure on corporations to reduce fossil fuel consumption, reduce carbon emissions and make less of an impact on the environment have made these considerations a real factor in business decisions. In simple terms, this is the concept of doing more with less. DWCs not only give processing plants a lower-CAPEX means of providing the distillation tools to meet a plant's processing objectives, but they also provide improvement on the environmental impact. These advancements make sense for the business world—i.e., they allow changes that improve business economics while simultaneously enabling operators to do more with less, thereby reducing their impact on the environment.

As previously noted, it is common to reduce construction materials of the major processing equipment by 30% when using a DWC design over a conventional one. If the volume of metal and other construction materials needed to build a plant is reduced, then the mining, shipping and processing of the metal ore could be reduced, which would reduce the shipping of this metal to fabrication shops, the fabrication of finished products and the shipping of the products, all of which could potentially lead to a savings of 30% in environmental impact. If all businesses could similarly reduce their environmental impact in building new distillation columns, buildings and other business-related assets, then this would have a significant environmental impact.

Light ends processing. Processing of light ends is commonly required in many different processing units. Common applications include:

- Saturated gas plants (SGP)
- FCC gas concentration plants
- Coker gas plants
- NGL gas plants
- Flare gas recovery.

DWCs can be used in these applications, as well as others, to lower CAPEX and OPEX and to reduce the impact on the environment.

Saturated gas plants. A simplified process flow diagram (PFD) of a common conventional SGP configuration is shown in FIG. 1. Numerous deviations have been used in the flow scheme for SGPs over the years. Designs include complex configurations with refrigeration units; more moderate designs (such as that shown in FIG. 1); lower-cost, simple designs with low LPG recovery; or no SGP where the FCC gas concentration unit processes the saturated gas streams.

Within the design of SGPs such as that shown in FIG. 1, many variations have been used. Debutanizers have been installed upstream of the deethanizer, the primary absorber has been separated from the deethanizer, sponge absorbers have been omitted, intercoolers have been used and not used on the primary absorber, refrigeration systems to supply cold absorption oil have been included, and other deviations have resulted in variations of this basic flow scheme.

Regardless of which conventional PFD has been implemented, the conventional SGP design requires numerous columns to provide quality molecular management and component recoveries. In FIG. 1, the seven product streams (offgas, propane, isobutane, normal butane, isopentane, normal pentane and heavy naphtha) require seven to eight columns to fractionate the crude unit naphtha and lighter compounds into the streams shown in FIG. 1 for sale or further processing. One

technology[a] used in SGPs significantly reduces CAPEX.In three vessels, the DWC technology can produce the same product streams as shown in FIG. 1.

FIG. 2 is one configuration of the proprietary technology[a] for SGPs. The sponge absorber, primary absorber, deethanizer and depropanizer are combined into a single vessel; the debutanizer and deisobutanizer are combined into a second vessel; and the dependentanizer and deisopentanizer are combined into a third vessel. The conventional process flow configuration with seven vessels has been combined into three by utilizing DWC technology. In addition, the required number of condensers, reboilers and pumps is less. Fewer pieces of equipment are needed to construct, operate and maintain. This is the future of all technically advanced SGP designs.

The dependentanizer and deisopentanizer have been combined into a single vessel producing isopentane (iC_5), normal pentane (nC_5) and heavy naphtha streams. This design works well when producing a high-purity nC_5 stream feeding a C_5 isomerization unit. If the isomerization unit is for C_5/C_6 isomerization, then a different configuration is used for the DWC. In this case, a four-cut DWC that produces iC_5, nC_5/C_6, benzene and benzene precursor concentrate, and heavy naphtha streams is the optimum design configuration. High-purity streams are obtained with optimal control of benzene and benzene precursors.

Similarities exist in the design of DWCs to conventional FCCU, coking unit and SGP designs. The proper DWC design takes advantage of these similarities, which have been proven in numerous units operating for years. Using a stabilized naphtha stream as a source of lean oil enables improvement in propane recovery. It is more common to use debutanized naphtha as the lean oil, but naphtha that has been stabilized more thoroughly offers an even better lean oil for propane recovery. The composition of this lean oil stream, along with other operating conditions, determines the vapor/liquid equilibrium at the top of the absorber.

Using lean oil that has been only debutanized will produce enough gasoline-range components in the primary absorber offgas so that a sponge absorber is often used downstream to recover these components. However, when utilizing lean oil that has been more deeply stabilized, it is sometimes possible to eliminate the sponge absorber from the process. In this case, the gasoline components in the offgas are sufficiently low to allow for this design.

The gas compressor discharge cooler and receiver provide multiple functions. The heat of compression must be removed by this exchanger. The separation of the vapor and liquid phases occurs in the receiver before the two phases are fed to the primary absorber and the deethanizer. If fed as a single stream to a single column, the phases are more difficult to separate and, if not separated, could result in premature column flooding. Combining the deethanizer offgas and the primary absorber bottoms with the gas compressor section discharge provides another stage of absorption to improve propane

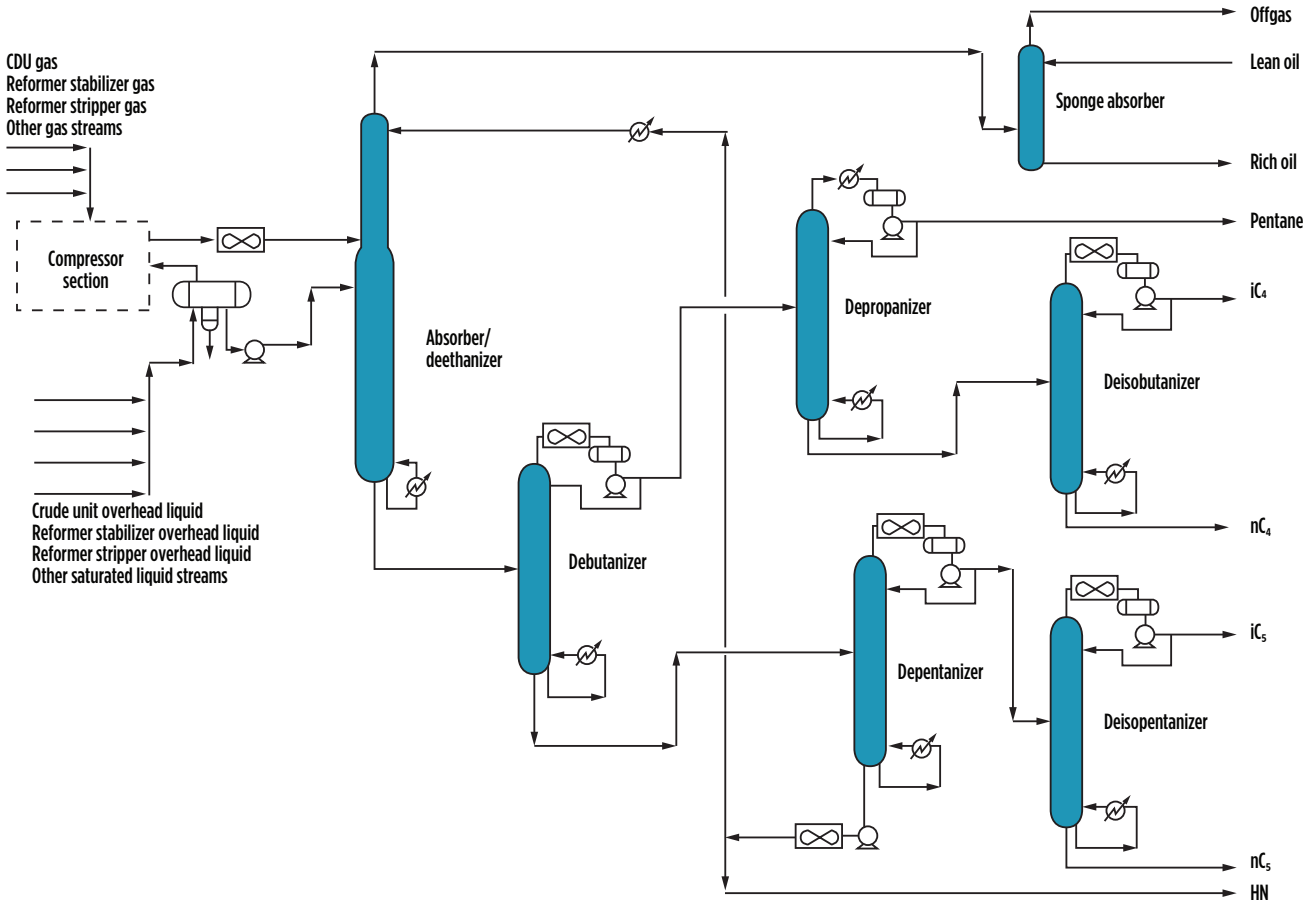

FIG. 1. Conventional SGP simplified PFD.

recovery. The high-pressure receiver also provides the settling time necessary to remove water from the system that otherwise can lead to water entrapment issues. These and other similarities are utilized to provide an effective and reliable design.

The DWC design utilizes two advanced separation units.[b,c] These units are based on well-proven designs that optimize plant CAPEX and maximize product purity to achieve maximum recovery. In comparing FIGS. 1 and 2, seven conventional vessels are combined into three vessels, using DWC technology to provide significant savings in CAPEX and plot space. Not only are the number of vessels reduced, but also the number of foundations is reduced by having fewer columns. The amount of vessel metal is reduced significantly, as is foundation load and material cost. A significant reduction in column insulation, ladders, platforms, etc., is achieved. The number of condenser systems (exchangers, drum, pumps, controls) is reduced from five to two, and the number of reboiler systems is reduced from six to five.

The DWC SGP design can easily operate over the typical range of SGPs and is a lower-CAPEX solution. The simplistic design configuration helps achieve equal or better product recoveries and purities, as compared to any conventional system, but at lower CAPEX. This SGP design can be used without the addition of a high-cost refrigeration system to provide propane recovery of greater than 97%. Molecular management and light ends recovery will become more important than ever to enable shifts to petrochemical feedstock and higher-octane gasoline production. DWCs offer lower-CAPEX means of attaining these demands.

DWC internals design. Some in the industry have expressed reluctance to use DWC technology. However, the introduction of packing internals has been a topic of interest over the past century and, as with DWCs, there was a reluctance to use packing at that time. Great success has been experienced in using packing instead of trays. At the same time, some significant failures have been experienced by those who did not possess adequate design knowledge. DWC internals are no different. Hundreds of applications using DWC designs with success already exist. However, to create this success requires detailed knowledge in designing the process and the column internals.

While a DWC tray can be similar to a conventional tray, it also has some distinctive features that allow proper tray operation. FIG. 3 shows a shop setup of two-pass trays for a DWC that has since been installed. To some degree, the tray is no different than a standard tray design, but here each tray is segmented on each side of the dividing wall.

The basic tray operation is essentially no different than a conventional design. However, there are many enhancements in the design, especially in the transition areas. The proper splitting of vapor and liquid to the two sides of the wall, and how to achieve this, are also important. In addition, the shape of the tray leads to changes in operating parameters, such as weir loadings, which must be taken into consideration. While a DWC tray has similarities to a conventional tray, it also has differ-

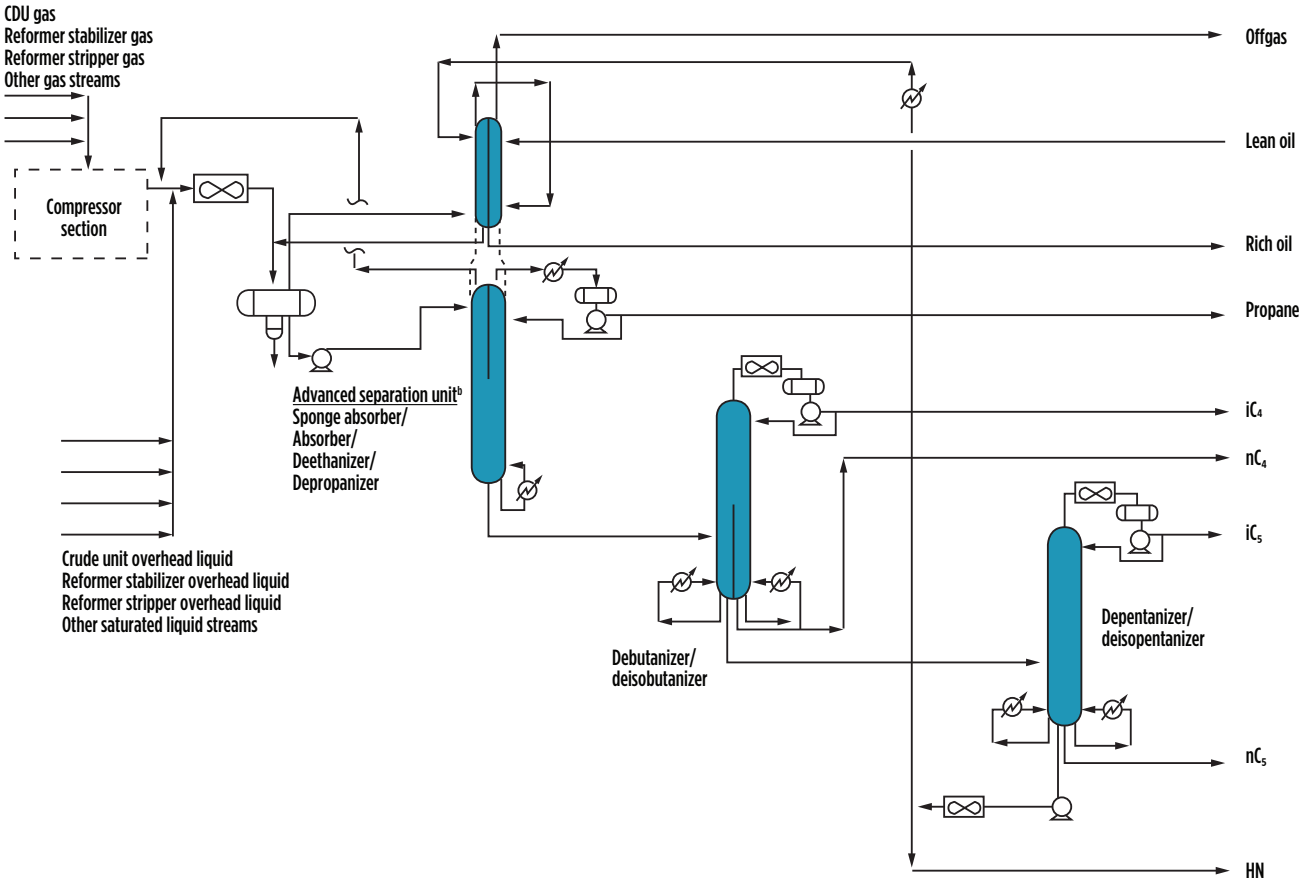

FIG. 2. SGP utilizing proprietary LPG[b] and GWC[c] technologies.

ences that must be taken into account for proper tray operation.

For an equivalent selection of column internals, the design of a DWC tray can provide the same reliability and fouling resistance as a conventional tray design; there is no difference in a DWC from a conventional design. Both require someone who understands the process and how to properly design the column internals and incorporate reliability and fouling resistance into the design as dictated by each process. The selection of the type of column internal is as important with a DWC as it is with a conventional column. If structured packing does not work in a conventional gas plant depropanizer, then it should not be expected to be adequate for use in a DWC that is being used as a depropanizer. As with any technology, the limitations in use must be understood.

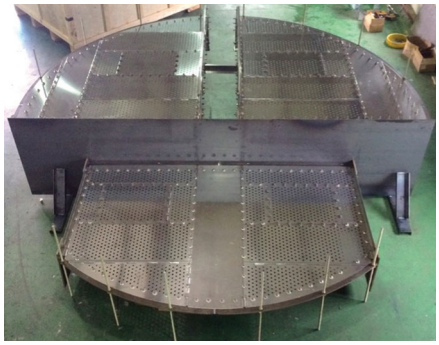

FIG. 3. Shop setup of trays for a DWC.

FCC gas plants. As is seen in the processing schemes for the gas plants shown, the gas plants can be designed in a similar fashion. The primary difference is driven by processing saturates or a combination of saturates and olefins, the value of the products, capital cost limitations and the overall plant design configuration. The compositional difference for the processing of light ends with olefins changes the downstream processing of the gas plant products and leads to variations in the gas plant design.

Consider the similarities and differences in design for an FCC gas plant that processes olefins compared to an SGP. A simplified PFD of a common, conventional FCC gas concentration plant configuration is shown in **FIG. 4.** Those familiar with FCC gas concentration plants know that numerous deviations in the PFD have been used over the years. Depropanizers have been installed upstream of the debutanizer, the primary absorber has been stacked on top of the deethanizer, dependentanizers have been installed in front of the debutanizer, intercoolers have been used on the primary absorber, refrigeration systems to supply cold absorption oil have been used, and other deviations in the process flow scheme have resulted in variations of this basic flow scheme.

Regardless of which conventional process flow scheme has been used, the conventional designs require five to six columns to fractionate the FCCU naphtha and lighter compounds into the streams shown for sales or further processing. The FCCU gascons utilizing the DWC process significantly reduces CAPEX. The DWC process can produce the same product streams shown in the conventional processing scheme of **FIG. 4,** with the same or improved purity and recoveries in two vessels. **FIG. 5** is one configuration of a proprietary technology[a] for FCC gas concentration plants. The sponge absorber, primary absorber, deethanizer and C_3/C_4 splitter are combined into a single vessel,

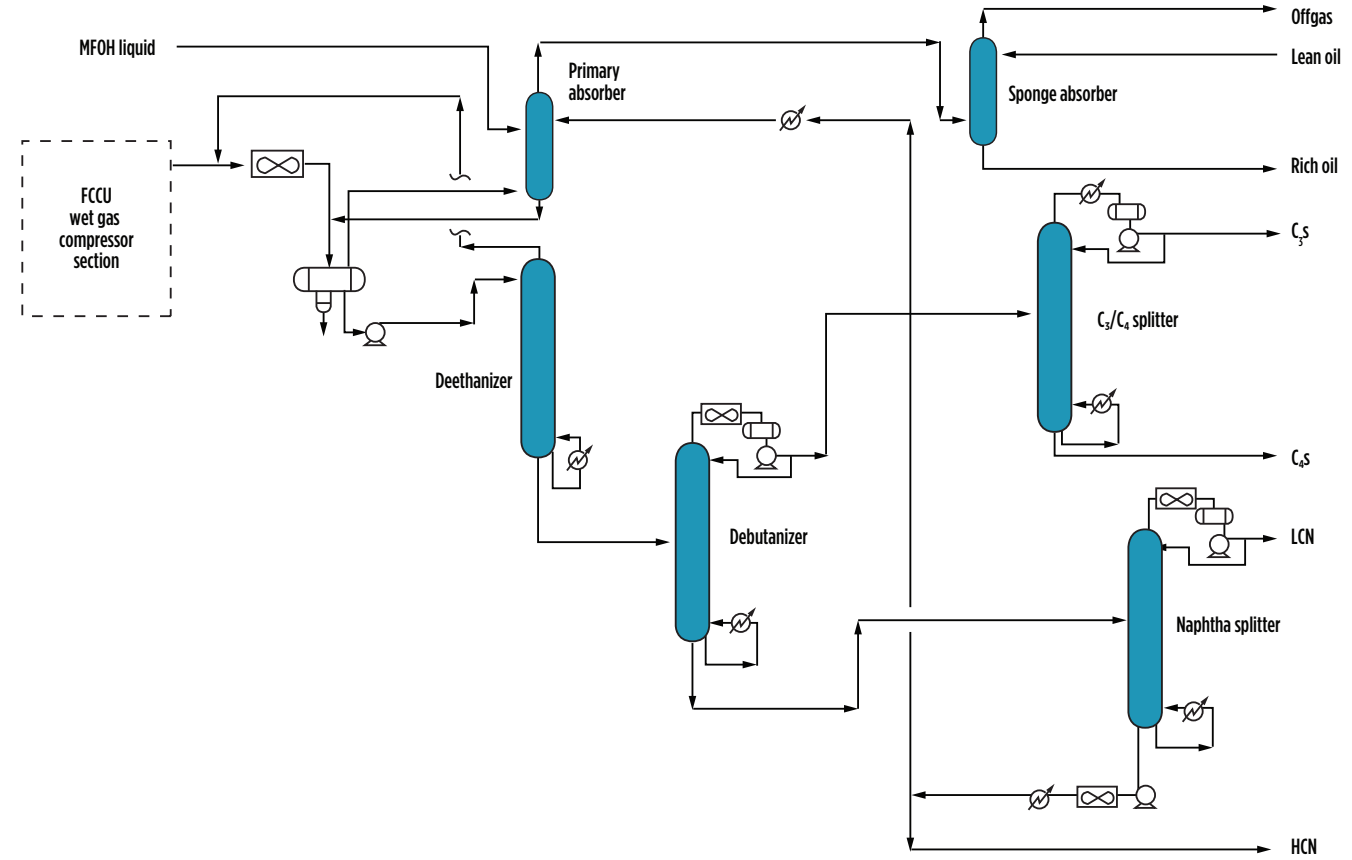

FIG. 4. Conventional FCCU gascon simplified PFD.

and the debutanizer and naphtha splitter are also combined into a single vessel. The conventional process flow configuration with six columns has been combined into two vessels by utilizing DWC technology.

As with the SGP, similarities exist in the design of the DWC technology compared to a conventional FCCU gas concentration plant design. The proper design takes advantage of these similarities, which have been proven by numerous FCCUs in operation for years. Using a stabilized naphtha stream as a source of lean oil enables improvement in propylene recovery. It is more common to use debutanized naphtha as the lean oil; however, naphtha that has been more deeply stabilized is more effective for propylene recovery.

As with the previously described SGP design, the composition of the lean oil stream, along with other operating conditions, determines the vapor/liquid equilibrium at the top of the absorber. Using lean oil that has only been debutanized results in enough gasoline-range components in the primary absorber offgas that a sponge absorber is normally used downstream to recover these components. Sometimes, when utilizing lean oil that has been more thoroughly stabilized, the sponge absorber may be eliminated. The gasoline components in the offgas are sufficiently low to allow for this design.

The wet gas compressor discharge cooler and high-pressure receiver provide for the removal of heat of compression, separate the vapor and liquid phases prior to the column, and combine the deethanizer offgas and the primary absorber bottoms with the wet gas compressor section discharge, which provides another stage of absorption, thereby improving propylene recovery. Separating the phases prior to the column helps eliminate issues with premature flooding of the column, especially if significant swings occur in the proportion of C_2– components in the feed to the gas plant. The high-pressure receiver also provides the settling time necessary to remove water from the system that otherwise can cause water entrapment problems. These and other similarities are utilized to provide an effective and reliable design.

Experienced operators of FCC gas concentration units understand the problems associated with water entrapment. Some have utilized inferior design configurations that have operated adequately; however, as FCC shifts toward maximum propylene operation and design to increase propylene recovery, the design of the system becomes more important. Inferior designs will not work. As refiners shift from maximum gasoline mode to maximum propylene production, the problem with water entrapment becomes worse.

The DWC design utilizes two advanced separation units.[b,c] These units are based on well-proven designs that optimize plant CAPEX and maximize product recovery and purity for maximum recovery. Six conventional columns are combined into two vessels using DWC technology to provide significant savings in CAPEX and plot space. A significant reduction in column insulation, ladders, platforms, etc., is seen. The number of condenser systems (exchangers, drum, pumps, controls) is reduced from three to two, and the number of reboiler systems is reduced from four to two.

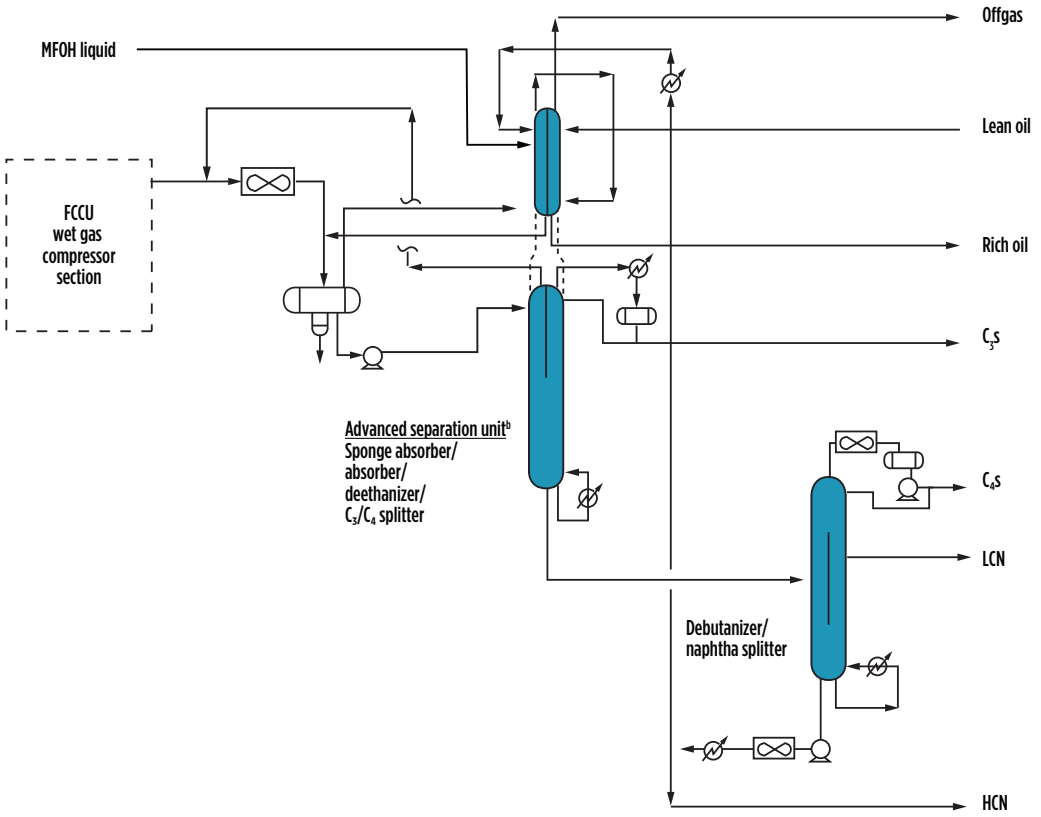

FIG. 5. FCCU gas concentration plant utilizing proprietary technologies.[b,c]

To better understand the reasons for the reduction in CAPEX, a design combining the primary absorber and sponge absorber columns is studied. In this design, the primary absorber, sponge absorber, deethanizer and C_3/C_4 splitter are combined, which reduces the number of foundations from four to one. For simplicity, however, it can be assumed that only the primary absorber and sponge absorber are being combined. In this case, two columns have been combined, with a common wall separating them. Typically, gas plants are designed for operating pressures of 180 psig–450 psig (12.66 kg/cm^2–31.64 kg/cm^2). This requires thick vessel walls, whereas the pressure differential across the wall separating these two columns is only about 2 psi (0.14 kg/cm^2), resulting in a thin wall for construction.

Combining the two columns in this manner results in an approximately 30% reduction in metal. The quantity of column insulation is reduced by a similar amount. The vessel ladders and platforms can be reduced essentially by half. Only one instead of two foundations needs to be designed and constructed. The reduction in vessel weight reduces the foundation load, which reduces the construction cost of the foundation. These and numerous other reasons are why DWCs are characterized by significant CAPEX savings.

The DWC FCC gas concentration unit design can easily operate over the typical operating range of FCCUs and is a lower-CAPEX solution. The simplistic design provides for achieving equal or better product recoveries and purities as a conventional system at lower CAPEX. FCC gas concentration design can be used without the addition of a high-cost refrigeration system to provide propylene recovery of greater than 97% in FCCUs designed for maximum gasoline mode.

Changes in global refinery product demand will continue to drive changes in the optimum configuration and operation of FCCUs. Petrochemical market demand will continue to rise, with an expected declining or flat market demand for refined products. As high-compression engines become more prevalent, an increase in the percentage of high-octane gasoline blending components required for the gasoline pool will be necessary. Shifting the FCCU operation to increase propylene and butylene for petrochemical feedstock and higher-octane gasoline production is a piece of the puzzle. Proprietary technology[a] offers a lower-CAPEX means of attaining these demands.

Takeaway. The distillation technology[a] discussed in this article provides designs that can significantly reduce CAPEX and OPEX while improving refinery molecular management and lowering the impact on the environment. This technology not only improves business economics, but also helps reduce fossil fuel consumption, carbon emissions and impacts to the environment. HP

NOTES

[a] GT-DWC Advanced Distillation
[b] GT-LPG Max
[c] GT-DWC

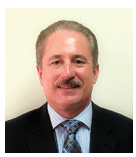

GARY R. MARTIN is Business Segment Leader for dividing wall column (DWC) technology at Sulzer GTC Technology. He develops new technology utilizing DWCs and creates marketing for DWC technology. Previously, he was President of Process Consulting Services. His experience has included conceptual process design and process design packages for large capital projects, optimization and troubleshooting services to the refining industry worldwide. Mr. Martin earned a BS degree in chemical engineering from Oklahoma State University, and has published more than 60 technical papers.

J. E. ECHENAGUCIA, Heatoil Solutions LLC, Venezuela

Reverse refining: A novel approach to the refining process

The crude oil refining processing sequence is based on the separation of distillate products from heavier ones and concentrating the heavy molecules of the barrel for processing at the end of the refining run. Processes developed to convert the concentrated bottom of the barrel into valuable distillates include hydrocracking or coking (hydrogenation or carbon rejection methods). In essence, the processes to convert the long-chain hydrocarbons—which are heavily concentrated in the bottom of the barrel—are complex, costly and limited to larger-sized units (e.g., 30,000-bpd minimum crude throughput).

Reverse refining. This article will detail several benefits of first converting the heavy molecules of the barrel at the beginning of the refining run before the separation and treatment of the end products are performed. In this alternative, converting asphaltenes into aromatics and saturates (i.e., aromatic, cyclic and paraffins) is accomplished at the beginning of the refining process sequence.

It is a better alternative to use a lower-cost thermal cracking process (i.e., visbreaking) to reduce the asphaltenes to a minimum before the crude enters the atmospheric distillation process. Using a thermal cracking process, converting the asphaltenes at the beginning of the refining process has the following advantages:

- It allows the refiner to purchase less-expensive crude (such as heavy or extra-heavy crude) and to convert it to its appropriate quality prior to the refining process. By adjusting the heavy ends conversion and the production of distillates before entering the refining process, this minimizes the tedious blending required to optimize the crude-quality feed to the process plants. This alternative could save refiners $10/bbl–$15/bbl.
- It optimizes the crude-quality feed to the refinery. Using the present conventional refining process flow is complex and costly; however, the reverse refining method is a simpler alternative.
- This process significantly lowers crude acidity and sulfur content by cracking the naphthenic acids and converting the sulfur molecules in crude oil into hydrogen sulfide (H_2S). Naphthenic acids are converted into saturated molecules, while the H_2S is separated from the upgraded crude to be treated in the acid gas plant. The result is a reduction of metal corrosion of the crude feed to the refining process.

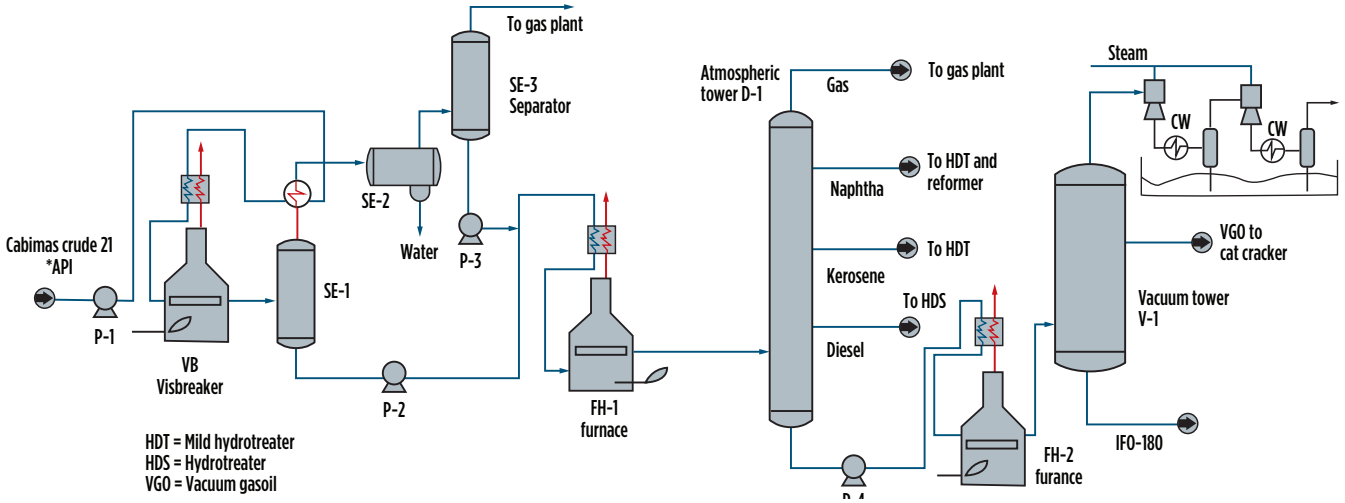

FIG. 1. Reverse refining process flow diagram.

In addition, the sulfur content of the heavy molecules of the barrel is reduced below 0.5 wt% to comply with International Maritime Organization (IMO) requirements.
- Converting the heavy, 530°C residue into distillate before it enters separation and treatment units replaces the investments in more costly and complex residue conversion units, such as delayed coking and hydrocracking.
- It simplifies the process flow scheme of the refinery for a deep conversion of the crude barrel, thus significantly reducing the capital investment and operational costs of the refining process.
- The proposed refining process allows for the construction of small, low-cost modular refineries, which can help supply local market demand. These units can be built near oil production fields, thus reducing the crude diluent and/or heating aspects of transportation costs.

This reverse refining method saves on capital and operational costs, leading to higher margins.

TABLE 1. Crude assay of Cabimas crude oil

Analysis	Component	Value
Specific gravity, ASTM D4052	API gravity at 60°F	21.3
Specific gravity, ASTM D4053	Specific gravity at 60°F, gr/cc	0.9261
Sulfur, ASTM D4294	Sulfur content, wt%	1.98
Micro carbon residue test, ASTM D4530	Micro method carbon residue, wt%	7.69
Total acid number, ASTM D664-A	Acid number, mgKOH/gr	1.01
Vapor pressure-crude oil, ASTM D6377	VPCR, psi	3.2
Viscosity, kinematic at 60°F, ASTM D445	Kin viscosity at 60°F, cSt	274.9
Viscosity, kinematic at 40°F, ASTM D446	Kin viscosity at 40°F, cSt	68.07
Pour point, ASTM D5950	Pour point calculated, °F	50.8
Bromine no., UOP 304	Bromine no., grBr/100 gr	4.22
Metals ICP-AES D5708	Nickel, ppm wt	30
Metals ICP-AES D5708	Iron, ppm wt	3.3
Metals ICP-AES D5708	Vanadium, ppm wt	277
Metals ICP-AES D5708	Sodium, ppm wt	7.4
Metals ICP-AES D5708	Nickel-vanadium index, ppm wt	307
Metals ICP-AES D5708	Silicon, ppm wt	< 1
Metals ICP-AES D5708	Phosphorous, ppm wt	< 1.01
Simulated distillation curve, ASTM D7169	**°C**	**°F**
Initial boiling point	36	96
5 wt%	137	279
10 wt%	195	383
20 wt%	274	525
30 wt%	336	637
40 wt%	397	747
50 wt%	455	851
60 wt%	516	960
70 wt%	583	1,081
80 wt%	651	1,204
85 wt%	684	1,263
86 wt%	691	1,276
90 wt%	721	1,329
91 wt%	729	1,345
92 wt%	739	1,363
Final boiling point	792	1,457

Capital cost comparison: Reverse refining vs. traditional refining. The following details a capital investment cost comparison between the processes to convert vacuum residue into distillates. A comparison is made of the traditional refining sequence vs. the reverse refining process. The crude oil selected for this comparison is Cabimas (Venezuela), with an API gravity of 21.3°. The Cabimas crude assay is shown in TABLE 1.

Traditional refining. Cabimas crude yields, along with the results of processing it by delayed coking and slurry-bed hydrocracking technologies, are shown in TABLE 2. The second column shows the original Cabimas crude assay wt% yields. The third and fourth columns show the Cabimas crude yields processed through traditional refining—i.e., using a delayed coker or hydrocracker slurry-bed reactor for vacuum residue conversion.[1,2]

Feeding 20,000 bpd of Cabimas crude to the traditional refining atmospheric distillation column results in approximately 12,666 bpd of atmospheric residue. This atmospheric residue is fed to a vacuum tower, where approximately 6,224 bpd of Cabimas vacuum residue will be produced. The vacuum residue must be sent to a coking unit or hydrocracker to convert it into distillates. TABLE 3 details the costs of processing and converting 20,000 bpd of Cabimas crude into distillates, using the traditional refining scheme.

The updated 2020 plant costs were estimated using costs published in literature.[3,4] The capital cost of vacuum residue upgrading in the traditional refining scheme is between $122 MM and $162 MM.

Reverse refining. The reverse refining process converts the Cabimas crude into distillates, using the visbreaker process before the final separation and treatment process take place (FIG. 1). After the crude passes through the visbreaker's reactors, water is separated and the gas product flows to an acid gas separator drum to be split into two fractions: a light fraction is taken to an acid gas separator, and the higher fraction is sent to the atmospheric preheating furnace. In the

atmospheric distillation tower, gas, naphtha, kerosene and gasoil are separated into products that will be hydrotreated to final specifications. The atmospheric residue goes to the vacuum tower (V-1), where vacuum gasoil (VGO) is separated as a final product and part of the VGO is left in the residue to adhere to viscosity specifications in IFO-180. The rest of the VGO should be sent to the catalytic cracker and alkylation units to be converted into gasoline and diesel products.

Reverse refining is an ideal alternative for the construction of small, low-cost deep conversion modular refineries, which can help supply local market demands. These units could be built near oil production fields to lower crude diluent and/or heating transportation costs.

All processes involved in this model are commercial processes that have been in operation for more than 80 yr. The visbreaking process was developed and put into commercial use in the 1930s. The process has been used in the traditional refining sequence to convert atmospheric and vacuum residue (maximum of 10° API) into distillates. The viability of using the visbreaker process for crude conversion was proven with lab equipment, followed by a 240-bpd pilot plant installed at the Tia Juana oil field in Venezuela (FIG. 2). The results of a crude oil run in April 2018—at maximum reactor severity temperature—for 11° API Tia Juana Heavy crude are shown in TABLE 4. As illustrated, the crude conversion in the visbreaker process is very efficient, improving all chemical properties of the original crude.

TABLE 5 shows the comparison of Cabimas crude yields, using other available residue conversion technologies vs. reverse refining. In this case, the thermal cracking units were run at maximum severity; therefore, the overall selectivity of the process resulted in a higher naphtha yield. The selectivity of the process can be adjusted in the thermal cracking units to modify the yield pattern, as required.

The data in TABLE 5 shows that the reverse refining scheme generates 35 wt% additional distillates when compared with the crude oil assay yields. The delayed coker generates a 5% gain in distillates, but with a 23 wt% loss in crude to coke. The slurry-bed hydrocracker generates 21 wt% more distillates vs. the original crude distillates content.

TABLE 6 shows the estimated capital expense for the process equipment shown in FIG. 1. Besides the benefits previously mentioned, there is a sizable reduction in capital investment by using the reverse refining scheme. Pilot plant capital costs were used as the basis for visbreaking capital cost estimation.

Takeaway. The refining process sequence is based on reducing heavier hydrocarbons and contaminants into a minimum volume, followed by using more expensive and complex technologies to convert the concentrated residue into valuable distillates.

This article has shown that reversing the present refining process sequence—

FIG. 2. View of the 240-bpd coil visbreaker pilot plant.

TABLE 2. Cabimas crude assay and other vacuum residue conversion technologies

Components	Cabimas crude assay, wt%	Delayed coker[1], wt%	Slurry bed[2], wt%
Sulfur	1.98	0.79	0.5
H_2S	0	0.59	3
Natural gas	0.17	10	11
Naphtha	5.45	16	17
Kerosene	11.37	3.41	6
Gasoil	18.5	17	48
Vacuum gasoil	26.69	29	12
Residue (> 530°C)	35.84	0	2.5
Coke	–	23.21	–
Total	**100**	**100**	**100**

TABLE 3. Traditional refining scheme: Capital expenditure of residue conversion plants

Unit	$/bbl (2020)	Plant capacity, bpd	Distillation, $	Coker, $	Hydrocracker, $
Atmospheric distillation	1,400	20,000	28,000,000	–	–
Vacuum distillation	1,256	12,666	15,908,496	–	–
Delayed coker	12,640	6,224	–	78,671,360	–
Residue hydrocracker	19,125	6,224	–	–	119,034,000
		Total	**43,908,496**	**122,579,856**	**162,942,496**

TABLE 4. Crude run at the 240-bpd pilot plant using Tia Juana Heavy crude

Sample	Viscosity, cSt	°API	Sulfur, wt%	Water, %	Salt, %	Acidity, mg KOH/gr	Pour point, °C	Flash point, °C	Ramsbottom carbon, %	Nitrogen, ppm
Original crude	57.9	11.14	2.63	2.5	1.2	3.6	27	65	2.6	5,860
Upgraded crude	5.72	30.55	0.95	0.5	0.8	0.18	7	43	0.93	1,030

	Saturate, aromatic, resin and asphaltene (SARA) analysis									
Sample	Saturated	Aromatics	Resins	Asphaltenes	Aniline point, °C	Bromine no.	H/C ratio	Flash point, °C	Ramsbottom carbon, %	Nitrogen, ppm
Original crude	20.5	48.5	12.9	18.1	1.2	10.7	1.52	65	2.6	5,860
Upgraded crude	23.6	53.2	12.7	10.5	0.8	1.2	1.71	43	0.93	1,030

Sample	Thermal stability, %	Oxidation stability, %	P value
Original crude	18.1	9.23	4.4
Upgraded crude	10.5	0.14	2.9

TABLE 5. Cabimas crude yields using residue conversion technologies

Components	Cabimas crude assay, wt%	Delayed coker[1], wt%	Slurry bed[2], wt%	Reverse refining, wt%
Sulfur	1.98	0.79	0.5	0.25
H_2S	0	0.59	3	1.73
Gas	0.17	10	11	9.76
Naphtha	5.45	16	17	34.78
Kerosene	11.37	3.41	6	4.98
Gasoil	18.5	17	48	23.75
VGO	26.69	29	12	23.51
Residue (> 530°C)	35.84	0	2.5	1.25
Coke	–	23.21	–	–
Total	**100**	**100**	**100**	**100**

TABLE 6. Reverse refining scheme: Capital cost of residue conversion plants

	$/bbl	Plant capacity, bpd	Total cost, $
Visbreaker plant and separators	2,590	20,000	51,800,000
Atmospheric distillation unit	1,600	20,000	32,000,000
Vacuum distillation unit	1,300	2,000	2,600,000
		Total	**86,400,000**

converting the asphaltenes into aromatics and saturates before the products are separated and treated—has several advantages, including:

- When processing Cabimas crude, the reverse refining scheme generates 35 wt% additional distillates. Delayed coking generates a 5 wt% distillate gain, but an overall loss of crude into coke of 23 wt%. Hydrocracking technology generates 21% additional distillates when compared to the original crude oil assay distillates content.
- This scheme allows the refiner to buy a less expensive crude (such as heavier, sour and/or higher-acid crude).
- It is no longer necessary to buy several qualities of crudes to obtain the optimum refinery crude diet.
- This process reduces crude acidity and sulfur content to the low limits required by environmental regulations prior to entering a refinery's separation and treatment equipment.
- It allows the refiner to change product slates by changing the severity of the visbreaking process.
- There is a lower capital cost for the reverse refining scheme. The capital cost for reverse refining is 29%–53% lower than delayed coking and hydrocracking technologies.
- This scheme allows refiners to build small-capacity (e.g., less than 5,000 bpd), modular refineries or crude upgrading plants near or within oil production fields to either sell product in the local market or prepare it for export. HP

LITERATURE CITED

[1] Jarullah, A., "Delayed Coker," *Petroleum Refining—Fourth Year,* Tikrit University, Iraq.
[2] Biswas, G., "Residue Hydrocracking Technologies," Chevron Lummus Global.
[3] Pelegry, E. A., *et al.,* "The Oil and Gas Value Chain: A Focus on Oil Refining," Orkestra–Instituto Vasco de Competitividad, November 2018.
[4] Kaiser, M., "A Review of Refinery Complexity Applications," *Petroleum Science,* 2017.

JORGE ENRIQUE ECHENAGUCIA earned a PhD in chemical engineering from Virginia Polytechnic Institute. He has 47 yr of experience in the areas of crude oil production and refining. Dr. Echenagucia is the CEO of Hot Oil Engineering LLC, focusing on the process development of low-capacity, deep-conversion modular refineries.

M. BROOKS, AspenTech, Alamo, California

If you want AI to overcome limitations, give it more scalability

Artificial intelligence (AI) has caused a significant buzz not only within the hydrocarbon processing industry but also in everyday activities. AI seems to be everywhere. It is in autonomous vehicles, it can recognize images of people and cats vs. dogs, and bank and credit card companies use it for fraud detection, among others. The application of AI is seemingly endless.

Since 2015, AI has become more pervasive and obvious as Alexa, Siri and Google Assistant help us when asked. Even AI-powered washing machines can cut laundry time, and product and services companies use AI to tell us what books we might like to read, what music we can enjoy and what movie will fit the bill for Friday night.

The essence of AI is about learning from data and using it to determine the probability of future outcomes based on the patterns learned from the past. This emulates a human characteristic. If you watch a specific area, situation or process long enough, you may develop insights. When similar things occur again, you could guess with some accuracy what is going to happen next. Other people have read the books you have and based on recognizing similar patterns, Amazon suggests you will enjoy another title just as much as others who read the same books. It sounds simple enough, but is it?

The Challenge with AI. Standard AI can recognize patterns but cannot reason why things occur the way they do without substantial help from humans. We often hear that AI sees correlations, which may be simplistic and just happen without being linked. AI cannot determine why it happens—i.e., the causation. For example, data from literature[1] showed an interesting correlation: the more lemons imported to the U.S. from Mexico, the fewer U.S. highway fatalities occurred. Correlation does not necessarily mean causation—no one would seriously believe there is cause-and-effect in the referenced example; however, the problem is that AI cannot tell the difference. It turns out that humans are better at judgment and have the ability—unlike AI—to assess whether the observed correlations make sense. Consequently, despite such challenges for AI technology within industrial manufacturing, there appears to be great potential and opportunities if AI applications are tempered appropriately to overcome the limitations.

AI can create more value than is currently extracted from industrial data, especially since most data is used for viewing trend charts for scarce insight development. Intelligent data gathering and grouping with AI-driven analytics can greatly assist in helping people make more accurate judgments and better decisions. The overarching goal of AI is to uncover new and better business processes that promise significant, positive business outcomes across key areas, such as manufacturing operations profitability, safety, environmental impact and corporate social responsibility.

To be effective, AI cannot be just a technology thrown at problems. We can refer to the adage "people, process and technology" to gain solace. We believe that the importance of incorporating domain knowledge is seriously overlooked by startup companies and service providers who are trying to enter the space. Industrial AI is the realization that scalability of any solution is the most important factor.

The dimensions of industrial AI. Industrial AI incorporates several important dimensions. These include the following:

- Many people must be able to use AI. To be pervasive, it cannot just belong to data scientists. Plant personnel must be able to build and deploy AI solutions based on what they know now. This is very similar to the iPhone, which contains deep technology, but the user does not need to know it since an elegant screen and a finger as a pointer complete the task. Consequently, with industrial AI, the competence level of workers is elevated and gravitates to making judgements on potential outcomes rather than doing the continuous and repeated heavy-lifting of deep analytics.
- Industrial AI solutions fit current work processes well without huge departures.
- Judgement from workers' domain knowledge is imparted as the industrial AI solution building process begins. This is where domain knowledge from workers provides guardrails around an AI solution to ensure it will realize true causation rather than simple correlation. Embedding is simple and easy so that users can insert what they know (e.g., when an event occurs, this sensor shows a condition and then "this" will happen). Those are the clues that form the guiderails that influence the solution direction and the best outcomes.
- With industrial AI, the step-by-step work process is built into the application building to make it simple and easy (e.g., booking a plane ticket or ordering a product on a website).
- As much judgment as possible must be built into the application to assist the user even further, adding even more domain knowledge. Industrial AI does not use

AI to just analyze the new data when a solution goes live. Instead, with or without user help, embedded AI helps define the solution strategy to select the right data sample times and data groupings for training and testing. This helps discover hidden and potential unknown relationships between events that occur and different data types—referred to as "feature selection" by the data science community.

- Industrial AI uses a combination of AI analysis and human judgement in the beginning to determine which data is valuable and which must be discarded. Most AI detects anomalies, so getting the right baseline is extremely important for accurate detection of abnormal conditions and to eliminate false positives.
- Industrial AI ensures that it is simple, easy and rapid to cover different types of equipment. This includes not only big machines that spin but all equipment (e.g., rotating, static, mobile, process and mechanical). Scalability also guarantees that what is learned as normal behavior and explicit failures on one machine is spread rapidly without intense engineering effort—from one asset to many that are the same (e.g., providing all boiler feedwater pumps the same safety and breakdown protection).
- Application sustainability ensures industrial AI automatically adapts—with minimum effort—to changing process conditions, keeping the solution updated and on point without re-engaging engineering experts and data scientists.

Takeaway. Only with scalability capabilities can industrial AI deliver more accurate performance to enable better judgement and faster decision-making. The author's company recognizes that industry needs guardrails around AI-embedded products to ensure causation is found and not just simple correlation. Those combinations mean that the products provide assertive insights immediately within the alert messages to enable rapid human judgement and remove post-alert extended analysis. Lastly, industrial AI products uncover new business processes, simultaneously evaluating thousands of different scenarios to uncover optimal processes that tie to specific business goals. HP

LITERATURE CITED

[1] "Distinguishing between correlation and causation: A key to critical thinking," Oregon State University, February 2014, online: https://blogs.oregonstate.edu/econ439/2014/02/03/distinguishing-correlation-causation-key-critical-thinking/

MIKE BROOKS is an Asset Performance Management consultant at AspenTech. Previously, he was Chief Operating Officer of Mtell, which pioneered machine learning for managing the health of industrial equipment. Mr. Brooks also served as a venture executive with Chevron Technology Ventures and held senior roles at five startups. He began his career as an engineer at Esso and Chevron.

G. GOUS and **P. DE VAAL,** The University of Pretoria, Pretoria, South Africa

Integral vs. proportional gap for averaging level control

In process plants, many instances of level control are required to keep the material balance of the plant from integrating to undesired operating conditions. Level control of distillation column bottoms or reflux drums are good examples. Here, the column will overfill or de-inventorize if the average of the sum of the distillate and bottoms flow is not kept the same as the average feed to the column. While this condition must be met, the plant is simultaneously afforded the opportunity to let these levels drift away from setpoint (SP) to stabilize the flows that are manipulated to control the levels. If this is done correctly, a huge benefit can be achieved in terms of stability of downstream equipment. This is referred to as level buffering or averaging level control.

Some levels require very tight adherence to SP and averaging level control should not be applied. Examples of these systems include levels in knock-out pots where little volume is available to separate liquid and vapor streams. In these systems, vapor or liquid carryover into the wrong outlet can typically lead to severe process upsets or equipment damage; therefore, tight level control with aggressive tuning is applied.

If averaging level control is done incorrectly and the level controller's process variable (PV) is allowed to stray too far from SP, process issues—such as pump cavitation or liquid carryover—can occur. These process conditions should normally be avoided by using alarms to warn the operator of impending issues, as well as trips to prevent such occurrences. Alarms or trips are undesired occurrences, and care should be taken when tuning averaging level controllers, as frequent alarms or trips will cause operators to lose faith in the control solution and find ways to circumvent it.[1] This behavior sometimes influences process control engineers to forego the benefits of averaging level control altogether. Many instances can be found in industry where tight level control allows plant upsets to be propagated to downstream equipment, and often the effect of an upset is amplified rather than mitigated.

Many plants have feed drums and tuning these level controllers tightly essentially reduces a drum to nothing more than a pipe, wasting the initial capital outlay of installing the drum. In some instances, feed drums or tanks are used to ensure the availability of feed material during upstream process upsets—in these cases, levels are kept at a high SP, keeping the drum full in case of a disruption in feed flow. Additionally, a small amount of averaging level control can still provide substantial stabilizing benefits while keeping the level at a high average value.

Averaging level control methods can also be applied to integrating variables other than levels. A typical example is a gas/vapor pressure that is controlled by manipulating the gas flow into or out of a vessel or pipeline.

Many averaging level controllers are deployed using PI, gap or non-linear controllers and tuning rules exist to optimize their performance.[1,2,3]

Discussion. A typical PI controller equation that is commonly used in industrial distributed control systems (DCSs) is shown in Eq. 1:[4]

$$\delta OP = K_c \times \left[\left(E_n - E_{n-1} \right) + \frac{ts}{T_i} E_n \right] \quad (1)$$

where:

δOP = change in controller output
K_c = controller gain, a tuning variable
E_n = PV error (PV-SP) at the current execution cycle
E_{n-1} = PV error at the previous execution cycle
ts = execution cycle time of the DCS
T_i = integral tuning constant.

When a level is subject to a disturbance, the PV will begin moving away from SP, causing PV error (E_n) to increase if the disturbance moves the PV upward. Eq. 1 shows that while the PV is moving away from SP, the proportional action (Eq. 2) and the integral action (Eq. 3) will have the same sign:

$$K_c \times \left[\left(E_n - E_{n-1} \right) \right] \quad (2)$$

$$K_c \times \left[\frac{ts}{T_i} E_n \right] \quad (3)$$

While the PV is moving away from SP, both proportional and integral will work together to reject the disturbance.

When enough control action has been taken to reduce the rate of change of the level to zero, proportional action will have reduced to zero because ($E_n - E_{n-1}$) will be zero. The integral action will keep manipulating the OP to reduce E_n to zero.

Next, the level will begin returning to SP. During this phase, proportional and integral will oppose each other. Integral action will still attempt to reduce error (E_n) to zero, while proportional will react to the reduction in error ($E_n - E_{n-1}$ will now be negative) by moving the OP in the opposite direction. It can be seen as integral driving the error to zero while

proportional is applying the brakes to prevent the PV from overshooting SP.

The PI tuning should be such that during this phase the proportional control is strong enough to not permit the integral action to cause overshoot. If this is not done, a slow cycle in the level will result, negating the desired benefits of averaging control. In gap and non-linear controllers, this effect is made worse by the decrease in proportional tuning when the PV is close to SP.

When conducting averaging control, the dilemma is that weak proportional control is needed to allow the level to deviate from SP to minimize OP movement. However, the need to have the integral action weaker than proportional during the phase when the PV is returning to SP remains. Therefore, in averaging level control the integral action must be tuned very weakly to prevent the level from cycling.

Very weak integral action means that the level will take a very long time to return to SP. When using typical PI tuning for averaging level control,[1,2,3] it will typically take more than six times longer to return the level to SP than the time it takes to turn the level after a disturbance, as can be seen in **FIG. 1.** Depending on the frequency of disturbances, this may be a problem as new disturbances may occur while the PV is still far away from SP.

To enable more aggressive tuning when the PV is close to limits while still allowing the controller to slow down the approach to SP enough to prevent overshoot, the integral gap controller (IGC) is proposed. Defining an integral gap as a set distance above and below SP where less integral control action is taken when the level is close to SP (error is small)—while taking more aggressive integral action when the level is farther from SP (error is large)—takes care of the potential overshoot when the level is returning to SP. This is done by changing the value of T_i in Eq. 1 from a larger number ($T_{i\ in\ gap}$) to a smaller number ($T_{i\ outside\ gap}$) when the PV moves outside the gap.

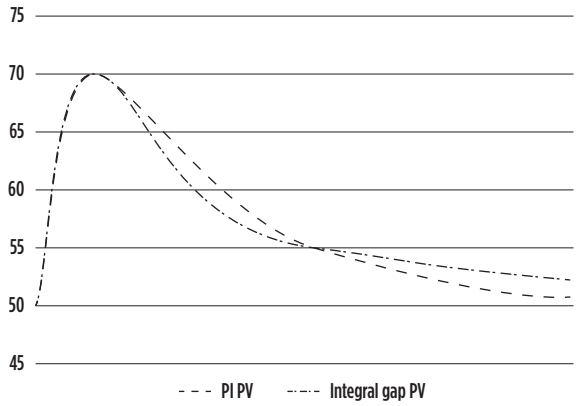

FIG. 1. PV response of PI and IGC to a positive disturbance.

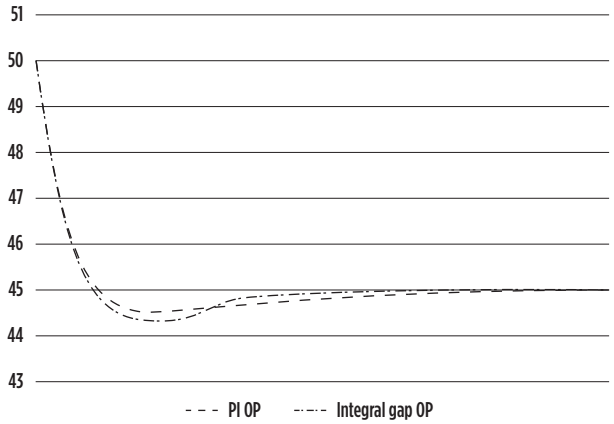

FIG. 2. OP response of PI and IGC to a positive disturbance.

When this is done, a disturbance will start the level moving away from SP. Proportional control will counteract the increase in level while little integral action will be taken. Once the level moves outside of the defined gap, integral action will increase to assist the proportional in changing the direction of the level until the level will start moving back to SP. Proportional control will work in the same direction as integral, both attempting to turn the level back to SP.

Once the level has turned, the increased integral action will still be applied, increasing the rate at which the level will return to SP. At this stage, proportional control will start working against the integral action, attempting to slow down the return to SP. As the integral action is still tuned aggressively, it should overshadow the proportional, causing the level to quickly return to SP.

Once the level moves back into the gap, decreased integral action will decrease the effect of moving the PV back to SP. Proportional action will still react to the decrease in error, slowing the rate of change of the level and preventing overshoot or a possible cycle. If tuning is applied incorrectly, the proportional may overpower the decreased integral action in the gap to the point where the level will again not reach SP in the desired timeframe.

Tuning the IGC is done by setting:

- The width of the integral gap (how far the PV must be from SP before the integral action is increased)
- The tuning constant for the integral action when the PV is in the gap ($T_{i\ in\ gap}$)
- The tuning constant for the integral action when the PV is outside the gap ($T_{i\ outside\ gap}$).

The tuning of the proportional gain (K_c) is done as for a typical PI controller.

By setting the gain, the integral tuning and the gap correctly, the IGC can:

- Avoid causing overshoot
- Aggressively return the PV to SP while the error is large
- Slow down the controller while the error is small.

Simulation. To demonstrate the principle, a level was simulated and controlled using a typical DCS used in industry. The IGC was compared to a PI controller that was tuned to prohibit the level moving further than 20% from SP when the maximum disturbance of 5 m^3/hr occurs. To illustrate the outcome of using the IGC, the gap size as well as the amount of integral action taken inside and outside the gap were changed.

Control performance indicators like integrated absolute error (IAE) or integrated squared error (ISE) are typically not used when considering averaging level control, as the controller is only required to maintain the level between limits without minimizing the error between SP and the PV. With

averaging level control, the performance indicators considered typically focus on minimizing the movement of the OP, like the variance of the OP derivative (VOD)[5,6,7] as shown in Eq. 3 or the average of the absolute move of the OP (AAMO) shown in Eq. 4:

$$VOD = \sqrt{\frac{1}{N}\sum_{i=1}^{N}\left[(OP_i - OP_{i-1}) - \mu\right]^2} \quad (3)$$

where:

N = number of execution cycles

OP = controller output

μ = mean of the OP for all execution cycles.

If the IGC is tuned aggressively, the controller will move the OP past the steady-state value and then change direction. To show this behavior, the AAMO metric (as shown in Eq. 4) was developed as an additional performance indicator.

$$AAM = \left[\sum_{i}^{N} abs\left(OP_i - OP_{i-1}\right)\right] / N \quad (4)$$

where:

N = number of execution cycles

OP = controller output.

As the advantage of the IGC is that it repositions the system quicker by bringing PV back to SP faster than a normal PI controller, it is worthwhile to also consider performance metrics that measure the control performance, such as integrated absolute error (IAE) and integrated squared error (ISE). Specifically, the ISE should be considered, as the IGC will aggressively counteract PV error when the PV is outside the integral gap while acting less aggressively when the PV is inside the gap. The ISE will provide a better indication of whether the IGC does this successfully.

The difference between a PI averaging level controller with typical tuning and an IGC is shown in **FIGS. 1** and **2.** Both controllers were tuned to reject a 5-m³/hr step disturbance with a high limit set at 70%.

The IGC was tuned with a 10% gap on either side of SP: $T_{i\ outside\ gap} = 96$ and $T_{i\ in\ gap} = 256$.

The IGC gap was set to 10% and **FIGS. 1** and **2** show how the more aggressive control action decreased when the PV returned to less than 60%. Studying the OP trajectory also shows how the proportional action that was increasing the OP on the return of the PV towards SP made larger OP moves than the decreased integral action that was still moving the OP downwards. This caused the PI controller to overtake the IGC and have less remaining PV error towards the end of the test.

Even though the intent of the IGC is to reach SP sooner than the traditional PI controller, tuning the IGC this way has merit as small disturbances that occur while the PV is close to SP will be rejected less aggressively, and return to SP will also be done slowly, leading to improved averaging level control on smaller disturbances.

FIG. 2 also shows the obvious disadvantage that bringing the level back to SP sooner will require slightly larger OP moves. This disadvantage must be offset by the advantage of being ready for a subsequent disturbance sooner.

TABLE 1 shows that the IGC performed better on the squared error metric, as it brought the PV closer to the SP in a shorter time. The VOD showed that the IGC was slightly gentler with the OP movements, while the AAMO penalized the IGC for overshooting the steady-state value more than the PI controller.

This could be a typical way of tuning the IGC controller that would quickly bring the PV back into the gap and then act less aggressively to prevent overshooting SP. This would also enable the controller to be gentler when smaller disturbances occur that do not push the PV outside the gap.

For the IGC to reach SP sooner than the PI controller, either the integral action in the gap can be increased or the size of the gap can be decreased.

FIGS. 3 and **4** compare the performance of the IGC with more aggressive integral action in the gap with the PI controller.

These figures show how the IGC was able to get to SP sooner but had to move its OP faster to do so.

TABLE 1. Performance metrics, gap = 10%, $T_{i\ outside\ gap}$ = 96 and $T_{i\ in\ gap}$ = 256

	IAE	ISE	VOD	AAMO
PI	3,139	40,519	0.0395	0.0142
IGC	3,204	37,546	0.0392	0.0149

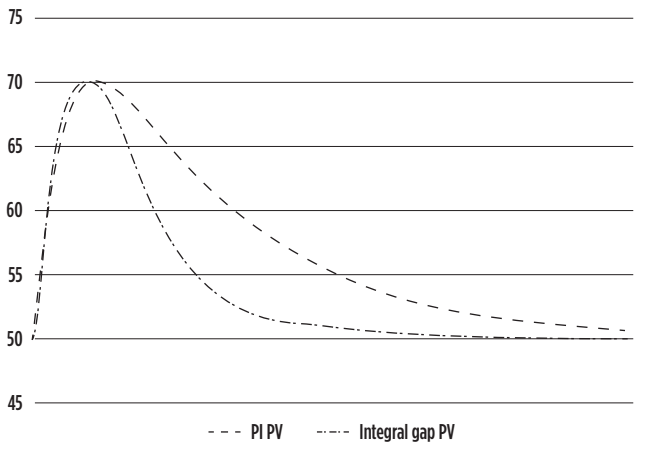

FIG. 3. PV response of PI and more aggressive IGC to a positive disturbance.

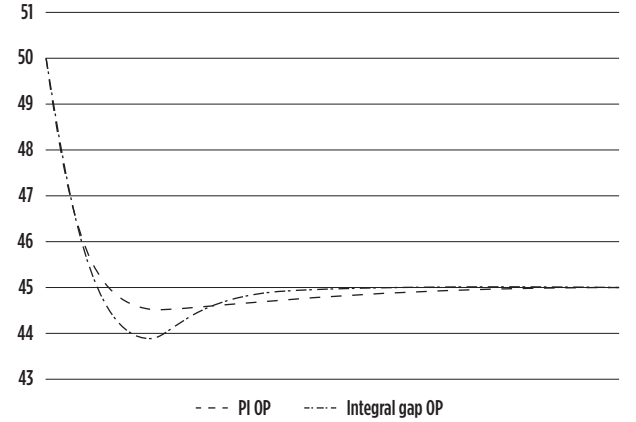

FIG. 4. OP response of PI and more aggressive IGC to a positive disturbance.

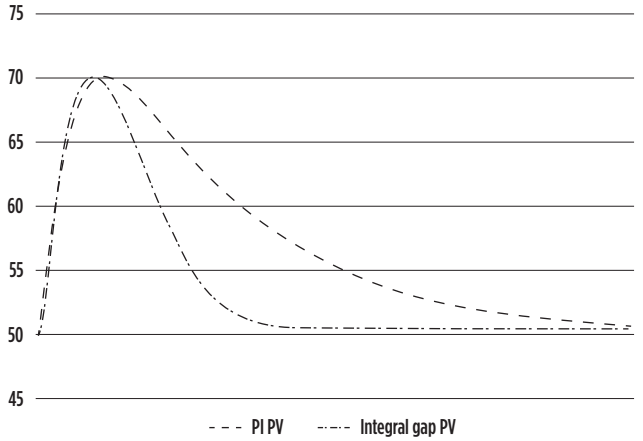

FIG. 5. PV response of PI and IGC with a 5% gap.

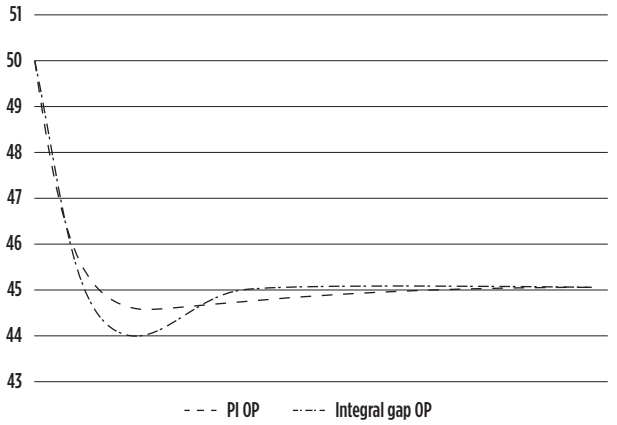

FIG. 6. OP response of PI and IGC with a 5% gap.

In **TABLE 2,** the IAE and ISE both show the positive effect of the IGC bringing the PV back to SP much faster, while the VOD and the AAMO both show how it had to move the OP faster and overshoot the steady-state value more.

The PV can also be brought back to SP faster by decreasing the size of the gap, as shown in **FIGS. 5** and **6.** Because the controller will then apply the full effect of the integral action for a longer time, the integral action in and outside of the gap will also have to be adapted to prevent overshoot.

The smaller gap meant that the controller had less opportunity for the proportional action to counter the prolonged aggressive integral action outside the gap. Therefore, the integral action inside the gap had to be extremely weak to prevent overshoot.

Once again, the metrics (**TABLE 3**) show how the IGC managed to bring the PV back to SP at a small penalty in terms of increased OP movement.

Takeaway and recommendation. When averaging level control is applied where concurrent disturbances may cause the level to go outside limits, the IGC will enable the process control engineer to return the PV to SP faster, without the risk of starting a cycle on the plant. This will be accompanied by a slight increase in OP movement.

While the PV is close to SP, the IGC will make small moves, minimizing OP variance.

TABLE 2. Performance metrics, gap = 10%, $T_{i\ outside\ gap}$ = 48 and $T_{i\ in\ gap}$ = 124

	IAE	ISE	VOD	AAMO
PI	3,139	40,519	0.0395	0.0142
IGC	1,753	23,369	0.04	0.0171

TABLE 3. Performance metrics, gap = 5%, $T_{i\ outside\ gap}$ = 48 and $T_{i\ in\ gap}$ = 1,024

	IAE	ISE	VOD	AAMO
PI	3,139	40,519	0.0395	0.0142
IGC	1,683	22,697	0.0405	0.017

The IGC can be used to return to SP as quickly as possible or to react slower to smaller disturbances. This is done by setting the size of the integral gap and correspondingly increasing or decreasing the integral tuning inside and outside the gap.

If PID-based averaging level control is done using a PI controller on a system where disturbances occur frequently, the level can be returned to SP much faster by deploying an IGC. If this is done, the level control is afforded the opportunity of recovering from the current disturbance before the next disturbance occurs, ensuring that the PV stays clear of alarm or trip limits.

The IGC should be tuned so that the proportional action is dominant while the PV is inside the gap and the integral action is dominant when the PV is outside the gap. By adjusting the tuning, the trade-off between minimizing OP movement and getting the PV back to SP in time for the next disturbance can be optimized.

If the level is subject to many smaller disturbances, the gap of the IGC can be increased for the controller to react slower to smaller disturbances. This will assist in minimizing OP variance. HP

LITERATURE CITED

[1] King, M., *Process control: A practical approach,* Wiley, 2011.
[2] Shinskey, F. G., "Special rules for tuning level controllers," Controls, 2005, online: www.controlglobal.com/articles
[3] Friedman, Y. Z., "Tuning of averaging level controllers," Petrocontrol, 1994, online: http://www.petrocontrol.com/papers/1994_Level.pdf
[4] Honeywell, "Honeywell Experion control builder components theory—Volume 1," pp. 406–410, 2005.
[5] Kelly, J. D., "Tuning digital PI controllers for minimal variance in manipulated input moves applied to imbalanced systems with delay," *The Canadian Journal of Chemical Engineering*, Vol. 76, Iss. 5, 1998.
[6] Lindholm, A., "Buffer management strategies for improving plant availability," Thesis, Lund University, 2009.
[7] Ogawa, S., B. Allison, G. Dumont and M. Davies, "A new approach to optimal averaging level control with state constraints," 41st IEEE Conference on Decision and Control, Las Vegas, Nevada, December 2002.

GUSTAF GOUS works as a Process Control Consultant at Analyte Control. He graduated from the Department of Chemical Engineering, University of Pretoria, with a B-Eng degree in chemical engineering in 1987, followed by a B-Eng (Honors) and an M-Eng degree. He is now occupied with pursuing a PhD.

PHILIP DE VAAL graduated from the Department of Chemical Engineering, University of Pretoria, with a BS degree in chemical engineering in 1976, followed by an MS degree and PhD. Dr. de Vaal is now an Emeritus professor of chemical engineering and previously served as the Head of this department from 2004–2020.

A. K. COKER, A.K.C. Technology; and **A. ALSUHAIBANI**, Texas A & M University, College Station, Texas

Optimize product blending using Excel spreadsheets and Lingo software—Part 2

This article is a continuation of Part 1, which appeared in the June issue.

Linear programming (LP) for blending. LP is an optimization model that can be used to good advantage despite the highly nonlinear characteristics of the fluid flow-cash flow model. These nonlinearities can be resolved within the framework of a linear program model by adding constraints to make the model piece-wise linear. This requires a powerful computer to solve such linear program models.

The structure of the linear program model closely follows the schematic in **FIG. 5.** For instance, each refinery is represented by a sublinear program model of 100 or more constraints. Furthermore, sublinear models are used to represent the movement of crude oil from the fields to refineries, and the transportation of finished products from refineries to market.

Areas where this technique is employed include:[3]

1. Blending gasolines
2. Refinery models
3. Allocation of transportation facilities for shipping products from refineries to terminals
4. Integrated operations, simultaneously considering complete refinery models (2) and transportation models (3)
5. Allocation of transportation facilities for shipping products from the crude oil field to refineries
6. Integrated operations encompassing 1–5.

The general linear programming problem is to find a vector $(x_1, x_2, \ldots x_n)$, where n is the independent variable, which minimizes or maximizes the linear form or the objective function, P as (Eq. 39):

$$P = c_1x_1 + c_2x_2 + c_3x_3 + \ldots\ldots\ldots\ldots c_jx_j + \ldots\ldots\ldots\ldots + c_nx_n \quad (39)$$

subject to the linear constraints (Eq. 40):

$$x_j \geq 0, j = 1,2, \ldots\ldots\ldots\ldots, n \quad (40)$$

and (Eqs. 41–43):

$$a_{11}x_1 + a_{12}x_2 + \ldots\ldots\ldots\ldots a_{ij}x_j + \ldots\ldots\ldots\ldots + a_{ln}x_n \leq b_i \quad (41)$$

$$a_{il}x_1 + a_{i2}x_2 + \ldots\ldots\ldots\ldots a_{ij}x_j + \ldots\ldots\ldots\ldots + a_{in}x_n \leq b_i \quad (42)$$

$$a_{ml}x_1 + a_{m2}x_2 + \ldots\ldots\ldots\ldots a_{mj}x_j + \ldots\ldots\ldots\ldots + a_{mn}x_n \leq b_m \quad (43)$$

where a_{ij}, b_i and c_i are given constants and m < n.

One way of looking at the model is that the structure of the fluid-flow portion is represented by the following constraints (Eqs. 44 and 45):

$$A \times X = b \quad (44)$$

subject to

$$X \geq 0 \quad (45)$$

Conversely, the cash flow aspect of the model is represented by minimizing or maximizing $C \times X$, where $C = (c_1, c_2, \ldots c_m)$ is a row vector, $X = (x_1, x_2, \ldots x_m)$ is a column vector, $A = (a_{ij})$ is a matrix and $B = (b_1, b_2, \ldots b_m)$ is a column vector.

The objective function (P) is usually the octane number of the blend that must be maximized. In some instances, the objective function can be the minimized cost or setting the Reid vapor pressure (RVP) to a certain value. The primary constraints variables (x_1 to x_n) are the volume of each cut of a blend, which must be greater than zero. Other constraints include the capacity of the tank in which the sum of x_1's will not exceed, as well as any blend properties. Therefore, a_{i1} to a_{mn} are the properties or their indices for components 1 to n, and b_i to b_m are the targeted blending properties of their indices.

In most blending cases, two or more properties are required to be adjusted by the addition of modifiers to the blend. For example, oxygenates are added to enhance gasoline octane number and n-butane is added to adjust the RVP. Determining the

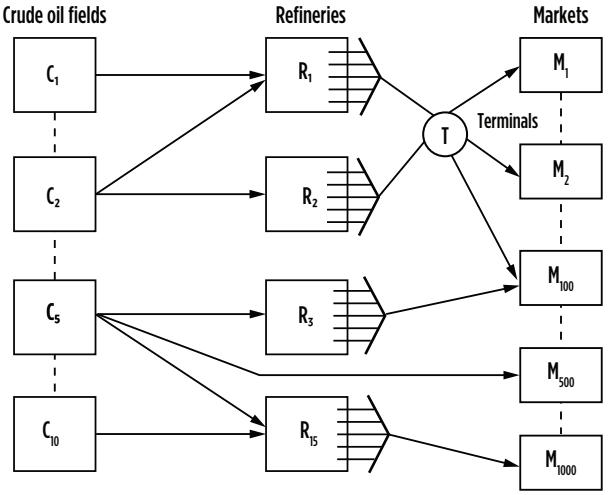

FIG. 5. Fluid flow model.

quantities of the additives becomes more difficult in non-linear properties cases. Determining the amounts of these blends is based on solving two or more equations with two or more unknowns, depending on the property equations.

A typical refinery optimization problem can be split into sub-problems using a spatial decomposition scheme proposed by Jia and Ierapetritou.[4] These sub-problems are solved as independent optimization problems, and the combined results are considered an approximate solution to the overall refinery optimization problem.

Several commercial tools are available for solving standalone refinery optimization problems, including software products for online and offline blending optimization problems[a,b]; products for online and offline blending optimization[c,d,e]; and online optimization solutions for primary and secondary process units[f,g].

FIG. 6 shows a schematic decomposition of the refinery optimization problem, and **FIG. 7** shows an overview of petroleum refining and blending processes.

Mathematical formulation. The problem formulation includes multiple blenders and storage tanks, as shown in **FIG. 6.** Properties of the final products are modelled using blend laws that relate the final product property to the quantities and properties of feed components. Blend product properties are either linearly or non-linearly blended based on the volume or mass of the feed components. For example, the RON of the blend is modelled by linear blend laws, while the RVP of the blend is modelled by non-linear blend laws. The blend laws used to estimate product property based on volume/mass fraction or volume/mass flow and property of feed components are:

1. Linearly blended by component fractions in tanks: the property of product blend is a linear function of component volume/mass fractions and properties (Eq. 46):

$$PE_j = \sum_i X_i BV_{i,j} \quad (46)$$

where X_i is the volume/mass fraction of component i in the product tank.

2. Linearly blended by component flows in blend headers: the instantaneous property of the product blend is a linear function of component volume/mass flowrates and properties (Eq. 47):

$$PE_j = \frac{\sum_i F_i BV_{i,j}}{\sum_i F_i} \quad (47)$$

where F_i is the volume/mass flowrate of component i to the blend header.

Blend optimization is subjected to different constraints types, including operational (equipment limits on component flow), inventory (volume limits on feed components) and quality (analyzer limits and tank property specification).

Solving the problem. Solving the proposed problem in real time is one of the main requirements; however, if this is impossible, then the intermediate iteration result after a fixed time interval should be feasible and better than the previous iteration results. This requirement ensures that a feasible solution is provided for cases where the solver cannot converge in the available time for a real-time optimization. The proposed problem is solved using a developed solver[h] due to its feasible region search robust nonlinear programming (NLP) solver and meets all solution requirements.[4]

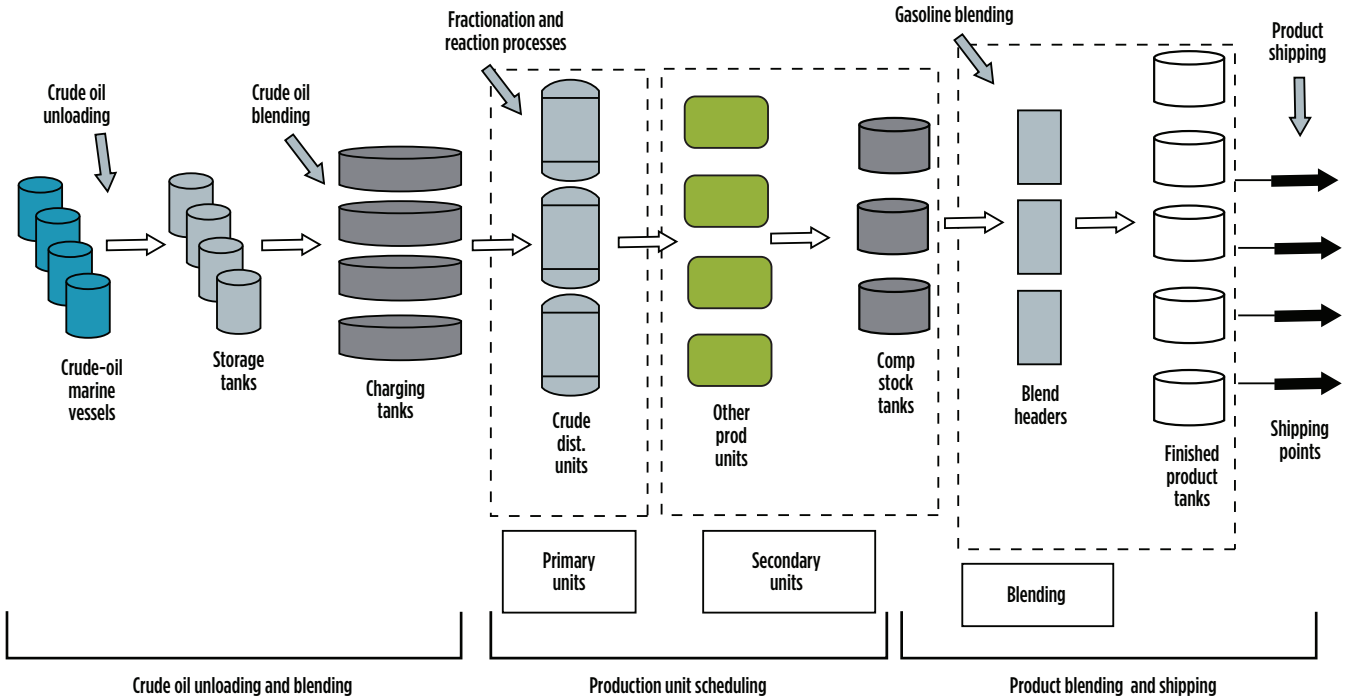

FIG. 6. Schematic division of refinery-wide operation.

NLP is an optimization problem that minimizes (or maximizes) a nonlinear objective function subject to linear or nonlinear constraints. Problems formulated as NLP are more accurate compared to their LP counterparts since most chemical processes are nonlinear in nature. Refinery models that account for the nonlinear relationship of process variables are more reliable and more closely represent refinery systems. The general representations of NLP problems are shown in Eqs. 48, 49 and 50:

$$\text{Minimize/maximize } f(x) \ldots\ldots\ldots\ldots x = [x_1, x_2, \ldots\ldots\ldots\ldots x_n]^T \quad (48)$$

$$\text{Subject to:} \quad h_i(x) = b_i \ldots\ldots\ldots i = 1,2, \ldots\ldots\ldots\ldots m \quad (49)$$

$$g_j(x) \leq c_j \ldots\ldots\ldots j = 1,2, \ldots\ldots\ldots\ldots r \quad (50)$$

In these formulation, bilinear and trilinear terms, and basic mathematical functions can be found. In Eqs. 48–50, the objective function $f(x)$, the equality constraint $h_i(x)$ or the inequality constraint $g_j(x)$ must be nonlinear.

The challenge in modelling using the NLP formulation is achieving a reasonable convergence. This is largely because many real-valued functions are non-convex. Convexity of a feasible region can only be guaranteed if constraints are all linear. Furthermore, it is difficult to determine whether objective functions or inequality constraints are convex or not. However, a convexity test can be carried out to satisfy conditions of optimality referred to as Kuhn-Tucker (KKT) conditions. Most algorithms embedded in commercial solvers terminate when these conditions are satisfied within some tolerance. For problems with several variables, KKT solutions can sometimes be found analytically, and the one with the best objective function value is chosen.

Unlike LP, NLP is reported in a significant number of publications in refinery problems involving blending relation and pooling. Moro, *et al.*[5] developed a non-linear optimization model for the entire refinery topology that considers all process units and includes non-linearity due to blending. Pinto, *et al.*[6] extended this work, as did Neiro and Pinto[7] for multi-period and multi-scenario cases involving nonlinear models. They considered nonlinearity in the development of the scheduling model for refinery production with product blending. Furthermore, Hamisu[8] considered nonlinearity in the development of a scheduling model for refinery production with product blending.

Example 2. A blend is performed for LSR gasoline, hydrocracker gasoline, fluid catalytic cracking (FCC) gasoline and n-butane. Calculate the amount of each component that must be added to produce gasoline blend of maximum octane number and 12 psi RVP. The properties of each cut are shown in **TABLE 3.** The olefin contents in each cut are assumed to be zero. The maximum blend storage capacity is 15,000 bbl. Recalculate if the available amount of FCC gasoline is 6,000 barrels.

The objective function is maximizing the octane number. Since the olefin contents are zero, Eqs. 51–56 are used:

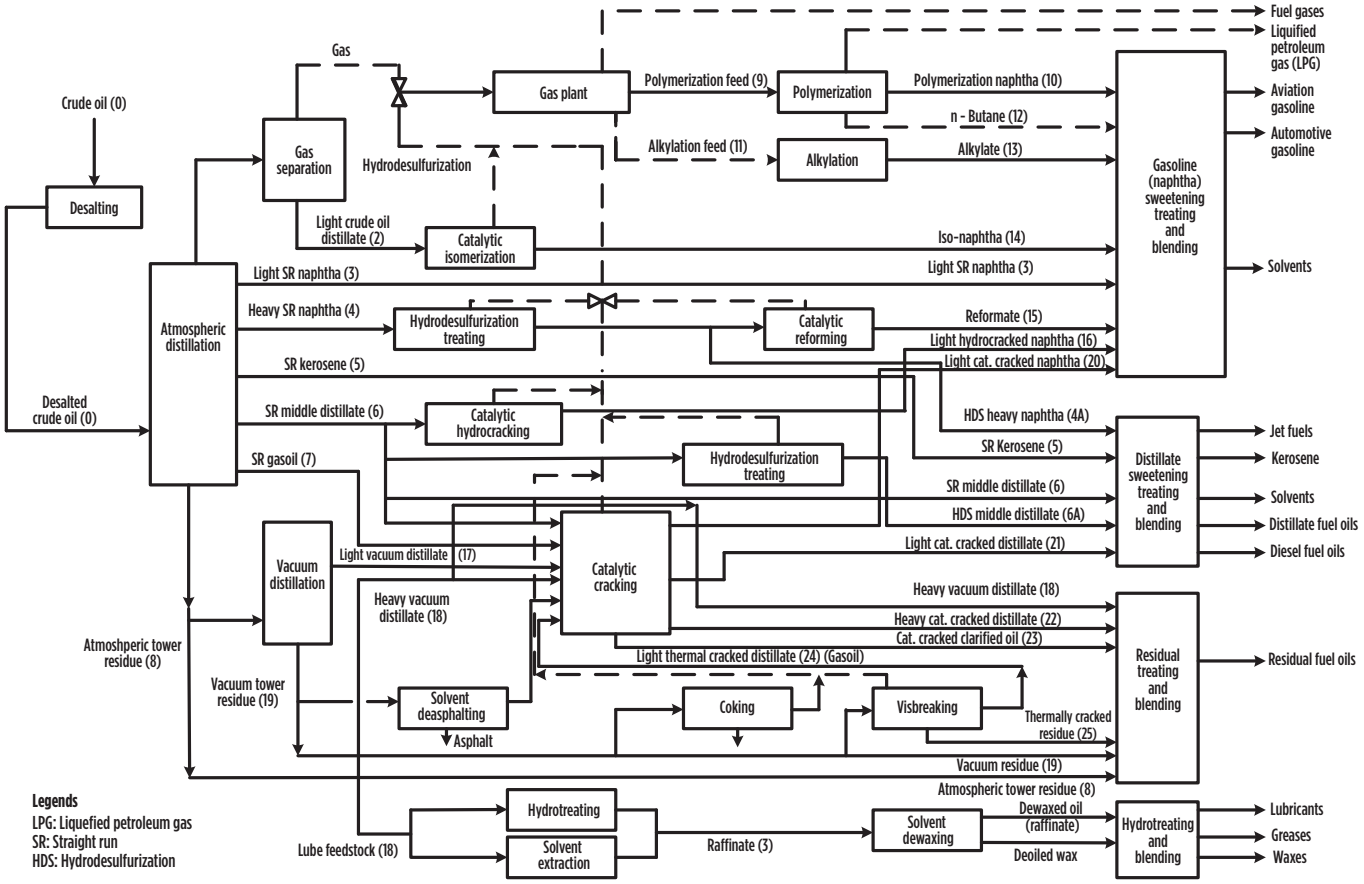

FIG. 7. Overview of petroleum refining and blending processes.

$$R = \bar{R} + 0.03324\left[\overline{RJ} - \bar{R} \times \bar{J}\right] + 0.00085\left[\left(\overline{O^2}\right) - \overline{O^2}\right] \quad (51)$$

$$RON_{Blend} = \bar{R} + 0.03324\left(\overline{RS} - \bar{R} \times \bar{S}\right) \quad (52)$$

where:

$$\bar{R} = (91)\frac{X_1}{X_T} + (89.5)\frac{X_2}{X_T} + (97)\frac{X_3}{X_T} + (93)\frac{X_4}{X_T} \quad (53)$$

$$\bar{S} = (91-81)\frac{X_1}{X_T} + (89.5-85.5)\frac{X_2}{X_T} + (97-96)\frac{X_3}{X_T} + (93-92)\frac{X_4}{X_T} \quad (54)$$

$$\overline{RS} = (91-81)\frac{X_1}{X_T} + (89.5-85.5)89.5\frac{X_2}{X_T} + (97-96)\frac{X_3}{X_T} + (93-92)\frac{X_4}{X_T} \quad (55)$$

$$X_1 \geq 0,\ X_2 \geq 0,\ X_3 \geq 0 \text{ and } X_4 \geq 0 \quad (56)$$

An additional constraint is shown in Eq. 57:

$$X_1 + X_2 + X_3 + X_4 < 15{,}000 \text{ barrels} \quad (57)$$

The constraint equation for the blend RVP can be obtained by calculating the RVP index from Eq. 58:

$$BI_{RVP_i} = RVP_i^{1.25} \quad (58)$$

where:

BI_{RVP_i} is the RVP blending index for component i and $RVPi$ is the RVP of component i in psi. Using the index, the RVP of a blend is (Eqs. 59–61):

$$BI_{RVP_i,Blend} = \sum_{i=1}^{n} x_{vi} BI_{RVP_i} \quad (59)$$

$$12.1^{1.25}\frac{X_1}{X_T} + 15.5^{1.25}\frac{X_2}{X_T} + 4.8^{1.25}\frac{X_3}{X_T} + 51.6^{1.25}\frac{X_4}{X_T} - 12.0^{1.25}\frac{X_T}{X_T} = 0 \quad (60)$$

or

$$22.56\frac{X_1}{X_T} + 30.755\frac{X_2}{X_T} + 7.105\frac{X_3}{X_T} + 138.3\frac{X_4}{X_T} - 22.33\frac{X_T}{X_T} = 0 \quad (61)$$

TABLE 3. Components properties for the blend

Component	Barrels	RVP, psi	RON	MON
LSR gasoline	X_1	12.1	91	81
Hydrocracker gasoline	X_2	15.5	89.5	85.5
FCC gasoline	X_3	4.8	97	96
n-Butane	X_4	51.6	93	92
Blend	X_5	12	Max	

Using the solver in an Excel spreadsheet to maximize RON, the objective function of Eq. 52 with the above constraints (Eqs. 56, 57 and 60), the results are:

RON = 96.54 and $X_1 = 0$, $X_2 = 0$, $X_3 = 13{,}259$ and $X_4 = 1{,}741$ bbl.

If a constraint for FCC gasoline (6,000 barrels) is added, the results for the maximum blend storage would be:

RON= 93.23 and $X_1 = 0$, $X_2 = 8{,}855$, $X_3 = 6{,}000$ and $X_4 = 145$ bbl.

Case study.[9,10] An oil refinery produces a stream of hydrocarbon-based fuel from each of four different processing units. The processing units have capacities of C_1, C_2, C_3 and C_4 bpd, respectively. A portion of each base fuel is fed to a central blending station where the base fuels are mixed into three grades of gasoline. The remainder of each base fuel is sold "as is" at the refinery. Storage facilities are available at the blending station for temporary storage of the blended gasolines, if required.

Let N_1, N_2, N_3 and N_4 be the octane ratings of the respective base fuels, and let S_1, S_2, S_3 and S_4 be the profit derived from their direct sale. Let O_1, O_2 and O_3 be the octane numbers of the three grades of gasoline that must be blended on any given day to satisfy customer demands D_1, D_2 and D_3. Let R_1, R_2 and R_3 be the minimum octane requirements of the three grades of blended gasoline, and let P_1, P_2 and P_3 be the profit per gallon that is realized from the sale of each grade of blended gasoline. Finally, let x_{ij} be the quantity of the *ith* base fuel used to blend the *jth* gasoline.

The octane number of each gasoline can be expressed as the weighted average of the octane numbers of the constituent base fuels. The weighting factors are the fractions of the base fuels in each gasoline. Therefore (Eqs. 62–64):

$$O_1 = \frac{x_{11}N_1 + x_{21}N_2 + x_{31}N_3 + x_{41}N_4}{x_{11} + x_{21} + x_{31} + x_{41}} \quad (62)$$

$$O_2 = \frac{x_{12}N_1 + x_{22}N_2 + x_{32}N_3 + x_{42}N_4}{x_{12} + x_{22} + x_{32} + x_{42}} \quad (63)$$

$$O_3 = \frac{x_{13}N_1 + x_{23}N_2 + x_{33}N_3 + x_{43}N_4}{x_{13} + x_{23} + x_{33} + x_{43}} \quad (64)$$

Develop a linear programming model to determine how much of each base fuel should be blended into gasoline and how much should be sold "as is" to maximize profit. Solve the model using numerical data in **TABLE 4** and below:

$$\text{Maximize } y = P_1(x_{11} + x_{21} + x_{31} + x_{41}) + P_2(x_{12} + x_{22} + x_{32} + x_{42}) + P_3(x_{13} + x_{23} + x_{33} + x_{43}) + (S_1/42)(42C_1 - x_{11} - x_{12} - x_{13}) + (S_2/42)(42C_2 - x_{21} - x_{22} - x_{23}) + (S_3/42)(42C_3 - x_{31} - x_{32} - x_{33}) + (S_4/42)(42C_4 - x_{41} - x_{42} - x_{43})$$

$$\text{Subject to } \sum x_{ij} \geq 42D_j$$

$$\sum x_{ij} N_i \; x_{11}N_1 + x_{21}N_2 + x_{31}N_3 + x_{41}N_4 \geq R_1(x_{11} + x_{21} + x_{31} + x_{41})$$

$$x_{12}N_1 + x_{22}N_2 + x_{32}N_3 + x_{42}N_4 \geq R_2(x_{12} + x_{22} + x_{32} + x_{42})$$

$$x_{13}N_1 + x_{23}N_2 + x_{33}N_3 + x_{43}N_4 \geq R_3(x_{13} + x_{23} + x_{33} + x_{43})$$

where x_{ij} = gallons of base fuel i used in gasoline j.

The model assumes full capacity production. The optimal value for the target cell is determined using a what-if analysis tool in the solver, which works by changing the values for parameters that are used to calculate the value of the target cell. The results of the optimization are:

y_{max} = 111,836,36 at x_{11} = 436,800, x_{41}= 109,200, x_{12} = 756,000, x_{42} = 294,000

x_{13} = 423,360, x_{43}= 332,640, all other x_{ij} = 0.

All x_{ij} expressed in terms of gal/d.

The same approach can be used to determine the optimum value of the target parameter when there are changes in other parameters, such as an increase or decrease in selling prices of one and/or all gasoline blends. The same calculation approach can solve for any changes in capacity (C), demand (D) or any other relevant parameter(s).

Alsuhaibani[11] employed a linear optimization programming method (LINGO) for the case study. **TABLE 5** shows the code and results and are in good agreement with the results obtained from the Excel spreadsheet.[12]

Takeaway. Linear programming includes two kinds of programs: a solver program and a mixed inter linear program (MILP). Microsoft Excel incorporates an NLP solver that operates on the values and formulas of a spreadsheet model. The solver uses the spreadsheet interpreter to evaluate the constraint and objective functions, and approximates derivatives using finite differences. The NLP solution engine for the Excel Solver is the generalized reduced gradient (GRG2) algorithm, and this has successfully been implemented in the examples and case study presented in this article and supported by the LINGO program. HP

NOTES

[a] AspenTech's Aspen Blend
[b] AspenTech's Aspen PIMS-MBO™
[c] Honeywell's EBC™
[d] Honeywell's OpenBPC™
[e] Honeywell's Blend™
[f] Honeywell's Profit Controller™
[g] Invensys' ROMeo™
[h] MINOS, developed by Stanford Systems Optimization Laboratory

TABLE 4. Numerical data

C_1 = 13,000 bpd	N_1 = 82 octane	S_1 = \$0.90/bbl
C_2 = 7,000	N_2 = 95	S_2 = 1.05
C_3 = 25,000	N_3 = 102	S_3 = 1.25
C_4 = 15,000	N_4 = 107	S_4 = 1.60
D_1 = 13,000 bpd	R_1 = 87 octane	P_1 = 3.5 /gal
D_2 = 25,000	R_2 = 89	P_2 = 4.5
D_3 = 18,000	R_3 = 93	P_3 = 6.0

Note: 42 gal = 1 bbl

TABLE 5. LINGO code, input and output for the case study

```
! Given;
P1 = 3.5;
P2 = 4.5;
P3 = 6;
S1 = 0.9;
S2 = 1.05;
S3 = 1.25;
S4 = 1.60;
C1 = 13,000;
C2 = 7,000;
C3 = 25,000;
C4 = 15,000;
N1 = 82;
N2 = 95;
N3 = 102;
N4 = 107;
D1 = 13,000;
D2 = 25,000;
D3 = 18,000;
R1 = 87;
R2 = 89;
R3 = 93;
! Maximize;
Max = P1 × (X11 + X21 + X31 + X41) + P2 × (X12 + X22 + X32 + X ) + P3 × (X13 + X23
+ X33 + X43) + (S1/42) × (42 × C1 − X11 − X12 − X13) + (S2/42) × (42 × C2 − X21
− X22 − X23) + (S2/42) × (42 × C3 − X31 − X32 − X33) + (S4/42) × (42 × C4 − X41
− X42 − X43);
! Subject to;
X11 + X21 + X31 + X41 = 42 × D1;
X12 + X22 + X32 + X42 = 42 × D2;
X13 + X23 + X33 + X43 = 42 × D3;
X11 × N1 + X21 × N2 + X31 × N3 + X41 × N4 > = R1 × (X1 + X21 + X31 + X41);
X12 × N1 + X22 × N2 + X32 × N3 + X42 × N4 > = R2 × (X12 + X22 + X32 + X42);
X13 × N1 + X23 × N2 + X33 × N3 + X43 × N4 >= R3 × (X13 + X23 + X33 + X43);
```

Variable	Value	Input/output
P1	3.5	
P2	4.5	
P3	6	
S1	0.9	
S2	1.05	
S3	1.25	
S4	1.6	
C1	13,000	
C2	7,000	
C3	25,000	
C4	15,000	Input
N1	82	
N2	95	
N3	102	
N4	107	
D1	13,000	
D2	25,000	
D3	18,000	
R1	87	
R2	89	
R3	93	

TABLE 5. LINGO code, input and output for the case study (cont.)

Variable	Value	Input/output
X11	409,500	
X21	0	
X31	136,500	
X41	0	
X12	682,500	
X22	0	Output
X32	367,500	
X33	415,800	
X43	0	
Y	1.11876E+07	

LITERATURE CITED

[1] Maples, R. E., *Petroleum refinery process economics,* 2nd Ed., PennWell Corp., January 2000.
[2] Healy Jr., W. C., C. W. Maasen and R. T. Peterson, "Predicting octane numbers of multi-component blends," Report number RT-70, Ethyl Corp., Detroit, Michigan, April 1959.
[3] Gary, J. H., G. E. Handwerk and M. J. Kaiser, *Petroleum refining: Technology and economics,* 5th Ed., CRC Press, Taylor & Francis Group, 2007.
[4] Jia, Z. and M. Ierapetritou, "Mixed-integer linear programming model for gasoline blending and distribution scheduling," *Industrial & Engineering Chemistry Research,* February 2003.
[5] Moro, L., A. Zanin and J. Pinto, "A planning model for refinery diesel production," *Computers & Chemical Engineering,* March 1998.
[6] Pinto, J. M., M. Joly and L. F. L., "Planning and scheduling models for refinery operations," *Computers & Chemical Engineering,* October 2000.
[7] Neiro, S. and J. Pinto, "Multiperiod optimization for production planning of petroleum refineries," *Chemical Engineering Communications,* Vol. 192, Iss. 1, 2005.
[8] Hamisu, A. A., "Petroleum refinery scheduling with consideration for uncertainty," PhD Thesis, Cranfield University, Cranfield, England, 2015.
[9] Aronofsky, J. S., "Linear programming—A problem-solving tool for petroleum industry management," *Journal of Petroleum Technology,* July 1962.
[10] Gottfried, B. S., *Spreadsheet tools for engineers: Excel 5.0 version,* McGraw-Hill College, March 1996.
[11] Alsuhaibani, A. S., Texas A & M University, private communications.
[12] Jiang, S., "Optimization of diesel and gasoline blending operations," PhD thesis, Centre for Process Integration, School of Chemical Engineering and Analytical Science, The University of Manchester, 2016.

A. KAYODE COKER is an Engineering Consultant for AKC Technology and has been a chartered chemical engineer for more than 30 yr. Dr. Coker is an Honorary Research Fellow at the University of Wolverhampton, U.K., a former Engineering Coordinator at Saudi Aramco Shell Refinery Company (SASREF) and Chairman of the department of Chemical Engineering Technology at Jubail Industrial College, Saudi Arabia. He is a Fellow of the Institution of Chemical Engineers, U.K. (C. Eng., FIChemE), and a senior member of the American Institute of Chemical Engineers (AIChE). He holds a BS (honors) degree in chemical engineering, an MS degree in process analysis and development and a PhD in chemical engineering, all from Aston University, Birmingham, U.K., as well as a Teacher's Certificate in education at the University of London, U.K. He has directed and conducted short courses extensively throughout the world and has been a lecturer at the university level. His articles have been published in several international journals. Dr. Coker is an author of six books on chemical engineering, a contributor to the Encyclopedia of Chemical Processing and Design, Vol. 61, and a certified trainer and mentor. He is a Technical Report Assessor and Interviewer for Chartered Chemical Engineers (IChemE) in the U.K. as well as a member of the International Biographical Centre in Cambridge, U.K. (IBC) as "Leading Engineers of the World" for 2008.

ABDULRAHMAN S. ALSUHAIBANI is a PhD candidate in the Chemical Engineering Department at Texas A&M University. His research is in the area of sustainable design of industrial systems. He has focused his research applications on important contemporary issues for sustainability, including CO_2 utilization and hydrogen economy. Prior to pursuing his PhD, Mr. Alsuhaibani worked for Saudi Aramco R&DC.

E. ÖZSAĞIROĞLU, T. Ö. ATAGÜN and E. ARICI,
Tüpraş, İzmit, Turkey

Debottleneck analysis on a coker debutanizer via simulation models

Production requirements for more valuable refined products and/or increased refining flexibility are increasing due to new regulations. Delayed coking units (DCUs) help refineries to achieve these goals and maintain sustainable profitability in shrinking market conditions. Therefore, it is important that DCUs must be problem-free facilities since any struggles in these units will negatively affect refinery margins.

A DCU consists of two primary sections: the coker section and the gas plant section. The coker section is designed to produce coke, light- and heavy-coker gasoils, unstabilized naphtha and overhead vapors. The unstabilized naphtha and overhead vapors are further processed in the gas plant section to produce treated fuel gas, LPG and stabilized naphtha. In the gas plant, stripper and debutanizer sections of the DCU are connected via streams and heating systems—therefore, a problem in any of these sections affects the other sections. The authors' refinery has struggled with a bottleneck problem in the debutanizer column at turndown conditions. The column's pressure profile increased rapidly and would trip the pressure safety valve (PSV) if feed decreased by 50%.

To solve the bottleneck in the debutanizer and stripper sections of the DCU, column models were prepared and validated with site data using a commercial simulation program. After this step, debottleneck studies were performed to solve the problem and sustain production without giveaways. These studies demonstrated that looking inside and outside the affected columns simultaneously can be a critical factor when evaluating possible solutions. The simulation study is a more comprehensive review to provide a guideline on anticipating, troubleshooting and overcoming bottleneck problems.

After implementing the simulation results to the field, the refinery's energy intensity value decreased 0.06 points and its carbon dioxide (CO_2) emissions decreased by 1,500 tpy.

Why was this study needed? After the startup of the DCU, it was observed that the debutanizer column performance was unstable, especially at a low feed rate. Sometimes, these instabilities resulted in a sudden pressure increase at the top of the tower, causing the PSV to trip. The aim of the project was to analyze the behavior of the debutanizer at turndown conditions and to eliminate the environmental effect by preventing a PSV trip.

To discover the bottleneck of the system, debutanizer and stripper column models—with condensers and reboilers—were simulated by using a proper data set. This set included capacity rate, maximum capacity and turndown capacity. Simulation models and data historian analyses were used simultaneously to determine the root causes of the problems.

The study's first phase focused on trying to discover processing problems via simulation models. The second phase was verifying the simulation results via data historian analysis. The third phase focused on improving solutions in the simulation models and then implementing them onsite. This study enabled plant personnel to detect trouble spots and to put forth solutions. It was essential to properly define the debutanizer feed; therefore, the stripper column was also covered in the simulation. Both columns needed to be simulated simultaneously, since these two systems were connected via outlet/charge streams and reboiler systems. All related operating parameters were revised to find the optimum unit operation according to unit capacity. Simulation model outputs were used to solve bottlenecks in the column's operation.

Main parameters used in the debottleneck study. Although DCUs are designed to maximize diesel cut, these units also produce a high amount of fuel gas, LPG and naphtha. LPG purity is higher vs. other LPG production units. LPG purity directly depends on the debutanizer column's performance. In addition, naphtha taken from debutanizer bottoms is sent to the naphtha desulfurizer. The stable flow of naphtha is required for the sake of catalyst activity. Consequently, the debutanizer column performance is important for the DCU. To illustrate this system, a schematic view of the process is shown in FIG. 1.

One of the main performance parameters in the debutanizer column is feed characteristic. To define feed characteristics properly, stripper columns and reboilers were simulated, as well.

Operational parameters that dramatically affect column performance were studied via simulation models. The following are operating parameters and their possible effects:

- **Stripper column bottom temperature.** Stripper column bottom temperature is a key parameter. The light ends and water should be separated in the stripper column, and it is not expected to carry these to the debutanizer column. For better operations, the stripper bottom temperature must be at an optimum by adjusting the stripper reboiler duty.
- **Debutanizer column recycle flowrate.** Recycle flow is supplied from the debutanizer overhead drum to the

debutanizer column. The aim of this recycle is to optimize column separation. Proper recycle flowrate is crucial for debutanizer operation.

- **Debutanizer column feed rate.** It was observed that the debutanizer column performance was fluctuating at a low debutanizer feed rate. Therefore, a column tray analysis was performed, and the weeping condition in all trays was obtained.
- **Debutanizer column bottom temperature.** The temperature at the bottom of the debutanizer was also one of the parameters affecting column performance. For the debutanizer top section load, the bottom temperature and reboiler duty needed to be optimized.

Simulation of the coker debutanizer and stripper columns. A commercial simulation program was used to achieve accurate simulation models on the stripper and debutanizer sections of the DCU. The configuration of the simulations covered rigorous column, condensers (heat exchangers and air coolers), reboilers, drums, pumps, valves and pipe segments.

The first step in simulation modeling of the unit was to carry out several selections and identifications. To estimate the properties of hydrocarbons, water and steam, appropriate property packages should be used. In this study, the Peng-Robinson equation of state (EOS) and ASME steam fluid packages were used. A unit process flow diagram was the basis for the simulation flowsheet.

The debottlenecking study via simulation models had the following primary equipment: a stripper column, a debutanizer column, condensers (heat exchangers and air coolers), reboilers and overhead receiver drums. The primary goal of the study was to investigate and provide solutions to a bottleneck problem in the debutanizer column section. Product back blend was used in all simulation case studies at the beginning of the detailed analysis. The base model of the stripper and debutanizer section of the unit was completed (at steady-state conditions, according to normal operational conditions) and then used for the bottleneck analysis.

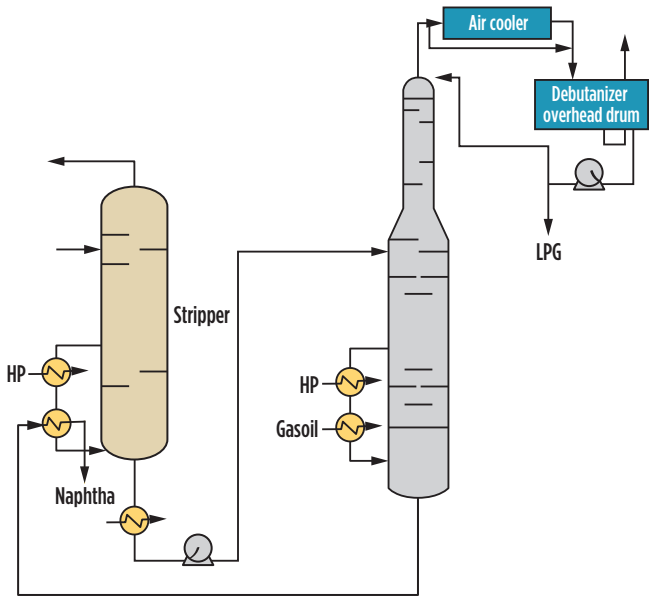

FIG. 1. Overview of the debutanizer and stripper sections of the DCU.

Simulation model validation. Simulation models were validated according to the unit's design data or field data before they were used in the study. The steps used during this validation are summarized here:

1. **Generation of the model, using field data:** Plant data (such as distillation, flowrates and operational data) and equipment process data sheets were used to configure the model. The debutanizer and stripper column models were completed according to steady-state operational conditions via two different data sets. Using different data sets, feed conditions were varied to obtain the most validated simulation models and to witness the effects of operational parameters on process dynamics, such as bottleneck conditions.
2. **Validation of the model results:** Based on predefined validation limits, the simulation results were validated according to plant data. Critical parameters for validating the simulation model include:
   - Product flowrates (LPG, light naphtha and heavy naphtha)
   - Product specifications for light naphtha, heavy naphtha (ASTM D86 T5-T95) and LPG (C_5 limit)
   - Temperature and pressure profiles of the stripper and debutanizer columns
   - Condensers (heat exchangers and air coolers) and reboiler outlet temperatures.
3. **Acceptance of the deviations from actual data:** When the model was compared with plant data, the results were acceptable if the difference was ±5%. These criteria were based on possible measurement errors and general refinery practice.

Debottleneck analysis. Before evaluating alternative solutions for a bottleneck analysis, the unit base model was created according to the 8-hr average values of a day when product and charge analyses were made, and production was stable. Because bottleneck problems occurred at low flowrates, the debottleneck study was performed via turndown simulation models. From the simulation model results, the authors observed the following:

- The simulation results showed weeping in all trays of the column at turndown conditions.
- The lower feed was raised to higher temperatures in the reboilers of the debutanizer column, with vapors remaining nearly unchanged at the top (given the weeping conditions).
- If the column began to weep, then there was no equilibrium in the trays, and the vapor from the feed (including the vapor produced by the reboiler) bypassed the trays on its way up the column. This typically causes higher pressure and very low tray efficiency.
- If the reboiler duty was kept the same, then more light components could reach the top of the column, thus increasing pressure and tripping the PSV.

This sequence obtained from simulation models was one of the bottleneck problems in the debutanizer columns section. The second problem included the following:

- During a troubleshooting review, it was also observed that water was continuously being removed from the debutanizer reflux drum.
- The reflux drum is equipped with a control valve on the water drain, which normally does not open during normal operating conditions.
- At lower feed loads, the control valve opening was high, which corresponded to the discharged water flowrate from the reflux drum. This was not an expected issue because dissolved water had to be taken from the stripper column—and the debutanizer feed had not contained water composition.
- Simulation models showed that stripper reboilers (these exchangers used hot debutanizer bottom products as heating fluid) did not have enough duty at lower feed rates.
- The lower feed fell to lower temperatures in the reboilers of the stripper column, and then water in the reboiled stream could not be removed.
- Water was carried via the stripper bottom to the debutanizer column at these conditions, thereby upsetting operations and tripping the PSV in the debutanizer.

Implementation of model results in the field. As a result of the simulation modeling, the stripper bottom temperature began to stay at optimum temperature (it was extracted from simulation models) and not carry light ends and water to the debutanizer column, especially at low feed rates. When the water reached the top of the debutanizer, there was a freezing risk that could result in a PSV trip. To prevent freezing and blocking, electrical tracing was used in pipelines and process instruments.

Following the implementation of these model results, high-pressure steam savings increased by 3.36%. Additionally, the refinery's energy intensity decreased by 0.06, while CO_2 emissions decreased by 1,500 tpy. This was achieved by reducing high-pressure steam consumption in the process via decreasing fuel gas rates at conventional boilers in the refinery. Avoiding PSV trips also helped the refinery decrease losses and mitigate environmental issues. This was an invaluable gain for the refinery's reputation.

Takeaway. This study analyzed the effects of each operating parameter, both individually and collectively. When a system is viewed in its entirety, some parameters have a snowball effect, while some have a diminishing effect. Therefore, before performing any debottleneck study in a process and/or in a specific section of a process, it is better to check the overall effects. In this case, by understanding and targeting the source of the bottleneck, the first step was obtaining the root causes of the problem based on the symptoms and on the unsteady operation of the stripper and the debutanizer under turndown loads. The second step was optimizing operating conditions according to the simulation results.

In many situations, it is uneconomical to solve the problem—especially for large-capacity units in a refinery—with conventional trial-and-error methods, which can cause off-spec products or upsets in refinery units. However, the authors found alternative solutions via simulation models and corrected the problems on the unit's data historian. After discovering the root causes of the problem, alternative solutions were applied on the models first, prior to implementing them onsite. This solved the problem in the most economical way. Therefore, to obtain a correct diagnosis of a problem, it is important to first understand the underlying principles before addressing the problem. HP

ERHAN ÖZSAĞIROĞLU is Simulation Superintendent under the Process and Equipment Development Department at Tüpraş headquarters. He previously worked as a senior process engineer and holds a PhD in chemical engineering from Istanbul Technical University.

TUĞÇE ÖZKURT ATAGÜN is the Process Superintendent at Tüpraş' İzmit refinery. She has been working for 8 yr, and is responsible for the following units: DCU, FCCU, the gasoline desulfurizer, the kerosene treater, and the LPG and SHU units.

ECEM ARİCİ is the Process Chief Engineer at Tüpraş' İzmit refinery. She is responsible for the kerosene treatment unit, the SHU and the LPG merox unit. She previously worked as an operations engineer and as a process engineer for the DCU. She earned a BSc degree in chemical engineering from Boğaziçi University in Turkey.

M. HOYME and J. MILLER,
Emerson, Marshalltown, Iowa

Extending proof test intervals by improving SIS final element reliability

Large chemical and refinery units often run up to 5 yr between plant outages, and many would extend that time even longer to maximize production. These processes usually involve hazardous chemicals and dangerous reactions and often employ a safety instrumented system (SIS) to protect equipment, personnel and the environment.

An SIS is critical for plant operations and must work reliably, a task made more difficult because safety equipment may not be called upon to function for years. Proof testing is required to verify the components of an SIS will function as intended, but these tests can often interrupt operations.

This article will discuss methods to mitigate the negative effects of proof tests on production, with suggestions included for implementation.

SIS protection. A SIS is a group of equipment intended to implement one or more safety instrumented functions (SIFs). SIFs are designed to respond to conditions within a plant that may be hazardous, or if left unchecked, generate a hazardous event. A SIS is composed of three major elements: sensor(s), a logic solver and a final control element (FIG. 1). Many facilities follow IEC 61508 or ISA 84.01 standards when designing their safety systems, with failure rates calculated to demonstrate their ability to perform the intended SIF.

The sensors are typically instruments used to measure process parameters, each of which sends measurement data to the logic solver. The logic solver is some type of an electronic safety controller, or possibly a simple hardwired device for the most basic of systems. In either case, it monitors the sensor readings and detects trip conditions. Should a trip be required, the logic solver activates the final element(s) to bring the plant to a safe condition.

The final elements are usually one or more valve assemblies, each of which must be driven to a predetermined position. Valves typically close to stop raw material feeds, block steam to turbines, isolate equipment or perform other operations. Valves may also be configured to open to vent process to flare systems, introduce a chemical to stop a reaction or perform other operations.

Reliability is obviously crucial for a SIF, as it is typically the last line of defense against a major incident. A SIF's reliability is indicated by its safety integrity level (SIL). A SIL 1 loop must work at least 90% of the time when called to function; a SIL 2 loop must work > 99% of the time and a SIL 3 loop must work > 99.9% of the time.

SIL calculations are used to determine the probability of failure on demand (PFD), and the SIF sensors, logic solver and final elements are chosen to satisfy the required SIL. Redundancy is not required but is often used to improve reliability; therefore, 2oo3 (two out of three voting arrangement) sensors and 1oo2 (redundant) final elements are common in SIL 2 and SIL 3 applications.

A SIF may fail in several ways, but failures generally fall into four categories: safe detected, safe undetected, dangerous detected and dangerous undetected. A safe failure is one that fails in a safe state, with either the final element tripping or a sensor calling for a trip. This may cause unplanned outages, but the SIF can still function.

Dangerous failures are more problematic, as they may disable the trip and block the safety function. Dangerous detected failures create a bad but manageable condition. The SIF cannot function, but the plant *knows* it cannot function and can work quickly to repair the condition and restore the safety function.

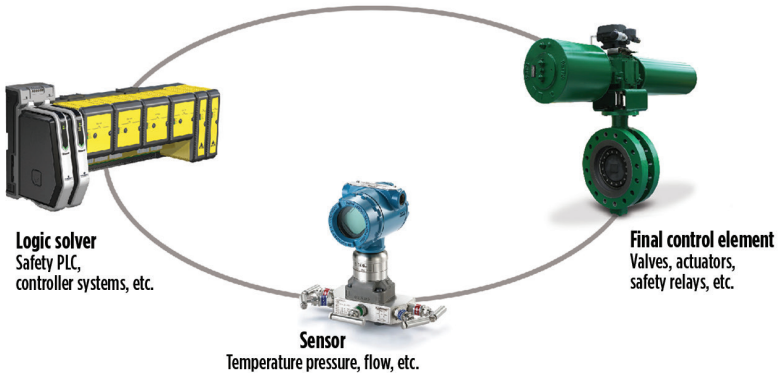

FIG. 1. A SIS provides an independent layer of protection against dangerous incidents and is composed of three major components: a logic solver, sensor(s) and final elements.

A dangerous undetected failure is a major incident waiting to happen. The SIF cannot function, and the operating unit is unaware of that fact. The operating unit will only discover the problem when a trip condition occurs, and the SIF fails to function.

Proof testing and diagnostics are key. Proof testing is a plant's main defense against dangerous undetected failures. To detect and minimize the probability of a SIF not functioning, plants must fully proof test all equipment on a routine basis. To achieve and maintain a SIL, the plant can either test more frequently, use components with lower failure rates or use components with a higher level of integrated diagnostics.

Many refining and chemical plants have SIL 2 and SIL 3 loops and run up to 5 yr between outages, creating extreme challenges for the safety system. Since a proof test will often trip a unit or even an entire plant, it usually can only be implemented during a full unit shutdown. Therefore, the operating unit must either devise a means to dramatically improve the reliability of the SIF components, or it must shut down more frequently to perform proof testing.

Safety equipment reliability. A SIF's SIL is determined by the PFD of the entire safety loop. This is determined by calculating the PFDs of each component and adding them together. When one evaluates the typical contribution of each component of the safety loop, final elements are found to be responsible for over 50% of the SIF loop failures (**FIG. 2**).

Sensors inherently have more diagnostics and can usually be tested while the plant is running, and it is relatively simple to implement redundancy and more advanced voting schemes to increase reliability. Furthermore, most sensors have no moving parts and, thus, have no wear parts, so long operating lives with minimal required maintenance is typical.

Most final elements are valves and have constant contact with the process media. These valves typically have minimal diagnostics, can go years without operating and cannot be fully tested without either shutting down the plant or isolating the valve needing testing through a bypass arrangement. Like most mechanical components, valves work best when operated periodically, which is often not possible with traditional installations. If a plant is looking to improve SIF reliability and extend proof test intervals, the final element is the first place to start.

Focus on final elements. A typical final element is composed of several components that might include a valve, actuator, solenoid, regulator, mounting brackets and couplings—and possibly positioners, I/P transducers and booster valves. Each of these components must function individually and in concert to ensure the safety function is achieved, whether that is to open or close the valve. Except for the positioner, many of these components offer few, if any, diagnostics, so failures tend to go undetected.

Engineering a final element can be a complicated task. It is usually some type of shutdown valve composed of several components, and each part must be carefully engineered to handle the process conditions and actuating torque, while working reliably despite very infrequent use in typical safety applications.

Normal and upset process conditions must be carefully evaluated and understood when choosing the shutdown valve and its actuator components. In addition, the proper combination of solenoids, mounting brackets, couplings and other critical hardware must be specified and carefully matched to the selected valve. When unsure of the sizing, the actuator will often be over specified above required safety margins, needlessly increasing the weight, size and cost of the final element. Therefore, careful design is required, often requiring the assistance of specialists.

TABLE 1. End user's SIL calculation comparison

	Traditional final element	Proprietary solution[a]
Proof test interval	6 yr	6 yr
PFD_{avg}	0.01	0.005
Risk reduction factor	96	189
SIL	1	2

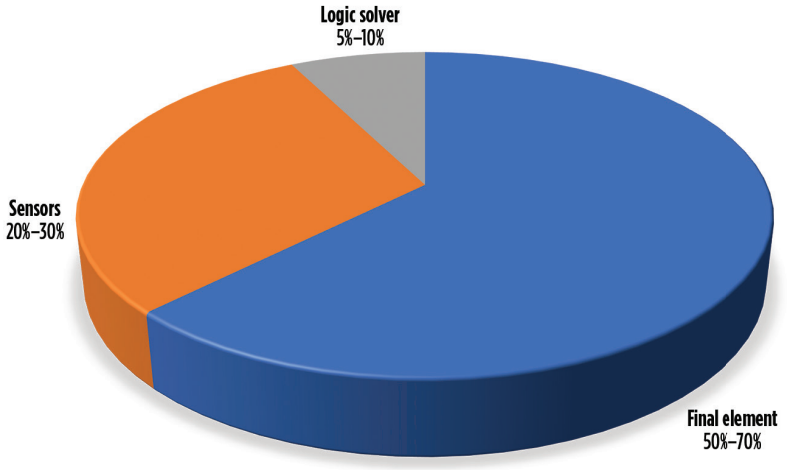

FIG. 2. An analysis of typical SIF loops shows that the final elements (typically valves) contribute approximately 50%–70% of overall safety loop failures.

FIG. 3. Proprietary final element solutions[a] are custom engineered shutdown valves provided as fully integrated, tested and certified final element assemblies, with the valve specifically designed for the application and each component carefully matched.

Improving final element safety and reliability. Final element safety and reliability can be improved by making use of fully integrated assemblies, partial stroke testing and increased diagnostics. Documenting and taking credit for unplanned trips can simplify compliance with test requirements.

Fully-integrated assemblies. Rather than having a user specify several individual valve components from different vendors, a single provider is now offering a complete final element assembly appropriate for a user's specific safety application (FIG. 3). This valve assembly is specifically engineered to satisfy the application requirements and is provided holistically as a fully tested and certified unit. The assembly is maintained from a total safety lifecycle perspective, rather than as a general service isolation valve. Each assembly is furnished with a single serial card delineating the details of every part, as well as a single SIL certificate and safety manual covering all components of the final element assembly.

These improvements in design and testing as an engineered solution and safety lifecycle approach to the final element provide a significantly improved PFD rate. In some cases, the failure rate of the assembly will be up to 50% less than the combination of the same components purchased individually, allowing a plant to significantly extend proof test intervals.

Partial stroke testing. A partial stroke test (PST) utilizes a custom solenoid or positioner to allow a valve to partially stroke toward its safe state (i.e., open or closed) during the test. While this does not constitute a full test since the valve is not completely stroked, it does show that the valve is not frozen in place and the solenoid and actuator components are functioning as designed. A PST is considered a diagnostic and partial test and can be used to improve a valve's overall reliability rating. The challenge of a PST is to avoid upsetting the process. If the valve strokes too far or moves too quickly, it will often introduce enough of an upset to shut down the process, so PST components must be carefully designed to avoid this situation.

Increased diagnostics. Significantly improved diagnostics are available with smart valve instrumentation, such as a digital valve controller (DVC), which can be installed on valves with analog or digital controls (FIG. 4). A DVC can monitor several parameters, including air supply pressure, actuator movement, seal performance, solenoid health and others. It can also be used to initiate and document a PST, and the improved diagnostics can be used to significantly reduce the PFD of the entire shutdown valve assembly.

Additionally, some DVCs can document and take credit for unplanned valve movement. Occasionally, an unexpected process upset will cause the logic solver to trip a SIS valve. If the valve position is historized using data from a digital positioner, the valve performance can be captured and documented as the trip sequence executes. Assuming the valve performs as expected, this data can be considered a fully executed proof test, thus resetting the proof test interval time.

Results. Implementation of these concepts has resulted in significant savings for several end users, with the reliability and integrity of the safety systems improved.

One end user wanted to achieve a 6-yr proof test interval for a SIL 2 loop. When they performed a component SIL calculation on a standard final element assembly, they could only achieve SIL 1 reliability at a 6-yr proof test interval, as shown in TABLE 1. However, a proprietary solution[a] was designed to meet SIL 2 requirements using the same components and still achieving a 6-yr proof test interval. This allowed the plant to safely extend its run time to 6 yr, generating millions of dollars in additional revenue.

In another case, a U.S. refinery had to shut down as a hurricane approached. Trips and shutdown valve performance were captured by a proprietary digital valve controller[b] as the plant was taken out of service. With this data used as documentation of proof testing, the plant avoided further downtime costing $2 MM/d.

Caveats. Implementation of each of these concepts requires careful design and engineering, coupled with close attention to operating procedures. Many chemical plants and refineries are already running with minimal onsite staff, exacerbating these issues. Because SIS installations are highly specialized, a plant may not have the specific required expertise on hand to implement changes and modify operating procedures, even for improvements expected to be highly beneficial.

These and other related issues can usually be effectively addressed by enlisting the services of a trusted partner, either an engineering or consulting firm or a supplier. This requires reliance on a third-party source, introducing cost and risks. However, in most cases, the return on investment can be justified.

FIG. 4. PST—via digital valve controllers—provides two methods to significantly improve shutdown valve reliability. These devices can perform a PST while ensuring the valve does not fully stroke. The digital valve controller shown can perform the PST, monitor valve components and initiate other tests.

Takeaway. Satisfying SIL requirements with extended proof test intervals can be very challenging, and many plants are looking for ways to further extend intervals safely. SIS final elements offer the greatest opportunity to extend proof test intervals through improved SIF reliability. PST, increased diagnostics, valve trip documentation and complete valve assemblies can dramatically improve final element performance, while continuing to meet the required SIL, even as production runs are extended. HP

NOTES

[a] Fisher™ Digital Isolation™ Solutions from Emerson
[b] Fisher™ FIELDVUE™ DVC6200 digital valve controller

MIKE HOYME is a Product Manager for Fisher Rotary Valves. He is a certified functional safety professional with 10 yr of valve engineering and product management experience. He strives to create final elements for SISs that both improve safety and process uptime. Mr. Hoyme earned a BS degree in mechanical engineering from the South Dakota School of Mines and Technology.

JUSTIN MILLER is a Senior Sales Engineer for Emerson's flow controls products, specializing in the chemical industry. Previously, he spent 6 yr in product management where he supported Fisher sliding stem valves. He is a certified functional safety professional with 9 yr of valve application and product management experience. He strives to help customers find the best possible solutions to challenging applications. Mr. Miller earned a BS degree in mechanical engineering from Iowa State University.

R. KADIKAR, ITT Corp., Vadodara, India

Is coating required on stainless-steel components?

Stainless steel is a generic term used for a large group of corrosion-resistant alloys containing at least 10.5% chromium (Cr), and possibly containing other alloying elements like nickel (Ni), molybdenum (Mo), manganese (Mn) and nitrogen (N).

Stainless steels are divided into five categories based on their microstructure and properties:

1. Austenitic stainless steel
2. Ferritic stainless steel
3. Martensitic stainless steel
4. Duplex stainless steel
5. Precipitation-hardened stainless steels.

These grades are further subdivided into super austenitic, super ferritic and super duplex stainless steel. Super (austenitic, ferritic and duplex) stainless steel grades may contain higher Cr, Ni, Mo and N, depending on their material type and grade.

Corrosion in stainless steels. In stainless steels, Cr content above 10.5% is necessary to form a stable passive chromium oxide (Cr_2O_3) layer. This passive layer protects underlying material from corrosion damage from the surrounding environment. The passive Cr_2O_3 film is extremely thin, approximately 10–100 atoms thick (approximately 2 nm); however, it prevents further oxygen diffusion into the base metal. A Cr_2O_3 passive layer in stainless steel acts as a defender of the material. Any mechanical activity, like grinding or cutting, damages the passive Cr_2O_3 layer. However, Cr has very high affinity with oxygen, and so it immediately reacts with surrounding oxygen and forms a passive Cr_2O_3 film, thereby protecting stainless steels. In a corrosive environment, damage to the passive layer cannot be restored, which leads to corrosion of the underlying material.

Generally, stainless steel suffers from corrosion damage in the presence of halides, such as chlorides, bromides, etc. Damage due to chloride presence is common in stainless steels around industrial areas, buried vessels under soil and/or water, and vicinity to a marine environment. These locations contain high chlorides and lead to chloride-related damage mechanisms.

Chloride ions from wet and humid environments can combine with Cr of the passive layer, forming soluble chromium chloride. As Cr dissolves, free iron (Fe) is exposed to chemically reactive surroundings containing chlorides, and the surface reacts with the corrosive environment to initiate corrosion. In this way, the chloride ion acts as a nemesis of the material.

Damage mechanisms of corrosion types. Depending on chloride concentration, temperature and operating conditions, chloride ions can cause three different corrosion damages in stainless steels:

1. Crevice corrosion
2. Pitting corrosion
3. Stress corrosion cracking.

Crevice corrosion is highly localized corrosion that occurs within the crevices and shielded areas on metal surfaces exposed to corrosives. A typical example of crevice corrosion is under-deposit corrosion, which forms below sand, dirt and corrosion products.

Pitting corrosion is an extremely localized attack that results in holes on metal surfaces. Pitting is one of the most destructive and insidious form of corrosion. It causes equipment to fail because of perforations with only a small percent of weight loss of the entire structure.

The damage mechanism for crevice and pitting corrosion is the same result: the passive Cr_2O_3 layer is damaged, and the chloride ion forms hydrochloric acid within the pits/crevices, thereby enlarging the pits and crevices over time.

FIG. 1A shows a typical crevice and pitting corrosion mechanism. **FIG. 1B** and **FIG. 1C** show how crevice and pitting corrosion looks in stainless steel.

Stress corrosion cracking involves the cracking and sudden rupture of equipment without any warning, which makes stress corrosion cracking in stainless steel more damaging to equipment, to personnel working around the equipment and to the surrounding environment. Austenitic stainless steel is susceptible to chloride stress corrosion cracking if the temperature is above 60°C (140°F). **FIG. 2** shows chloride stress corrosion cracking in austenitic stainless steel.

Critical factors that increase susceptibility for chloride damage in stainless steel involve chloride concentration, temperature, pH, oxygen and residual stresses for stress corrosion cracking. Increas-

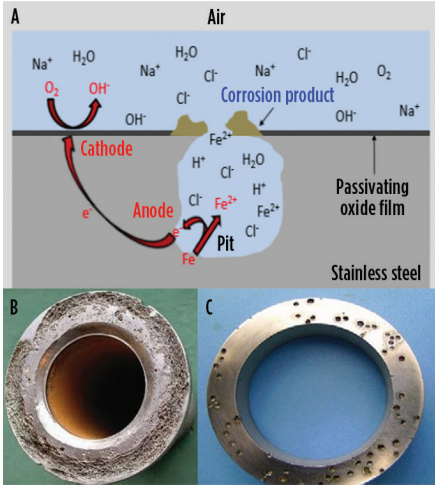

FIG. 1. Crevice and pitting corrosion mechanism (A), crevice corrosion appearance in stainless steel (B), pitting corrosion appearance in stainless steel (C).

ing the chloride content and temperature increases the susceptibility of stainless steel to corrosion. Susceptibility to corrosion increases with lower pH, and corrosion tendency decreases with higher pH. Excessively stressed and low-temperature components are highly susceptible to chloride stress corrosion cracking. Oxygen and oxidizers increase chloride stress corrosion cracking susceptibility; however, stagnant conditions and low oxygen availability increase the susceptibility for crevice and pitting corrosion.

In terms of chloride-related corrosion resistance, duplex and ferritic stainless steels offer better resistance. Precipitation and martensitic stainless steels offer the least resistance. Austenitic stainless steel offers intermediate resistance. However, material selection should be performed only after considering all of the previously specified critical factors.

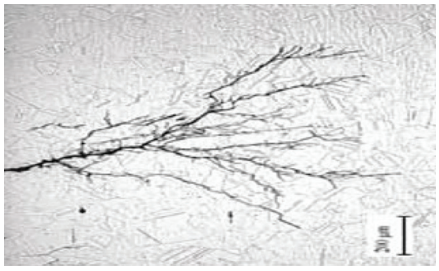

FIG. 2. Chloride stress corrosion cracking in austenitic stainless steel.

Duplex stainless steel has better resistance against chloride-related corrosion damage mechanisms; however, it is not immune to these damages. Its resistance against chloride is also dependent on the critical factors previously specified.

It is important that the coating is applied as per the manufacturer's coating application guidelines to avoid coating defects. Surface preparation and application are key to ensuring the coating integrity.

Microbiologically influenced corrosion (MIC). MIC is another form of corrosion that occurs in stainless steels. This type of corrosion is caused by living organisms such as bacteria, algae and/or fungi. It is often associated with the presence of tubercles or slimy organic substances. Often, the bacteria produce localized corrosion in the form of crevice or pitting corrosion. MIC is found in aqueous environments where stagnant or low-flow conditions exist and promote the growth of microorganisms.

These microbes fall into two basic groups: aerobic and anaerobic. The two groups are based on the environment the microbes prefer (with or without oxygen). Slime-forming bacteria comprise a diverse group of aerobic bacteria. Common anaerobic bacteria include sulfate-reducing bacteria (SRB) and organic acid-forming bacteria. In stainless steels, anaerobic bacteria are more harmful since they do not require oxygen for growth and, therefore, do not allow oxygen to reach the metal surface for passive film formation.

FIG. 3. Examples of MIC corrosion damage in stainless steel pipe.

Different organisms thrive on different nutrients, including inorganic substances (e.g., sulfur, ammonia, Fe, sulfate compounds and H_2S) and organic substances (e.g., hydrocarbons and organic acids). In addition, all organisms require a source of carbon, nitrogen and phosphorous for growth. Corrosion is often blamed on iron-oxidizing bacteria or sulfate-reducing bacteria. However, these organisms typically are only part of a complex colony of multiple types of interdependent organisms, each capable of creating byproducts that might be a food source for others.

These microbes tend to form colonies, with different characteristics appearing on the outside and inside. On the outside, slime-forming bacteria may produce polymers (slime) that attract inorganic material, making the colony appear as a pile of mud and debris. These aerobic organisms can efficiently use up all available oxygen, giving anaerobic microbes inside the colony a hospitable environment, which encourages enhanced corrosion under the colony. **FIG. 3** shows MIC damage in stainless steel pipe.

Coatings to prevent corrosion. Material selection is carried out based on the extreme corrosive conditions from the process fluid side and/or the external atmosphere. When stainless steel is selected, internal coatings are usually not required because the stainless steel corrosion resistance will protect against the internal process fluids. However, the possibility of corrosion from the external atmosphere still exists, which could require coatings on the external surfaces of stainless steel components to mitigate against chlorides and/or microbial corrosion damage.

The following conditions require external coatings on stainless steels to guard against external corrosion damage:

1. Equipment buried underground, where wet soil with chlorides and microbes is in contact with stainless steel

TABLE 1. Guidelines for coating austenitic stainless steel

Material	Temperature	Coating system
Austenitic stainless steel	–40°C–80°C (–40°F–176°F)	Two coats of epoxy with a top coat of polyurethane
	81°C–200°C (177°F–392°F)	Two coats of phenolic epoxy
	201°C–400°C (393°F–752°F)	Two coats of silicone

TABLE 2. Guidelines for coating duplex stainless steel

Material	Temperature	Coating system
Duplex stainless steel	100°C–200°C (212°F–392°F)	Two coats of phenolic epoxy
	201°C–400°C (393°F–752°F)	Two coats of silicone

2. Equipment submerged in wet pits, where salty water could be present and microbes are in contact with stainless steel
3. Equipment enclosed in insulation, where salty water from a marine environment or rain water containing some chlorides may accumulate on stainless steel.

All these conditions may cause accumulation of chlorides on the external surface. Similarly, underground buried and submerged equipment may encounter microbial activity. Both equipment scenarios can create an environment that is conducive for pitting, crevice and microbial corrosion, and even stress corrosion at moderate temperatures.

To maintain corrosion resistance against external crevice, pitting, stress corrosion cracking and MIC, the severity of corrosion should be assessed. One option to mitigate against corrosion is to select corrosion-resistant material to ensure internal and external corrosion-resistant conditions. The second option is to implement an external coating on stainless steel surfaces to avoid direct contact of corrosive species with the equipment external surface. The most economical way to protect against external damage is to apply a coating to exposed external surfaces, which will avoid direct contact of corrosive chlorides and microbes with the stainless steel components.

It is important that the coating is applied as per the manufacturer's coating application guidelines to avoid coating defects. Surface preparation and application are key to ensuring the coating integrity. For buried equipment, where regular coating inspection is not possible, the application of sacrificial or impressed-current cathodic protection, along with coating, can help improve design life and equipment integrity. Cathodic protection additionally protects equipment in case of coating damage due to defect or physical damage. **Note:** The selection of cathodic protection type and design is a wide subject and is not covered here.

Various international standards and company specifications prescribe coatings on stainless steel if corrosion conditions exist. For example, coating systems are used as specified in **TABLE 1** and **TABLE 2** for austenitic and duplex stainless steels, respectively.

Buried, submerged and insulated stainless steel components can encounter chloride and microbial corrosion attack. Stainless steels in these scenarios require external coating; otherwise, external coating on stainless steel components is not necessary. HP

RATNAKAR KADIKAR is Global Manager, Materials for ITT Corp. Industrial Process Group. He provides metallurgical and materials technology for ITT Corp.'s business, as well as technical support to ITT customers and product specialists. He has more than 21 yr of experience in corrosion monitoring, corrosion evaluation, material selection, failure investigation, heat treatment, micro-structural analysis and training on metallurgical aspects. He has also worked in corrosion loop risk-based inspection study, integrity operating window, cathodic protection, painting/coatings and residual life assessment of static equipment. Mr. Ratnakar holds BS and MS degrees in metallurgical engineering. He is a qualified NACE International Senior Corrosion Technologist and is API 571/API 653 certified.

MIKE RHODES, MANAGING EDITOR
Mike.Rhodes@HydrocarbonProcessing.com

Digital control of work (CoW) software system

Yokogawa RAP has launched RAP4, its trusted digital control of work (CoW) software. With significant new functionality, RAP4 provides a fresh intuitive gateway to a safer workforce culture.

Allied with the RAP Cortex knowledge base of potential hazards and mitigating controls, RAP4 is an intelligent alternative to the simple digitization of paper-based formats and continues to place risk assessment at the forefront of the permitting process.

This advanced and user-centric software has been given a full reconfiguration refresh, with updated and streamlined workflow processes throughout, taking the system to new levels of user friendliness. Additional permit and isolation functionality, as well as native Android and iOS applications, have also been added to further improve safety and efficiency.

The RAP4 system provides smart, simple, clear and intuitive modules with the intelligence to ensure complete CoW audit compliance and drive continuous safety improvement.

Through the RAP Cortex, all relevant hazards and controls can be easily accessed by following a best practice workflow process, resulting in a simple to follow system for all. Specific knowledge of permits and permitting processes is not required, thus making the software significantly more accessible to the people who actually do the work. RAP4 is highly configurable and drives continuous safety and risk assessment processes that are created directly as part of the permitting process, and it builds on earlier versions of this software to create an easy to access and intuitive gateway to digital CoW processes.

Rugged field transmitter

Endress+Hauser has released iTEMP TMT142B (FIG. 1), a new-generation smart temperature transmitter with Bluetooth. The transmitter delivers highly accurate and reliable measurements, wireless communication via Bluetooth, and user-friendly operation—all packaged in a robust single-chamber field housing. The technology offers significant improvements in process efficiency and plant availability while reducing costs.

In industrial process engineering applications, temperature transmitters are an important link between temperature sensors in the process and higher levels of automation. Measurement instruments are often installed in difficult-to-access locations, which frequently makes commissioning, operation and servicing more difficult.

To address these and other issues, the transmitter features a highly secure integrated Bluetooth interface that enables users to wirelessly visualize measured values, NAMUR NE 017 diagnostic information, as well as perform configuration tasks. The device is extremely easy and fast to operate using a phone or tablet and the Endress+Hauser SmartBlue app. No special tools are required. Access to the device is password-protected, and Endress+Hauser security provisions for Bluetooth communication comply with the highest standards.

The newly developed backlit display provides excellent readability under all environmental conditions, both in the dark and bright sunlight. Diagnostic messages are highlighted when the normally white background turns red.

The conversion of different sensor signals into a stable, standardized output signal (4 mA–20 mA) represents a logistical challenge, as it often requires multiple transmitter variations. To meet this challenge, the configurable single-channel device transmits converted signals from resistance sensors (RTD), thermocouples (TC), resistances (Ω) and voltage transmitters (mV) via the 4 mA–20 mA signal or the HART 7 communication.

The iTEMP TMT142B temperature transmitter is designed for safe operation in hazardous areas, as certified by international approvals (ATEX, CSA C/US, IECEx). Safe operation is enhanced by the incorporation of an integrated overvoltage protection that protects the device from damage and permits continued functionality after common upset events.

FIG. 1. Endress+Hauser's iTEMP TMT142B new-generation smart temperature transmitter with Bluetooth.

Extended centrifugal pump capabilities

Reliable, leak-free pumping of hazardous, more challenging chemicals is a prerequisite in all chemical processing applications and seal-less, magnetically driven pumps are the established preferred option. The Finish Thompson ULTRA-Chem (UC) series of Tefzel (ETFE) lined centrifugal pumps (FIG. 2) represents a good example of well-engineered and durable leak-free pumps. Following recent modifications, new options are resulting in extended capabilities and a wider performance envelope.

Available from Michael Smith Engineers Inc., the UC series of pumps now includes the UC436L model, which features smaller impeller trims to allow for lower flows and heads, and the UC3210 model, which has been uprated for two-pole motors. The new two-pole motor option operates at a higher rotation speed than the existing model and enables the pump to generate higher flows at higher heads, thereby extending its performance range. Also, the innovative single-piece snap fit impeller/inner drive magnet feature has

FIG. 2. The Finish Thompson ULTRAChem (UC) series of Tefzel (ETFE) lined centrifugal pumps.

FIG. 3. Cast Aluminum Solutions' new CAST-X high-temperature heater line.

FIG. 4. Sensor Networks Inc. and Cosasco have partnered for their first collaborative product: Echo Point®

also been extended through all models in the ULTRAChem range, helping to simplify maintenance and reduce servicing costs.

As with all the Finish Thompson ULTRAChem pumps, these new options combine a tough ductile iron casing with an ETFE lining to ensure outstanding corrosion resistance and feature powerful neodymium magnets that drive the impeller through a carbon-filled PTFE lined barrier for dependable, leak-free operation.

In addition, the pumps incorporate other features that optimize efficiency and performance, ensuring minimal wear on components, lower running costs and extended periods between routine servicing. For example, a Dri-coat silicon carbide bearing/shaft option prevents catastrophic failure in the event of short-term dry-running. Also, a two-piece dynamically balanced outer drive magnet with multiple pole options matches drive to motor for greater efficiency.

This outer drive magnet incorporates Finish Thompson's "Easy-set" mounting system so that the drive magnet can be fitted to the motor shaft without having to measure the magnet set-height. This ensures a perfectly set magnet that removes the potential cause of misalignment and so improves safety and reliability.

Other features include a Kevlar reinforced barrier, which reduces the air gap between driven and driving magnet and so maximizes magnetic power to transmission. Using Kevlar for the barrier reinforcement enables maximum working pressure to be increased to 300 psi (20.7 bar).

These latest options and features further underline the effectiveness of ULTRAChem pumps as an ideal choice for extreme pumping applications. These typically occur in chemical manufacturing, blending and distribution, water treatment, plating and surface treatment applications, paper mills, fume scrubbers and other similar challenging situations that demand robust and reliable leak-free pumping.

High-temperature industrial heater line

Cast Aluminum Solutions (CAS), a supplier of specialized heaters for oil and gas applications, has launched its new CAST-X high-temperature heater line (**FIG. 3**), which features operating temps to 1,110°F (600°C).

Flammable liquids and gases can be safely heated using CAST-X high-temperature heaters, even under significant operating pressures: CAST-X high-temperature heaters can safely heat natural gas, diesel fuel, jet fuel, alcohols, hydrocarbons and more. Process gases such as nitrogen, argon, CO and CO_2 (even in a cryogenic state) are also well-suited for CAST-X high-temperature heaters.

Available in two primary sizes, CAST-X high-temperature heaters are an easily-integrated "inline heater" with industry-standard flow tube sizes, and are compatible with most worldwide voltages. CAST-X HT 500 has power to 1,500 W, and a ¼-in. fluid/gas flow tube. Available with a certified explosion proof terminal enclosure (for hazardous locations) or with no terminal enclosure (for inert applications), these units have a very small footprint. CAST-X HT 2000 accommodates higher-flow applications, with power to 6 kW and a ½-in. flow tube; it is available with either an explosion-proof or a water-resistant terminal enclosure.

All CAST-X heaters have a unique "no contact design," where the heated media never contacts the heating element. The heated media (which can be liquid or gas) flows through a spiral-wound, stainless-steel or Inconel flow tube, which is isolated inside the heater body—high-performance heating elements are also integrated within the heater body. This design is much safer and cleaner than standard immersion heaters, where media is in direct contact with heating elements.

Technology partnership

Sensor Networks Inc. (SNI), a leader in non-intrusive, wireless ultrasonic sensor technologies, and Cosasco, a technology leader in intrusive corrosion monitoring, have produced their first collaborative

product: Echo Point® by Cosasco (FIG. 4), a non-intrusive metal loss monitoring instrument for critical assets. This technology accurately measures wall thickness (as well as internal pitting), operates under ultra-high temperature, and utilizes the industry-standard Wireless HART technology.

Available in three different transducer models, the sensor attaches easily to an asset's outer surface with clamps or a magnetic base and can measure through surface coatings in many applications. Echo Point features an embedded temperature sensor in the tip of the product, is a hazardous-location certified instrument and rated for Class I, Div. I, Zone 0 atmospheres.

Cosasco will provide an interactive experience with the data through the Cosasco Data Online management system via HART-IP, Modbus TCP/IP, or OPC to DCS and SCADA systems.

Improving fuel economy and energy efficiency

ExxonMobil has announced its new SpectraSyn™ MaX next-generation polyalphaolefin (PAO) base stock, designed to provide a low-viscosity, low-volatility balance and help enable improved fuel economy and energy efficiency.

SpectraSyn MaX leverages a unique PAO structure to provide low viscosity while improving or maintaining other key properties, including:

- Low volatility for reduced oil consumption
- Excellent low-temperature properties for optimal performance
- Improved oxidative stability for engine cleanliness and longer drain intervals
- Enhanced lubricity and traction for enhanced energy efficiency
- Improved flashpoint for safety.

Car manufacturers are under constant pressure to improve the energy efficiency and fuel economy of their vehicles. Ultra-low viscosity engine oils and electric vehicle (EV) driveline fluids are effective ways to help achieve those goals.

In fuel economy tests of various 0W-12 and 0W-8 lubricants, the blends formulated with SpectraSyn MaX outperformed alternatives made with different low-viscosity base stocks available on the market. Overall, SpectraSyn MaX provided versatile performance across various engine oil tests for fuel economy, durability and cleanliness.

While the trend towards lower viscosity grades has created some challenges for formulators, SpectraSyn MaX provides formulators with more formulation flexibility than existing low-viscosity base oils, allowing for the inclusion of additives—such as viscosity modifiers for improved fuel economy, detergents or dispersants for cleaner engines, and sulfur and phosphorous for better wear protection—without compromising performance.

For today's EV designs with integrated e-modules, SpectraSyn MaX comes with the added benefit of being a single-fluid solution that lubricates, cools and shows desirable electrical properties. SpectraSyn MaX also provides superior oxidative stability and can lower friction coefficient/torque loss, resulting in improved energy efficiency and extending the range of EVs. HP